

UNCLASSIFIED

AD NUMBER	
AD376586	
CLASSIFICATION CHANGES	
TO:	unclassified
FROM:	confidential
LIMITATION CHANGES	
TO:	Approved for public release, distribution unlimited
FROM:	Distribution authorized to U.S. Gov't. agencies and their contractors; Administrative/Operational Use; 07 OCT 1966. Other requests shall be referred to Air Force Systems Command Space Systems Division, Los Angeles, CA.
AUTHORITY	
31 Oct 1978, DoDD 5200.10; AFRPL ltr, 7 May 1973	

THIS PAGE IS UNCLASSIFIED

SECURITY

MARKING

The classified or limited status of this report applies to each page, unless otherwise marked.

Separate page printouts MUST be marked accordingly.

THIS DOCUMENT CONTAINS INFORMATION AFFECTING THE NATIONAL DEFENSE OF THE UNITED STATES WITHIN THE MEANING OF THE ESPIONAGE LAWS, TITLE 18, U.S.C., SECTIONS 793 AND 794. THE TRANSMISSION OR THE REVELATION OF ITS CONTENTS IN ANY MANNER TO AN UNAUTHORIZED PERSON IS PROHIBITED BY LAW.

NOTICE: When government or other drawings, specifications or other data are used for any purpose other than in connection with a definitely related government procurement operation, the U. S. Government thereby incurs no responsibility, nor any obligation whatsoever; and the fact that the Government may have formulated, furnished, or in any way supplied the said drawings, specifications, or other data is not to be regarded by implication or otherwise as in any manner licensing the holder or any other person or corporation, or conveying any rights or permission to manufacture, use or sell any patented invention that may in any way be related thereto.

CONFIDENTIAL

AFRPL-TR-66-222

TCO-58-10-6

Copy No. ~~8~~

DEMONSTRATION OF 156 INCH MOTOR WITH
SEGMENTED FIBERGLASS CASE AND ABLATIVE NOZZLE (U)

QUARTERLY TECHNICAL REPORT NO. 1

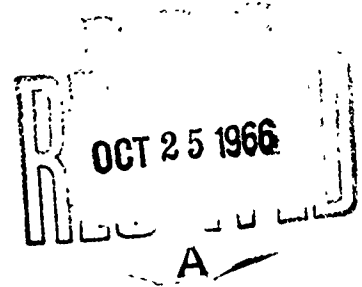
CONTRACT AF 04(611)-11603

7 October 1966

Prepared for

AIR FORCE
ROCKET PROPULSION LABORATORY
RESEARCH AND TECHNOLOGY DIVISION
AIR FORCE SYSTEMS COMMAND
Edwards, California

THIOKOL CHEMICAL CORPORATION
WASATCH DIVISION
Brigham City, Utah



IN ADDITION TO SECURITY REQUIREMENTS WHICH MUST BE MET, THIS
DOCUMENT IS SUBJECT TO SPECIAL EXPORT CONTROLS AND EACH
TRANSMITTAL TO FOREIGN NATIONALS MAY BE MADE ONLY WITH PRIOR
APPROVAL OF SSD (SSBS) LOS ANGELES AIR FORCE STATION, AIR
FORCE UNIT POST OFFICE, LOS ANGELES, CALIFORNIA, 90045.

CONFIDENTIAL

SPECIAL NOTICES

Qualified users may obtain copies of this report from the Defense Documentation Center.

Do not return this copy. When not needed, destroy in accordance with pertinent security regulations.

In addition to security requirements which must be met, this document is subject to special export controls and each transmittal to foreign nationals may be made only with prior approval of SSD (SSBS) Los Angeles Air Force Station, Air Force unit post office, Los Angeles, California, 90045.

CONFIDENTIAL

AFRPL-TR-66-222

TCO-56-10-6

DEMONSTRATION OF 156 INCH MOTOR WITH
SEGMENTED FIBERGLASS CASE AND ABLATIVE NOZZLE (U)

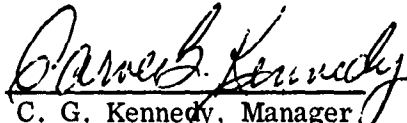
QUARTERLY TECHNICAL REPORT NO. 1

CONTRACT AF 04(611)-11603

7 October 1966

Prepared by

THIOKOL CHEMICAL CORPORATION
WASATCH DIVISION
Brigham City, Utah


C. G. Kennedy, Manager
Space Booster Development

DOWNGRADED AT 3 YEAR INTERVALS
DECLASSIFIED AFTER 12 YEARS
DOD DIR 5200.10

THIS MATERIAL CONTAINS INFORMATION AFFECTING THE NATIONAL
DEFENSE OF THE UNITED STATES WITHIN THE MEANING OF THE ESPI-
ONAGE LAWS, TITLE 18, U.S.C., SECTIONS 793 AND 794, THE TRANSMIS-
SION OR REVELATION OF WHICH IN ANY MANNER TO AN UNAUTHORIZED
PERSON IS PROHIBITED BY LAW.

Publications No. 1066-12163

0817-64-0995

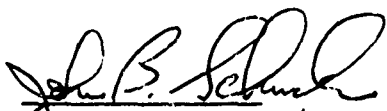
CONFIDENTIAL

FOREWORD

This quarterly technical report covers the work performed under Contract AF 04(611)-11603, "Demonstration of 156 Inch Motor with Segmented Fiberglass and Ablative Nozzle," for the period 2 May thru 31 Jul 1966.

This program is under the technical direction of John B. Schmuck, 1/LT, USAF, Project Engineer RPMBL, Air Force Rocket Propulsion Laboratory, Edwards AFB, California. Mr. William G. Morse is the Wasatch Division Program Manager for Thiokol Chemical Corporation. Mr. Robert F. Zeigler is the Project Engineer for the Wasatch Division.

Publication of this report does not constitute Air Force approval of the report's findings or conclusions. It is published only for the exchange and stimulation of ideas.



John B. Schmuck, 1/LT, USAF
Project Engineer

UNCLASSIFIED ABSTRACT

This program was established by the Air Force Rocket Propulsion Laboratory to demonstrate a segmented fiberglass case and an ambient pressure cured ablative nozzle in an actual motor firing. The development of manufacturing processes and handling techniques for the insulating and loading of a segmented fiberglass case is a primary objective of this program. The segmented fiberglass case was designed by Thiokol Chemical Corporation and fabricated by B. F. Goodrich Company under Air Force Materials Laboratory (AFML) Contract AF 33(657)-11303; the fixed ablative nozzle was fabricated by Thompson Ramo Wooldridge Incorporated under AFML Contract AF 33(657)-11301. The technical effort on this demonstration program was initiated on 2 May 1966. A subscale vessel was designed, fabricated, and tested during this first quarter to demonstrate joint sealing techniques for the 156 in. diameter segmented fiberglass case. The nozzle was delivered to the Wasatch Division, and effort in preparing the case segments for loading was initiated. The design of the 156 in. motor, including insulation, propellant grain, igniter, and ballistic performance, was completed.

TABLE OF CONTENTS

<u>Section</u>		<u>Page</u>
I	INTRODUCTION AND SUMMARY	1
	A. Introduction	1
	B. Summary	3
II	CASE	8
	A. Case Design Summary	8
	1. Design Criteria	8
	2. Structural	8
	3. Hydrotest	10
	4. Breakover Loads	14
	5. Bending Loads and Deflection at Horizontal Position	22
	B. Case Repair	28
	1. Repair Considerations	28
	2. Case Repair	28
	3. Effects of Repair on Case Design Strength	30
III	NOZZLE	47
	A. Nozzle Design Summary	47
	B. Nozzle Inspection	51
	C. Nozzle Performance Analysis	51
IV	JOINT SEAL	57
	A. Design Criteria	57
	B. Structural and Thermal Analysis and Summary	57
	C. Subscale Joint Seal Development	62
	1. Subscale Design	62
	2. Subscale Fabrication and Test	64
	3. Subscale Test Data and Analysis	70

TABLE OF CONTENTS (Cont)

<u>Section</u>		<u>Page</u>
V	INSULATION AND LINER.	77
	A. Design Criteria	77
	B. Material Selection.	77
	1. Insulation.	77
	2. Liner	81
	C. Material Configuration.	81
	1. Insulation.	81
	2. Liner	92
	D. Bonding Materials, Sealants, and Release Agents.	93
	E. Bond Verification Testing.	97
	1. Phase IA	97
	2. Phase IB	99
	3. Phase IIA	101
	4. Phase IIB	101
	5. Phase III	105
	6. Phase IVA	105
	7. Phase IVB	105
	8. Phase IVC	108
VI	PROPELLANT AND GRAIN	110
	A. Grain Design Summary.	110
	1. Ballistic Design	110
	2. Grain Stress Analysis	111
	B. Ballistic Performance	122
VII	IGNITION SYSTEM	137
	A. Ignition System Description	137
	1. Safety and Arming Device (S & A).	137
	2. Pyrotechnic Booster	140
	3. Initiating PYROGEN.	140
	4. Booster PYROGEN	141
	5. Igniter (Adapter).	141

TABLE OF CONTENTS (Cont)

<u>Section</u>	<u>Page</u>
B. Igniter Ballistic Design and Motor Ignition	
Transient	143
C. Igniter Insulation	153
1. Case Internal Insulation	153
2. Case External Insulation	153
3. Igniter Cap Insulation	153
4. Igniter Insulation Interfaces	154
D. Physical Characteristics, Ignition System	
Propellant, and Igniter Insulation	154
1. Stress Analysis	154
2. Igniter Weights	158
3. Ignition System Propellant	158
4. Insulation Ingredients, and Physical and Thermal Properties	160
5. Physical and Thermal Properties of Igniter External Insulation and Liner	160
E. Ignition Bench Tests	161
VIII PROGRAM SCHEDULE	163
A. Subscale Joint Seal Development	163
B. Motor Design and Analysis	163
C. Motor Insulation and Liner	164

LIST OF ILLUSTRATIONS

<u>Figure</u>		<u>Page</u>
1	TU-312L. 02 Motor Design	2
2	Program Schedule	4
3	Reports and Documentation List	5
4	Longitudinal Stresses and Radial Deflections of TU-312L. 01 Forward Skirt	12
5	Radial Deflections at 1,000 psi	13
6	Radial Deflections at Aft Joint (Top) and Forward Joint	15
7	TU-312 Handling Harness	16
8	Replacement Bladder Partially Installed	31
9	Vacuum Bag Installation Over Bladder	32
10	TU-312L. 02 Forward Segment	33
11	TU-312L. 02 Center Segment	34
12	TU-312L. 02 Aft Segment	35
13	Relative Deflections for a Clevis Leg	43
14	TU-312L. 02 Nozzle Design	48
15	Wall Mach Number vs Axial Position, Aft Case and Nozzle Inlet	53
16	Convective Heat Transfer Coefficient vs Axial Position, Nozzle Inlet	54

LIST OF ILLUSTRATIONS (Cont)

<u>Figure</u>		<u>Page</u>
17	Predicted Erosion, Char, and Ambient Temperature Profiles for TU-312 Nozzle	56
18	156-8 Motor Joint Seal	58
19	Displacements for the 156-8 Motor Seal	61
20	Subscale Test Assembly Design	63
21	Displacements for Subscale Seal	65
22	Subscale Insulation Showing Uncured Area	67
23	Test Assembly	71
24	Female Joint Insulation	71
25	Female Joint with Seal Installed	71
26	Vacuum Bag Compound Fill	72
27	Pressure Trace, Test No. 1, First Pressurization	73
28	Extensometer Trace, Test No. 1	73
29	Extensometer Trace, Test No. 1, First Pressurization	74
30	Pressure Trace, Test No. 1, Second Pressurization	74
31	Extensometer Trace, Test No. 1, Second Pressurization	75
32	Extensometer Trace, Test No. 1, Second Pressurization	75
33	Male Joint	76
34	TU-312L.02 Insulation Design Thickness	84
35	Predicted Erosion Rate of Silica Cloth Phenolic as a Function of Heat Transfer Coefficient	85

LIST OF ILLUSTRATIONS (Cont)

<u>Figure</u>		<u>Page</u>
36	Predicted Erosion Rate of Asbestos Filled NBR vs MACH Number in TU-312L.02 Motor Compared with Measured Erosion in Other Large Motors	86
37	Silica Cloth Erosion Rate vs Total Heat Flux	87
38	V-44 Erosion Rate vs Convective Heat Transfer Coefficient	88
39	Predicted Mach Flow and Heat Coefficient Through Aft Closure	89
40	TU-312L.02 Motor Aft Dome Total Heat Flux Variation on Silica Cloth	90
41	TU-312L.02 Motor Aft Dome Heat Transfer Coefficient Variation on Asbestos Filled NBR	91
42	Bond Test Apparatus Connected to Specimen	98
43	Apparatus for Testing Tenshear Plates Bonded in TU-312L.02 Case	98
44	Tenshear Test Apparatus	103
45	180 Deg Peel Test Specimen and Arrangement	104
46	Schematic Sketch of Half of TU-312 Center Segment Grain (Stress Analysis Grid Boundary)	112
47	Schematic Sketch of TU-312 Dome Segment Grain (Stress Analysis Grid Boundary)	112
48	Deformation of the TU-312 Center Grain at 60°F	114
49	Deformation of the TU-312 Forward Dome Grain at 60°F . . .	115
50	Deformation of the TU-312 Center Grain at 750 psi	117

LIST OF ILLUSTRATIONS (Cont)

<u>Figure</u>		<u>Page</u>
51	Deformation of the TU-312 Forward Dome Grain at 750 psi	118
52	Failure Criteria for TU-312 Grains.	119
53	TU-312L.02 Motor Chamber Pressure vs Time at 70°F	124
54	TU-312L.02 Motor Chamber Pressure vs Time at 100°F	125
55	TU-312L.02 Motor Thrust vs Time at 70°F (Vacuum Conditions)	126
56	TU-312L.02 Motor Vacuum Thrust vs Time at 100°F	127
57	TU-312L.02 Motor Vacuum Specific Impulse vs Time at 70 to 100°F	128
58	TU-312L.02 Motor Pressure Decay Rate vs Time at 70°F	129
59	TU-312L.02 Motor Pressure Decay Rate vs Time at 100°F	130
60	TU-312L.02 Motor Vacuum Thrust Decay Rate vs Time at 70°F	131
61	TU-312L.02 Motor Vacuum Thrust Decay Rate vs Time at 100°F	132
62	TU-312L.02 Motor Surface Area vs Time	133
63	TU-312L.02 Motor Throat Area vs Time	134
64	PYROGEN Ignition System	138

LIST OF ILLUSTRATIONS (Cont)

<u>Figure</u>		<u>Page</u>
65	TU-312L.02 Motor Igniter	139
66	TU-312L.02 Igniter Predicted Performance	142
67	Predicted TU-312L.02 Motor Ignition Transient	145
68	Predicted TU-312L.02 Motor Thrust vs Time During Ignition Transient (Utah Conditions)	146
69	Time from First Motor Chamber Pressure Rise to Initial Equilibrium as Function of Motor Characteristic Length	148
70	Summary of Analysis on TU-312L.02 Ignition System Condition II (MEOP = 1,000 psi)	155
71	Summary of Analysis on TU-312L.02 Ignition System Condition II (MEOP = 848 psi)	156

LIST OF TABLES

<u>Table</u>		<u>Page</u>
I	Fiberglass Design Requirements	36
II	Required, Original, and Remaining Glass Thickness and Safety Factors per Segment	42
III	Nozzle Insulation Materials	49
IV	Physical Property Test Results for Full Scale Nozzle Components	50
V	Insulation Ring	78
VI	Case Insulation	79
VII	Case Bladder	80
VIII	UF-2121 Liner	82
IX	UF-3119 Bonding Material	94
X	UF-3195 Bonding Material	95
XI	UF-1149 Bonding Material	96
XII	V-45 (Cured with Trevarno Cloth) Adhesion to UF-3119 (Phase IB)	100
XIII	Phase IIA Compatibility Test of Propellant to Insulation Bond	102
XIV	UF-2121 to MEK Wiped V-45 Bladder Material (Phase IIB)	102
XV	TU-312L.02 Igniter Compatibility Tests (Phase III)	106

LIST OF TABLES (Cont)

<u>Table</u>		<u>Page</u>
XVI	TU-312L.02 Inprocess Tests (Phase IV B).	107
XVII	TU-312L.02 Igniter Inprocess Tests (Phase IVC).	109
XVIII	Stress-Strain Conditions in the TU-312 Grains	116
XIX	Safety Margins for the TU-312 Loading Conditions (Worst Conditions Only).	120
XX	TU-312L.02 Rocket Motor Ballistic Performance Parameters.	123
XXI	TP-H1011 Propellant Composition	135
XXII	Ballistic Properties of TP-H1011 Propellant	136
XXIII	TU-312L.02 Igniter Predicted Performance	152
XXIV	Ignition System Structural Materials	157

SECTION I

INTRODUCTION AND SUMMARY

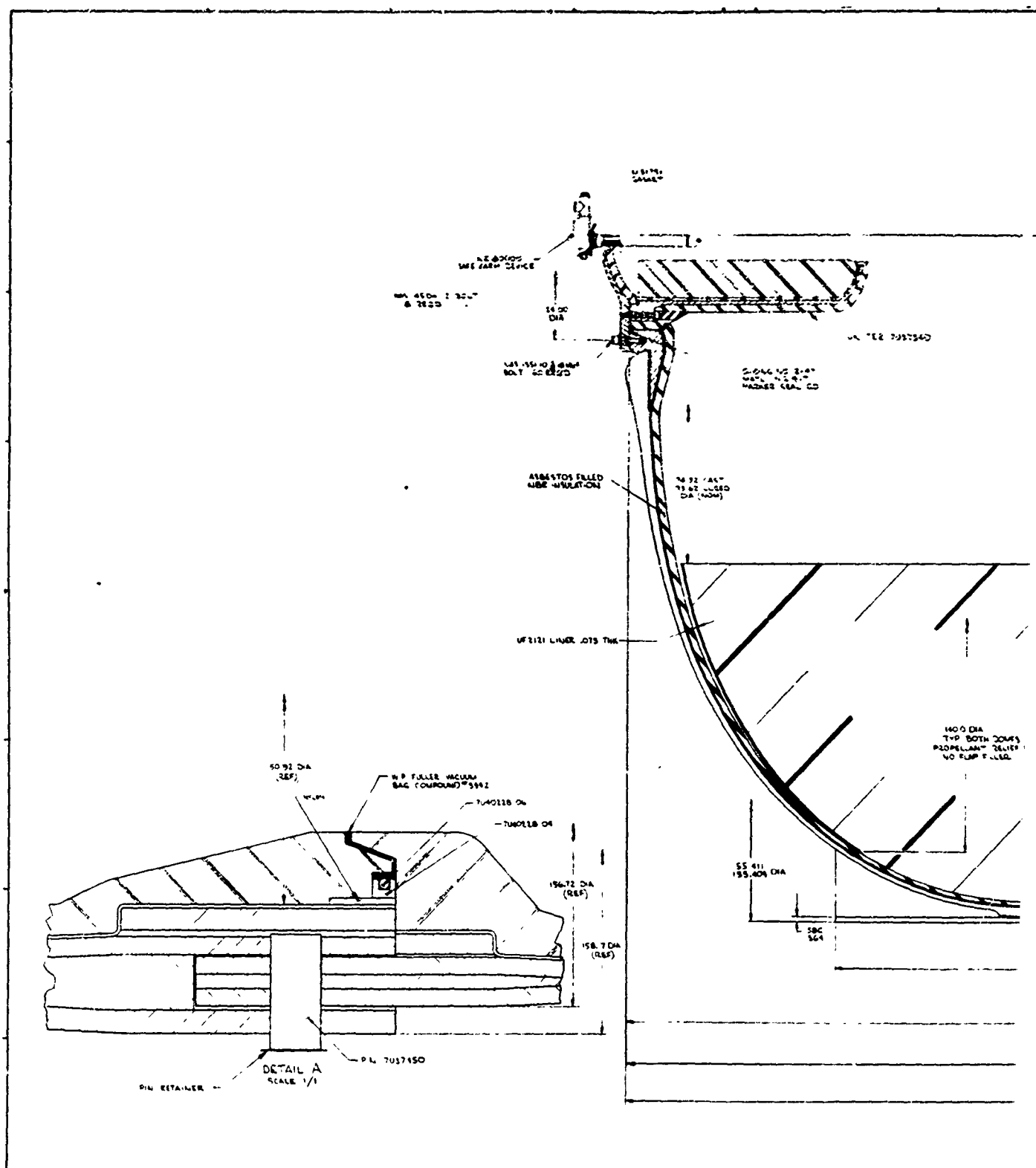
A. INTRODUCTION

This Quarterly Technical Progress Report reviews the work accomplished by Thiokol Chemical Corporation between 2 May and 31 July 1966 for the Air Force Rocket Propulsion Laboratory under Contract AF 04(611)-11603. The primary objective of this program is a demonstration static test firing of a segmented, flight-weight, 156 in. diameter, solid propellant motor (designated 156-8).

The demonstration motor described above will consist of a segmented fiber-glass case fabricated under Air Force Materials Laboratory Contract AF 33(657)-11303, with internal insulation, a segmented propellant grain, a head end ignition system, and a fixed ablative nozzle fabricated under Air Force Materials Laboratory Contract AF 33(657)-11301. The 156-8 motor (Figure 1) is designed to operate for approximately 120 sec and produce an impulse of approximately 120×10^6 lb-sec.

This report provides a discussion on progress to date on the following major areas of the program.

1. Design, fabrication, and test of a subscale vessel for the demonstration of a sealing concept for the segmented fiberglass case joints.
2. Replacement of the bladder in the segmented fiber-glass case.



10756 7057940

164" CAST
1650 LUGS
DIA 100"

164" CAST
1650 LUGS
DIA 100"

164" CAST
1650 LUGS
DIA 100"

80 0

1400 DIA
TYP. BOTH ZONES
PROPELLANT DEL. FLAP
NO FLAP T. LUGS

156 5
DIA

PROPELLANT DEL. FLAP
NO FLAP T. LUGS
1650 LUGS
DIA 100"

7057330 CASE, FWD SEC

161.890
162.770

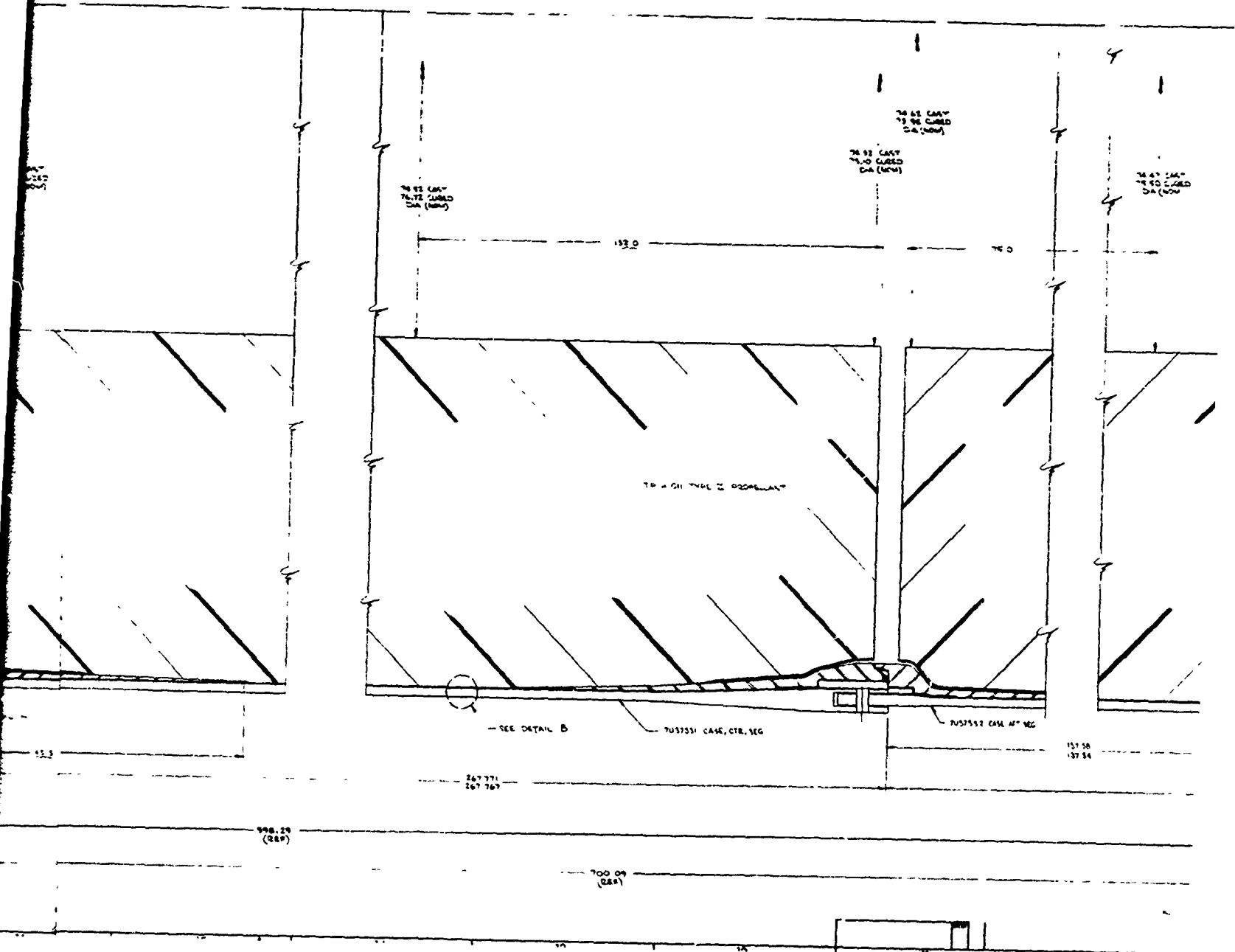
162.2070 DIA

161.815
162.750

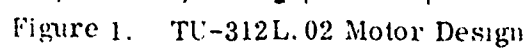
45.5

15.5

2



3



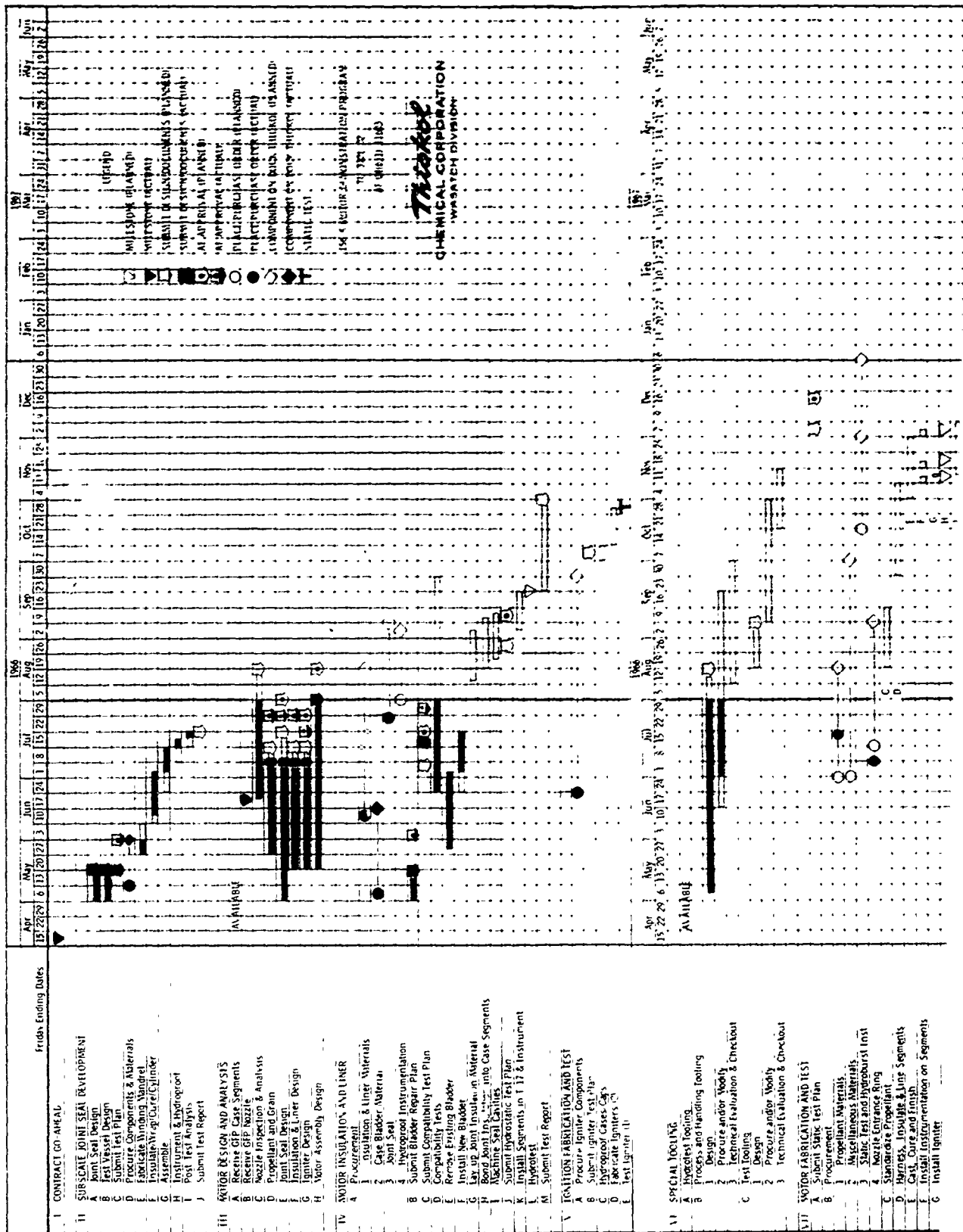
3. Design of the 156-8 motor, including the
 - (a) joint seal, (b) insulation and liner,
 - (c) propellant grain, and (d) ignition system.

B. SUMMARY

Work on the major areas tabulated above was completed during this quarter in accordance with the program schedule shown in Figure 2. All motor and component design effort was completed and all designs were transmitted to AFRPL for review and/or approval in accordance with the reports and documents shown in Figure 3.

The subscale demonstration vessel for the joint seal concept for the segmented fiberglass case was designed, fabricated, and successfully hydrotested to 1,100 psig. The vessel consisted of two open end 16 in. diameter steel cases fitted with fiberglass sleeves containing insulation cross sections the same as those designed for the 156 in. diameter case. The two cases were bolted together (end to end) with the joint seal located in the insulation. The subscale vessel was successfully tested three times. Each test consisted of two pressurizations to 1,100 psig for 120 seconds. The design, fabrication, and test of the subscale vessel is discussed in Section IV, Joint Seal.

The segmented fiberglass case was designed by Thiokol and fabricated by B. F. Goodrich Co under Contract AF 33(657)-11303 and is provided GFP to this program. Inspection of the case following hydrotest revealed a general unbonded condition between the fiberglass laminate and the rubber bladder. The unbonded condition, which was caused by two to three layers of dry fiberglass roving directly under the bladder, would have prevented adequate propellant bonding; therefore, the case bladder was removed from each case segment along with the dry fiberglass roving. A maximum of 2 1/2 layers of longitudinal glass and one layer of circumferential glass was removed from any one segment. Although the removal of some of the structural material reduced the safety factor, adequate safety factor remains because the case was originally designed for a burst pressure of 1,200 psig with a



Thiokol
CHEMICAL CORPORATION
MARS ROVER DIVISION

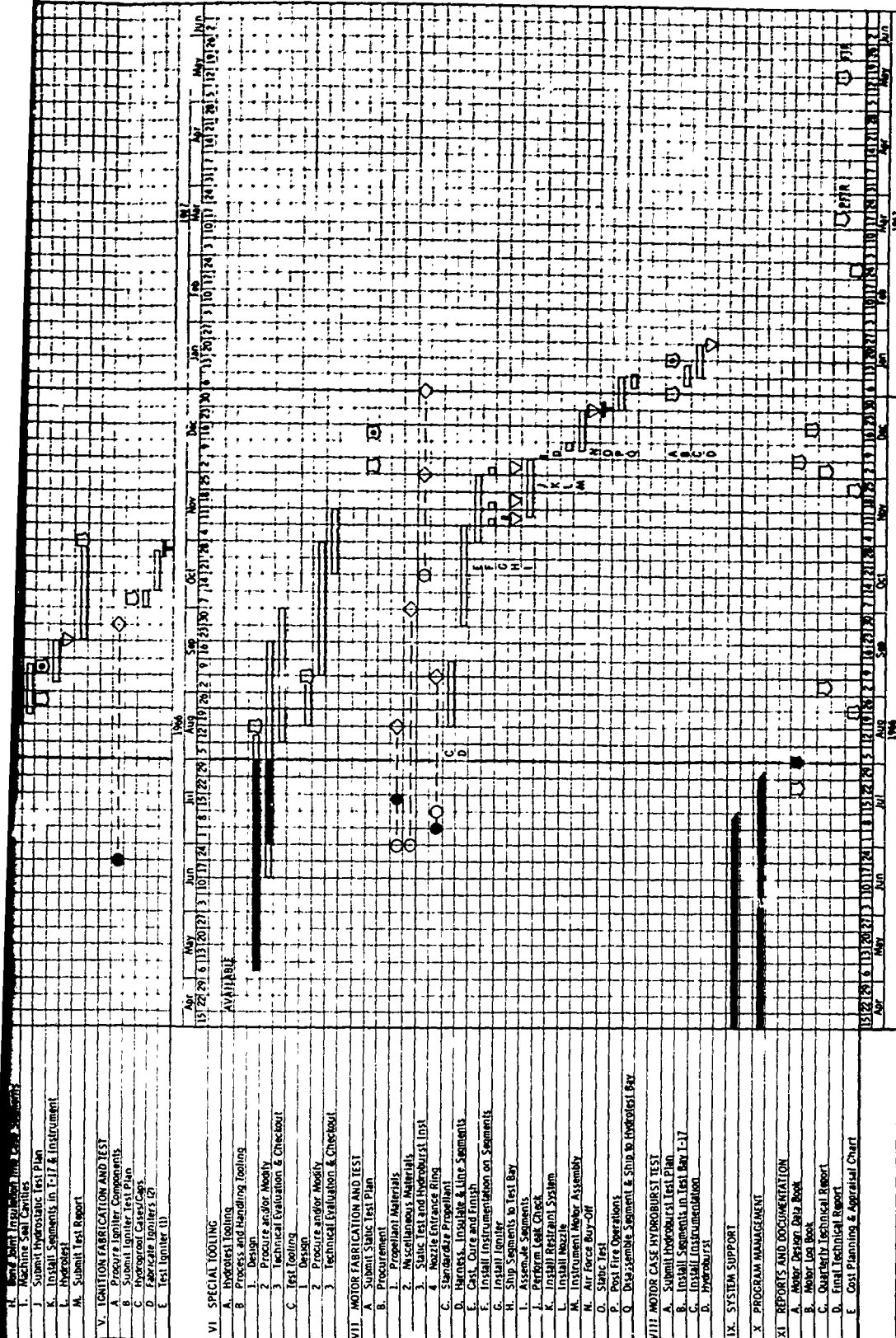


Figure 2. Program Schedule

2

REPORTS AND DOCUMENTATION
AF 04 (611)-11603
TU-312L.02

Thiokol
CHEMICAL CORPORATION
WASATCH DIVISION

DD-1423 LINE ITEM NO.	TITLE	DUE DATE FREQUENCY	AIR FORCE APPROVAL REQ'D DATE REQUIRED	AUTHORITY AFSCN 310-1	MAY	JUN	JUL	AUG	SEP	OCT	NOV
1	STILL PHOTO COVERAGE	END OF MONTH + 5 DAYS	NO	H-32-15.0				9 AUG			
2	MOTION PICTURE COVERAGE	END OF MONTH + 10 DAYS	NO	H-34-15.0							
3	DRAWINGS			E-13-21.0-1							
	A. MOTOR ASSEMBLY		YES				20 JUL	18 AUG			
	B. LOADED CASE		YES				1 JUL	10 JUL			
	C. INSULATED CASE		YES				1 JUL	5 AUG			
	D. IGNITER		YES				1 JUL	15 JUL			
	E. JOINT SEAL DESIGN		YES	S-10-20 MAY			1 JUL	10 JUL			
4	MOTOR DESIGN DESIGN DATA BOOK	18 JULY ONE TIME	REVIEW ONLY	C- -40.1				1 AUG			
5	DETAILED TEST PLANS	TEST-20 DAYS		T- -20.0	13 MAY						
	A. SUBSCALE JOINT SEAL DEVELOPMENT		YES		20 MAY						
	B. COMPATIBILITY TEST PLAN		YES				12 JUL	20 JUL			
	C. HYDROSTATIC TEST PLAN		YES					10 AUG			
	D. IGNITER TEST PLAN		REVIEW								
	E. MOTOR STATIC TEST		YES								
	F. HYDROBURST TEST PLAN		YES								
6	MOTOR LOG BOOK	INCREMENTALLY	YES	C- -44.0							
	A. FINAL RECEIVING INSPECTION FOR INSULATED AND LINED CASE										
	B. FINAL RECEIVING INSPECTION FOR THE LOADED CASE										
	C. FINAL RECEIVING INSPECTION FOR THE IGNITION SYSTEM										
	D. FINAL RECEIVING INSPECTION FOR THE COMPLETED MOTOR	TEST-7 DAYS									
8	STATIC TEST REPORTS			T-20-20.2							
	A. SUBSCALE JOINT DEVELOPMENT TESTS										
	B. COMPATIBILITY TESTS										
	C. CASE HYDROPROOF TEST										
	D. STATIC TEST QUICK LOOK										
	E. STATIC TEST REPORT										
	F. HYDROBURST										
9	TECHNICAL REPORTS			S-17-12.0-1							
	A. QUARTERLY TECHNICAL REPORT	END OF QUARTER + 30 DAYS	REVIEW FIRST QTR								
	B. FINAL TECHNICAL REPORT (DRAFT)	14 MAR '67	YES								
	C. FINAL TECHNICAL REPORT (FINAL)	12 MAY '67	NO								
10	COST PLANNING APPRAISAL CHART	END OF QUARTER + 20 DAYS	NO	A-15-17.0							
	OTHER REQUIRED SUBMITTALS										
	A. NOZZLE DESIGN REVIEW AND ANALYSIS RECOMMENDATIONS										
	B. BLADDER REPAIR PLAN		YES		13 MAY	24 JUN	18 JUL				
					20 MAY						

LEGEND

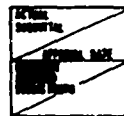
[illegible]

Figure 3. Reports and Documentation List

2

factor of safety of 1.2 and will be operated at a maximum pressure of 380 psig during static firing. A summary of the original case design and a complete discussion of the repair work performed is contained in Section II, Case.

The GFP nozzle designed and fabricated by Thompson Ramo Wooldridge Inc under Air Force Materials Laboratory Contract AF 33(657)-11301 was delivered to the Wasatch Division on 17 June 1966. The nozzle is being stored until handling tooling can be modified. A summary of the nozzle design is contained in Section III, Nozzle.

The joint seal concept, which was successfully demonstrated in subscale tests, consists of a spring loaded channel embedded in the asbestos filled NBR joint insulation. Although it was demonstrated in the subscale tests that the channel provides adequate sealing by itself, Thiokol plans to use vacuum compound in the joint, in addition to the channel seal, to provide thermal protection of the seal. Section IV, Joint Seal, contains a detailed discussion of the seal design.

The insulation for the 156-8 motor consists of asbestos filled NBR in the head-end, aft dome and joint areas and a silica/phenolic aft case insulation ring at the entrance to the nozzle. The asbestos filled NBR will be laid up in uncured sheets in molds, autoclave cured, and then bonded into the case segments. The insulation design uses a minimum factor of safety of 1.5. The silica filled NBR bladder in each case segment has not been included as part of the insulation thickness for design consideration. Insulation erosion rates and char rate data from various large motor firings have been used to optimize the insulation thickness design. The insulated segment case will be hydrostatically proof tested to MEOP (880 psig) prior to the lining and casting operations to assure functioning of the seal. In addition to the silica NBR bladder in each segment, only the joint insulation, which is required because of the joint seal requirements, will be installed in the motor case prior to hydrotesting.

UF-2121 liner material will be used in the 156-8 motor to provide the required propellant-insulation bond. This liner system is the standard Stage I MINUTEMAN liner, which has been successfully used on both the 156-1 and 156-7 demonstration motors. A verification test program will be conducted to verify the bond strength of the case insulation/liner/propellant interface with the actual materials that will be

used in the 156-8 motor. The case insulation and bladder surface will be primed with Koropon prior to applying the 0.060 in. minimum liner coating. A detailed discussion of the insulation and liner design is contained in Section V, Insulation and Liner.

A PBAA type propellant (designated TP-H1011) was selected for the 156-8 motor. This propellant is the same type used in the Stage I MINUTEMAN motor. Propellant materials have been ordered and propellant standardization will be conducted during the next quarter. The grain design incorporates a segmented, cylindrical perforated (CP) configuration. Propellant relief flaps are provided at both ends of each propellant segment. Propellant design data are presented in Section VI, Propellant and Grain.

The ignition system for the 156-8 motor will be a head end PYROGEN igniter. Two igniters will be fabricated: one for verification testing, the other for demonstration testing. A detailed discussion on the ignition system design is found in Section VII, Ignition System.

SECTION II

CASE

A. CASE DESIGN SUMMARY

1. DESIGN CRITERIA

The TU-312 rocket motor case has three filament wound, glass reinforced plastic segments designed for assembly at the test site.

The segmented case was designed for an internal ultimate pressure of 1,200 psig with a minimum positive factor of safety of 1.20 (factor of safety is defined as the strength of structure divided by the stress at design ultimate). A thrust loading of 1,600,000 lb at an internal chamber pressure of 1,200 psig was used for the design of the thrust skirt.

2. STRUCTURAL

The basic glass-resin structure is composed of S-994 HTS glass fibers and a resin system of Epon 826/NMA/DMP-30.

Glass strengths of 335,000 psi and 301,500 psi were used in the analysis for hoop and longitudinal glass requirements, respectively. The resin bulk factors for a 25 ± 2 percent resin content by weight were 1.7 for hoop glass and 2.0 for helical and polar glass, as well as for local longitudinal reinforcing glass. The band density was 170 ends/in.

The segments are assembled by means of mating clevis/tongue/pin joints. The tongue and clevis structures (composed of AM-355 steel sheet and fiberglass laminates) were designed to be critical in bearing. The design was based upon the

assumption that the most adverse tongue in clevis tolerance condition would be realized at some point on the joint circumference. The pin was designed to withstand shear and bending loads. The pin holes were match bored, and close tolerance pins were utilized.

The polar openings in the forward and aft domes are reinforced with forged 2014-T6 aluminum alloy rings.

The skirts on the forward and aft segments have identical thickness and composition because of a manufacturing feasibility of simultaneously winding the skirts. The thickness was determined from the loading induced on the forward skirt by the simulated thrust load and the weight of water incurred during hydrotest. An elastomeric material, Buna-N rubber, was bonded between the skirt and the dome to provide load transfer compatible with case deformation.

The design is summarized below by listing pertinent margins of safety.

Case wall, hoop glass

Forward segment	÷ 0.20
Center segment	+ 0.20
Aft segment	+ 0.21

Joint

Tongue	+ 0.27
Clevis	+ 0.21
Pin	>+ 0.20

Polar ring

Forward	+ 0.22
Aft	+ 0.56

Skirt

Compression	+ 0.75
Forward attachment	+ 0.54
Aft attachment	+ 1.11

3. HYDROTEST

The first TU-312 case hydrotest (conducted on 24 Aug 1965) developed a leak at the forward case joint at a pressure of 155 psig. Pressure was reduced immediately and the planned hydroproof test was aborted. Inspection of the case interior revealed that the bladder was torn in the area of the internal hoop ring on the forward segment clevis joint.

On 1 Oct 1965, the case was retested after additional seal material was installed at each joint. The case was pressurized to the hydroproof pressure of 977 psig at the rate of 6.5 psig/sec. After the pressure was held at 977 psig for 48 sec, the forward skirt crumpled just below the attachment shear ply. Since the failed skirt continued to transmit the 1,700,000 lb thrust and weight loading, the hydroproof pressure was held for the remainder of the scheduled 2 min cycle. Pressure was then reduced at the rate of 7 psig/sec.

Except for the skirt failure, the case performed as expected during the hydrostatic test. The joints showed no delamination or bearing deformation in the shim composite. The forward dome was crazed meridionally; however, cyclic tests of small pressure vessels, on which similar craze marks were found, have shown that any detrimental effect resulting from crazing is minor. The test verified the manufacturing methods, controls, and processes used to fabricate the segment joints and bond the skirts to the case.

A post test examination of the failed skirt revealed that the inner 0.16 in. (29 percent) of the skirt laminate was delaminated and had little longitudinal stiffness. The loss of 29 percent of the skirt laminate was responsible for the failure.

A skirt to replace the failed forward segment skirt was designed and wound at the Thiokol filament winding facility in Pocatello, Idaho, using U.S. Polymeric XF-7030 preimpregnated roving. The skirt was bonded onto the forward segment with a room temperature curing adhesive after removal of the failed skirt. The segments were reassembled into the hydrostatic test stand, instrumented, and successfully

hydroproof tested on 29 Mar 1966. An average hydroproof pressure of 980 psig was held for 123 sec, with a peak pressure of 1,003 psig occurring 7 sec after the start of the proof pressure hold.

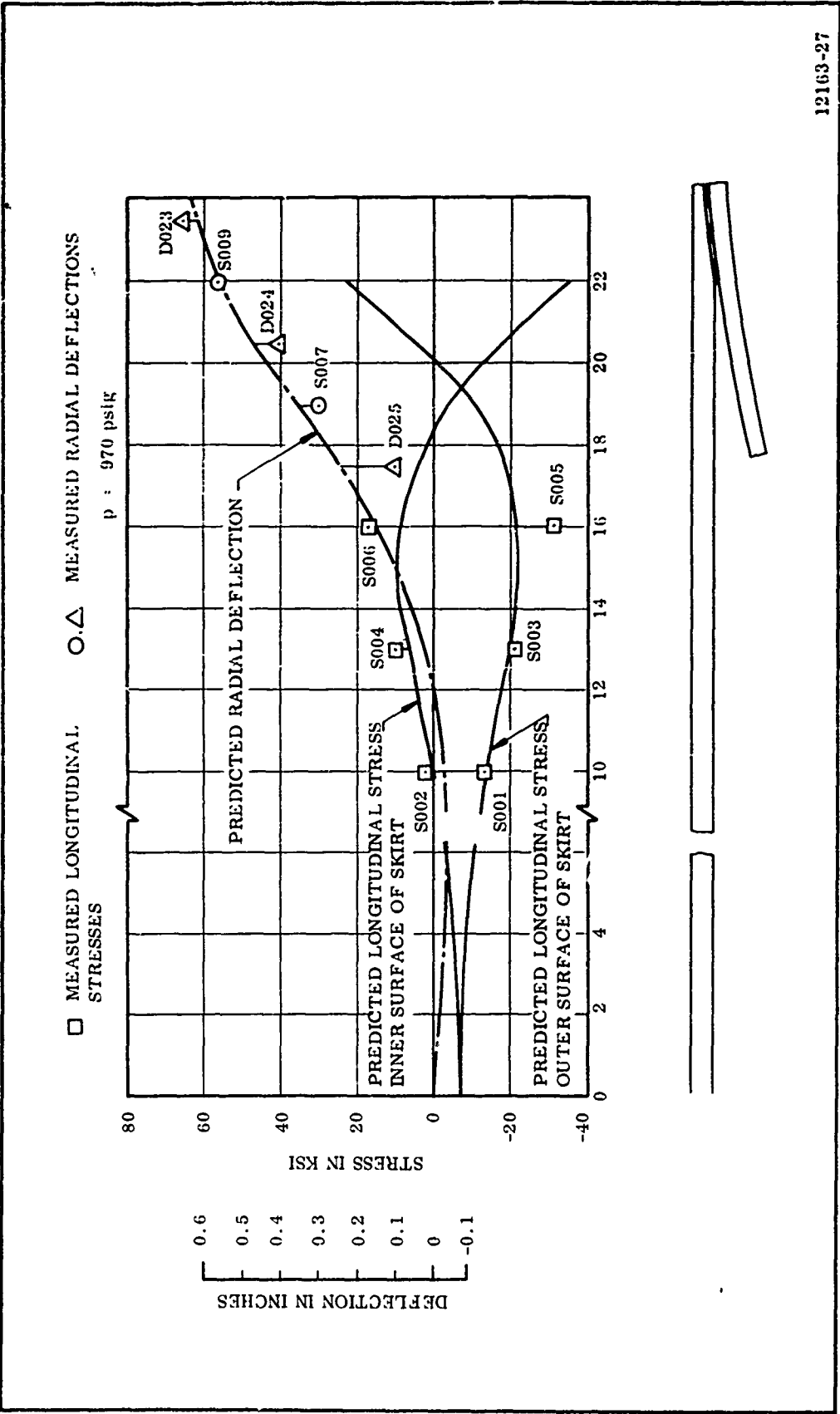
a. Forward Skirt Stresses and Deflections--Longitudinal strains were measured on both the inner and outer surfaces of the skirt at three stations to evaluate the bending effects. Circumferential strains and circumferential deflections were recorded at four additional stations, yielding added information concerning the deflections of the skirt under load.

The measured longitudinal strains were converted to stresses to permit a comparison with predicted stresses. The curves of calculated stresses and the stresses converted from longitudinal strain readings are shown in Figure 4. Predicted radial deflections and radial deflections converted from strain and extensometer readings are also shown.

Analysis of the differences between predicted and measured stresses and deflection showed that the skirt bends more sharply than predicted. Radial deflections imposed on the skirt by the case do not extend as far forward in the skirt as predicted, and bending effects are correspondingly higher. The differences between predicted and measured values are believed to be due to the "beam-column" effect, which is not included in the analysis.*

b. Radial Deflections--Circumferential extensometer readings of measured circumferential expansion were taken at 12 stations. Circumferential strains were measured at six additional stations. The circumferential deflections and strains were converted to radial deflections and are shown, with a side view of the case, in Figure 5. Note that where strain and extensometer readings were taken at essentially the same location, the extensometers indicated smaller deflections. The differences may have resulted from stretching the extensometer cables encircling the case or inaccuracy in the strain gage calibration factor.

*Large Segmented, Fiberglass Reinforced, Plastic Rocket Motor Cases, (U).
Interim Engineering Progress Report IR-8-150 (No. X).



12163-27

Figure 4. Longitudinal Stresses and Radial Deflections of TU-312.01 Forward Skirt

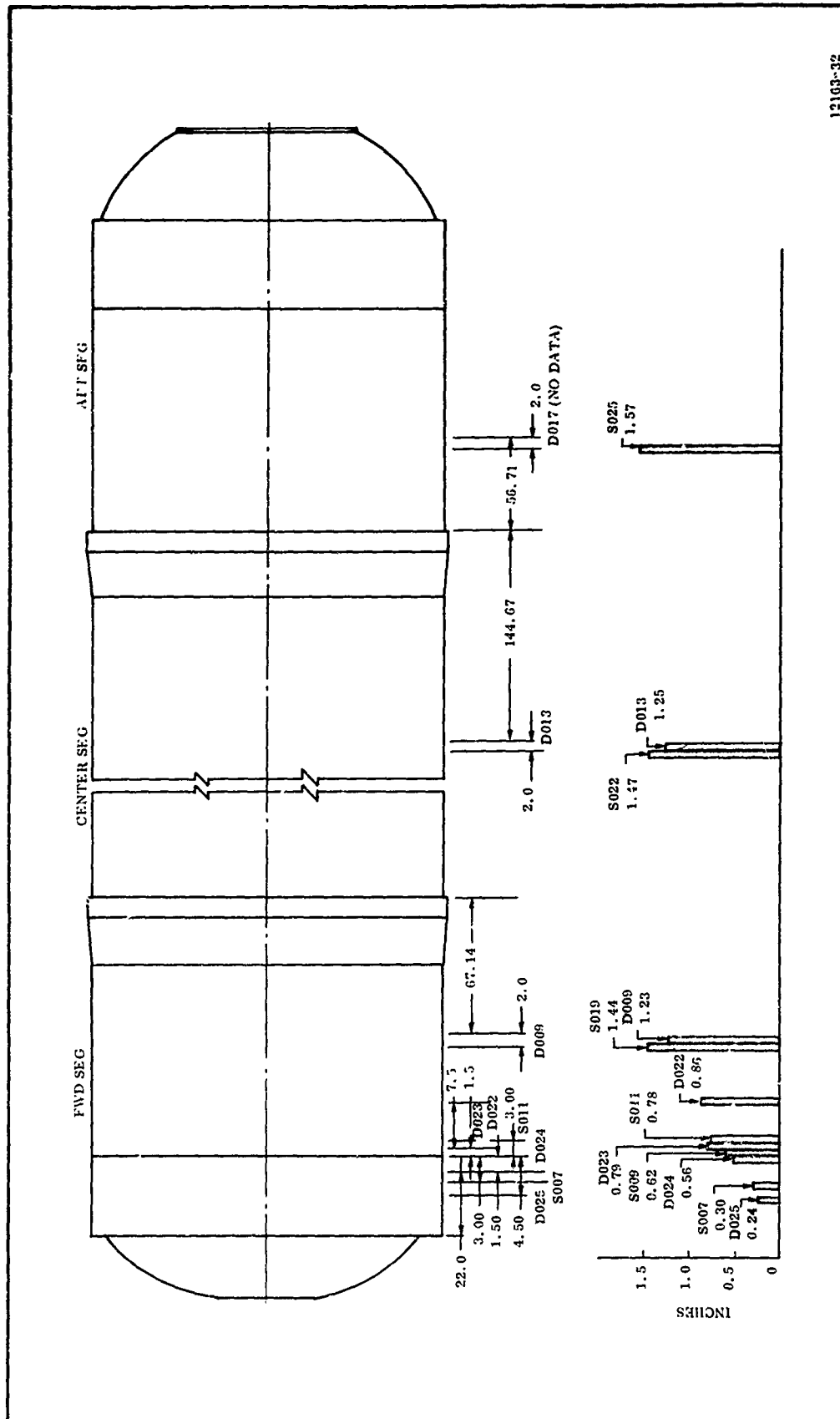


Figure 5. Radial Deflections at 1,000 psi

Radial deflections in the immediate areas of the joints are shown in Figure 6. These deflections are particularly gratifying because they are equal to the extensometer deflections in the centers of the segments and do not show any significant differences between the three stations at each joint. These data are considered conclusive evidence that the design objective of providing equal circumferential stiffness between joint areas and the basic segment walls was achieved.

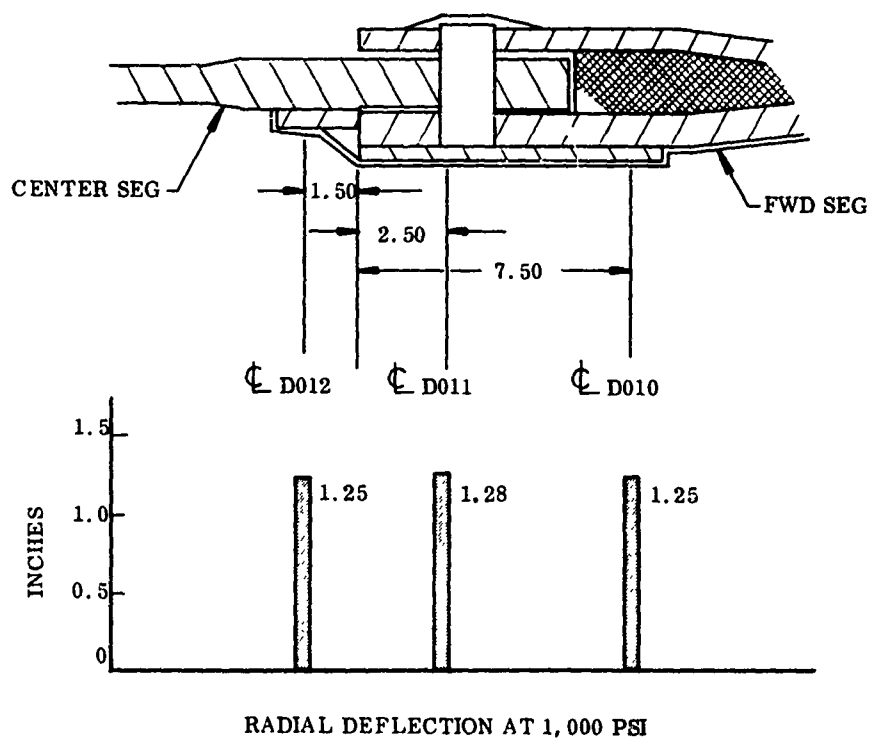
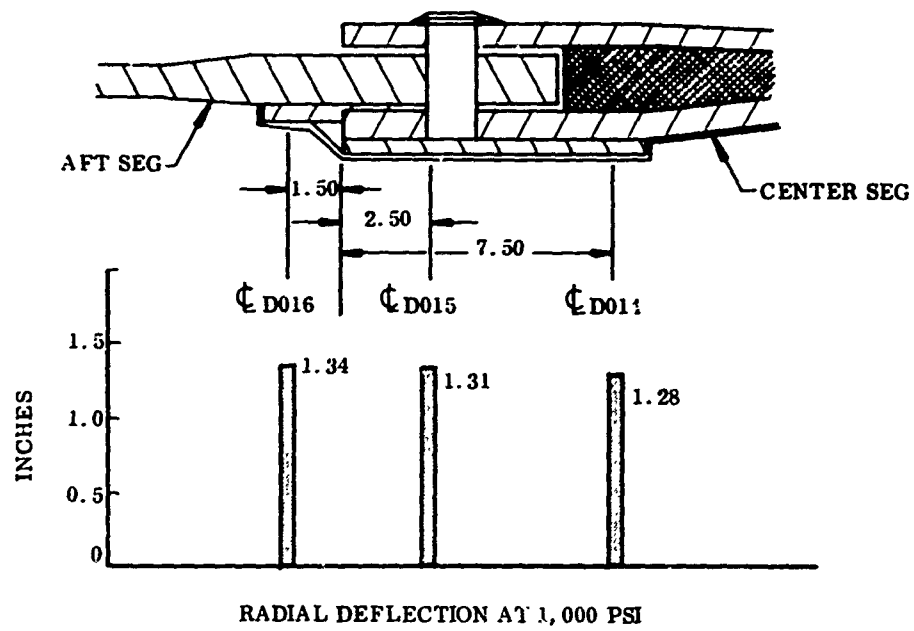
4. BREAKOVER LOADS

The analysis indicated that loads encountered during segment breakover were the most critical. For both of the end segments, the weakest areas were the bushings in the skirts (bearing loads due to transverse shear) and the rubber shear ply between the skirt and case (shear loads due to axial compression loads on the skirt). Based on 1 g loads, the calculated factors of safety for the forward and aft segments are +4.9 and +5.4, respectively, for the axial loading. Extremely high factors of safety were found for the shear loading conditions. For the center segment, the weakest area appeared to be the basic cylinder walls under a compressive axial load. Again, based on 1 g loads, the computed factor of safety is +4.6.

Loading at breakover based on a 1 g load with the center of gravity vertically in line with the support lugs was the most severe condition.

The handling harnesses (Figure 7) utilized the basic box rings used for the 156-6 and 156-7 motors, and is depicted on Drawing 2U25191. The skirts end rings are the same as those for the 156-7 motor. Each consists of a continuous box ring with segment bracketry which attaches to the skirts.

The segment joint harness rings utilize a box ring which has two semicircular segments such that the complete ring can be removed for static test. The box rings attach to segmented bracketry which are used for potting the case in the round condition and attaches to a continuous ring joint protector. The joint protector does not engage the tongue or clevis joint but compresses on the end of the segment. Rounding screws are mounted in the segmented bracketry. When in the rounded condition, the cases are potted to the harness with "Epocast", an epoxy potting compound.



12163-33

Figure 6. Radial Deflections at Aft Joint (top) and Forward Joint

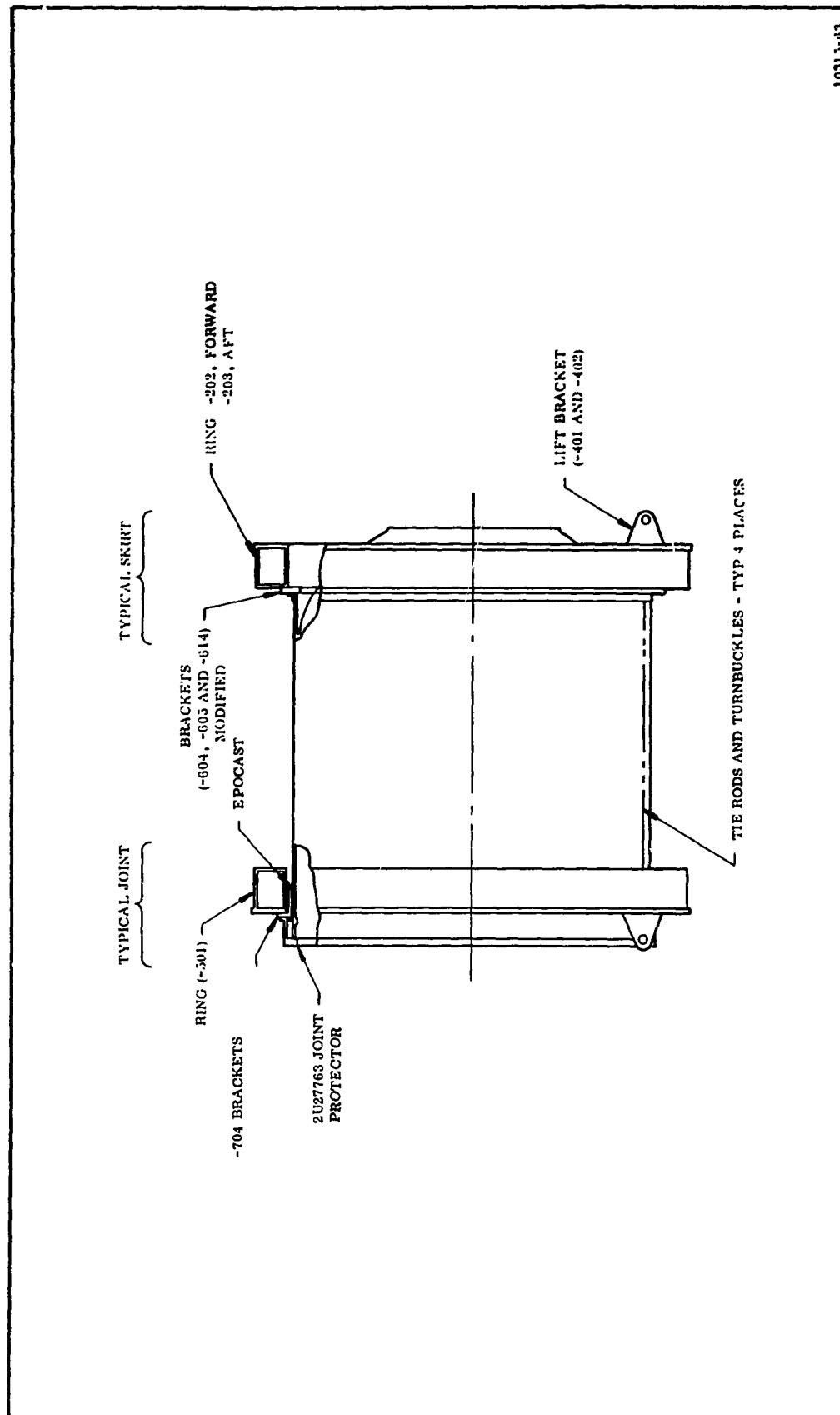
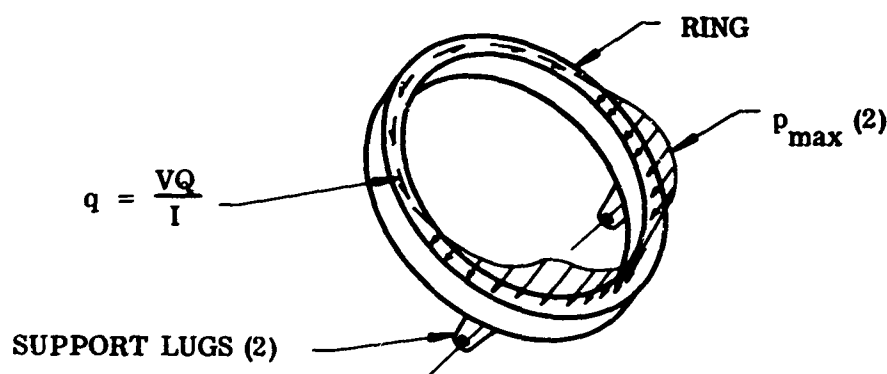


Figure 7. TU-312 Handling Harness

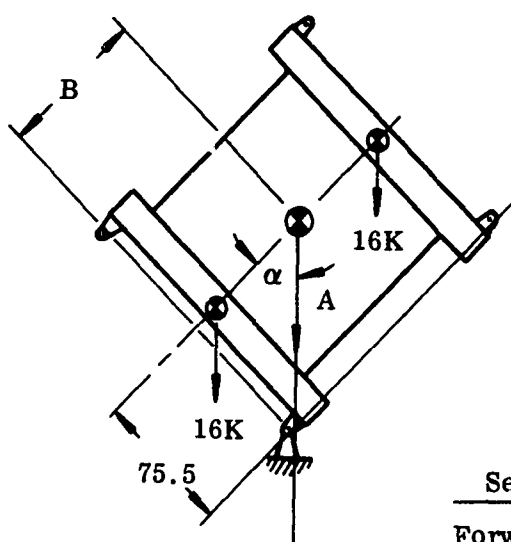
The harness rings on the ends of the segments are connected by eight tie rods, two in each of four locations. The tie rods are preloaded to provide for an axial compressive fit of the harness during handling of the loaded segments.

The handling load evaluations for the case are as follows:

Load Calculations



Pressure Profile Between Segment and Ring at Breakover

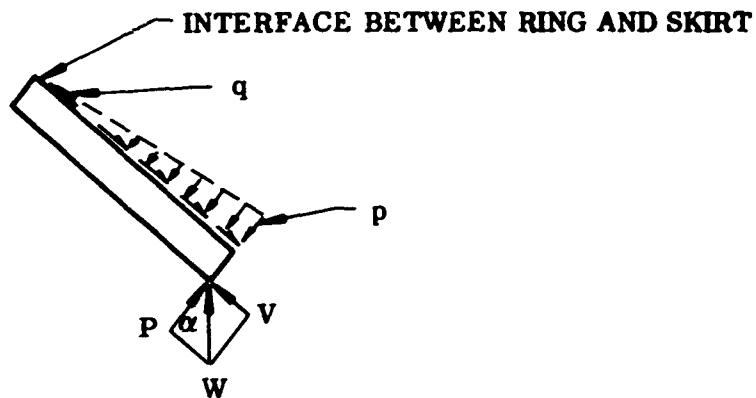


$$\alpha = \tan^{-1} \frac{75.5}{B}$$

Segment in Breakover Position

Seg	B (in.)	α
Forward	97	37° 58'
Center	139	28° 31'
Aft	81	42° 59'

Seg	COS	SIN
Forward	0.78837	0.61520
Center	0.87868	0.47741
Aft	0.73155	0.68179



Loading on Forward Ring

$$W = \frac{\epsilon \text{ Weight}}{\text{No. of Lugs}}$$

$$P = W \cos \alpha$$

$$V = W \sin \alpha$$

Seg	W lb/Lug	P lb/Lug	V lb/Lug	Pmax in. /lb
Forward	80,000	63,070	49,216	1,460
Center	134,000	117,743	63,973	3,091
Aft	77,500	56,695	53,614	1,312

$$P_{\max} = \frac{P\lambda}{2}$$

Damping function (λ) of the foundation.

$$\lambda = \sqrt[4]{\frac{K}{4EI_{x-x}}}$$

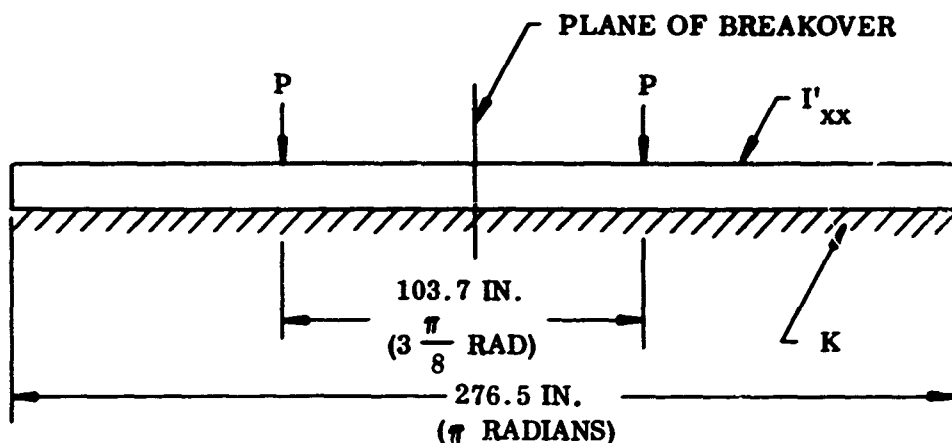
Where:

K = Foundation modulus

E = Modulus of elasticity of the beam

I_{xx} = Moment of inertia of beam in plane of
foundation per width of foundation

ANALYZED CONFIGURATION



Flat Pattern Layout of Ring (180 Deg Section)

$$I_{xx}^{FWD} = \frac{I_{xx}}{t_s^{FWD}} = \frac{3,275}{0.60} = 5,458 \text{ in.}^4/\text{in.} \quad (t_s = \text{skirt thickness})$$

$$I_{xx}^{AFT} = \frac{I_{xx}}{t_s^{AFT}} = \frac{3,275}{0.60} = 5,458 \text{ in.}^4/\text{in.} \quad \left(t_{SEG} = \text{thickness of segment wall} \right)$$

$$I_{xx}^{CTR} = \frac{I_{xx}}{t_{SEG}} = \frac{3,275}{1.0} = 3,275 \text{ in.}^4/\text{in.}$$

$$K = 3 \times 10^6 \text{ psi} = E\phi$$

$$E = 30 \times 10^6 \text{ psi}$$

$$\begin{aligned} \lambda^{AFT} = \lambda^{FWD} &= \left(\frac{K}{4EI_{xx}} \right) \frac{1}{4} = \left(\frac{3 \times 10^6}{4 \times 30 \times 10^6 \times 5,458} \right) \frac{1}{4} \\ &= \left(4.58 \times 10^{-6} \right) \frac{1}{4} = \left(2.14 \times 10^{-3} \right) \frac{1}{2} \\ &= 0.0463/\text{in.} \end{aligned}$$

$$\begin{aligned}
 \lambda_{CTR} &= \left(\frac{3 \times 10^6}{4 \times 30 \times 10^6 \times 3,275} \right) \frac{1}{4} = (7.63 \times 10^{-6}) \frac{1}{4} \\
 &= (2.76 \times 10^{-3}) \frac{1}{2} \\
 &= 0.0525/\text{in.}
 \end{aligned}$$

The shear load (v) is reacted by the bolts between the segments of the ring with the shear flow (q) of a $\frac{VQ}{I}$ type distribution.

It will be assumed that since the ring is very rigid, the shear flow (q) will be the same as if the total load (2v) were reacted at the mid point.

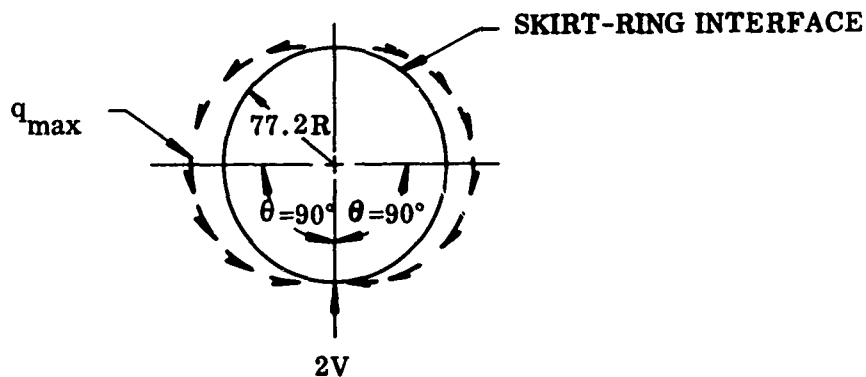
$$q = \frac{2 VQ}{I} = \frac{2 v \sin \theta}{\pi R_s}$$

Where:

θ = ARC distance from the mid point

R_s = Interface radius between the skirt and the ring

When $\theta \rightarrow 90^\circ$ $q \rightarrow q_{\max}$



$$q_{\max} \text{ FWD} = \frac{2 (49,216)}{\pi (77.2)} = 406 \text{ lb/in.}$$

$$q_{\max} \text{ CTR} = \frac{2 (63,973)}{\pi (77.2)} = 528 \text{ lb/in.}$$

$$q_{\max} \text{ AFT} = \frac{2 (53,614)}{\pi (77.2)} = 442 \text{ lb/in.}$$

The segment loading is summarized below.

<u>Segment</u>	<u>P_{max}</u> <u>lb/in.</u>	<u>q_{max}</u> <u>lb/in.</u>
Forward	1,460	406
Center	3,091	528
Aft	1,312	442

The segment allowable loads based on ultimates (weakest members) are summarized below.

<u>Segment</u>	<u>Load</u>		<u>Member</u>	
	<u>Shear</u> <u>lb/in.</u>	<u>Axial</u> <u>lb/in.</u>	<u>Shear</u>	<u>Axial</u>
Forward	15,936	7,200	Bushing	Shear ply (skirt attach)
Center	N/A	14,320	N/A	Cylinder
Aft	15,936	7,200	Bushing	Shear ply (skirt attach)

The factors of safety are shown below.

Axial

$$F.S. = \frac{N_s (ULT)}{P_{max}}$$

Shear

$$F.S. = \frac{F_B (ULT)}{q_{max} S_B}$$

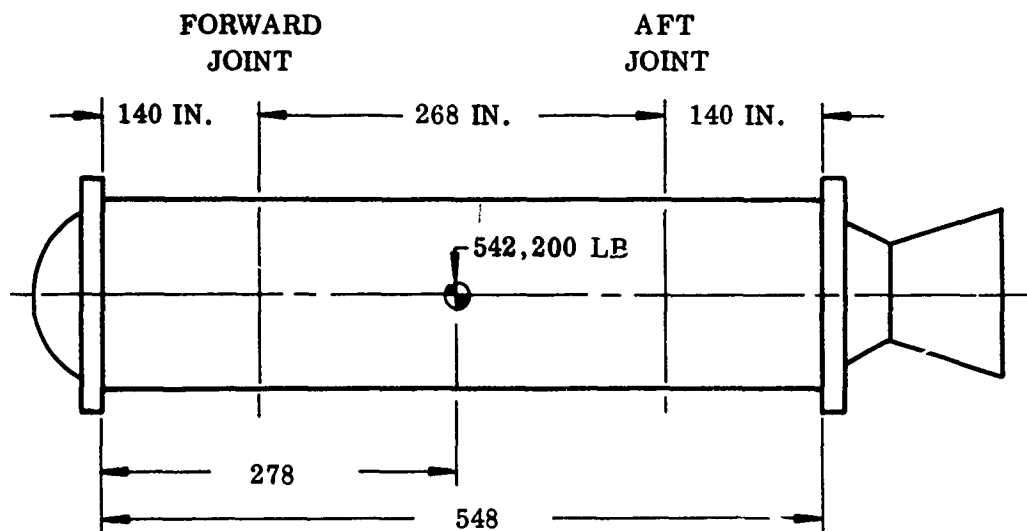
S_B = Bolt Spacing

<u>Segment</u>	<u>Axial</u>	<u>Shear</u>
Forward	+4.9	High
Center	+4.6	N/A
Aft	+5.4	High

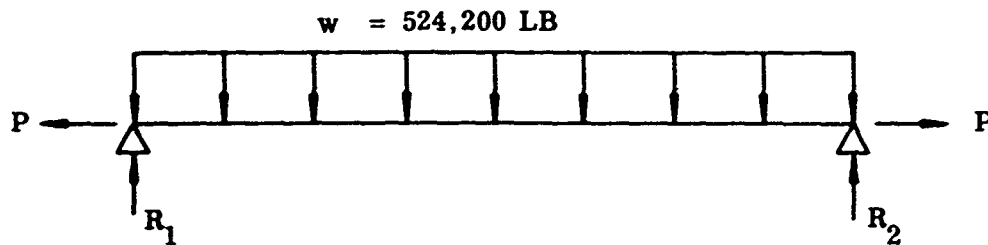
5. BENDING LOADS AND DEFLECTION AT HORIZONTAL POSITION

The case deflections during motor operation will reduce the actual longitudinal thrust measurements only 0.052 percent; however, a vertical component equal to 3.2 percent of the longitudinal thrust will be developed. This added vertical load (approximately 32,000 lb) is reacted by the aft motor support. The moment produced is transferred to the case through the aft skirt with a resultant stress level of 770 psi in the skirt just aft of the attachment. The structural analysis of this condition assumed an aft skirt effective thickness of 0.4 inch. The final conclusion as to the failure of the forward skirt during the hydrostatic test was that the skirt failed in buckling after the discontinuity loads had caused the inner skirt surface to delaminate, leaving an effective skirt thickness of 0.4 in. to carry the thrust and weight loading. Under these loads, the 0.4 in. thickness was critical in buckling. During motor operation, the loading on the aft skirt consists of the discontinuity stress induced by case pressure (28,000 psi) plus the stress induced by case deflection (770 psi) for a total stress of 28,770 psi. Since there is no axial load on the aft skirt, the stress is well below the compressive strength of the skirt laminate (60,000 psi), assuming an effective laminate thickness of 0.4 inch. Under this loading condition, a factor of safety in excess of 2.0 exists.

Loads and deflections are shown below.



Loads: (static)



$$R_1 = R_2 = \frac{1}{2} W = 262,100 \text{ lb} = V_1 = V_2$$

$$V_{\text{Center}} = 0$$

$$\begin{aligned} V_{\text{Fwd Joint}} &= \left\{ \frac{1}{2} W \left(1 - \frac{2X}{L} \right) = \frac{1}{2} 524,200 \left(1 - \frac{2 \times 140}{548} \right) \right. \\ V_{\text{Aft Joint}} &= \\ &= 128,183 \end{aligned}$$

Maximum moment: (at center)

$$M = \frac{1}{8} WL = \frac{1}{8} 524,200 \times 548 = 35,907,700 \text{ in. lb}$$

Moment at joints:

$$\begin{aligned} M &= \frac{1}{2} W X - \frac{WX^2}{L} = \frac{1}{2} 524,200 \cdot 140 - \frac{140^2}{548} \\ &= 27,319,621 \text{ in. lb} \end{aligned}$$

Deflection: (static)

Maximum (at center) -

$$Y_M = -\frac{5}{384} \frac{WL^3}{EI}$$

$$E_{\varphi} = 2.9 \times 10^6 \text{ psi}$$

$$I = \pi R^3 t = \pi 77.5^3 \times 1$$

$$= 1.462 \times 10^6 \text{ in.}^4$$

$$= \frac{-5}{384} \frac{0.5242 (548)^3}{2.9 \times 10^6 \times 1.462 \times 10^6}$$

$$= \frac{431.329}{1628.0832} = 0.265 \text{ in.}$$

At joints -

$$Y = -\frac{1}{24} \frac{WX}{EIL} (L^3 - 2LX^2 + X^3)$$

$$= -\frac{1}{24} \frac{0.5242 \times 0.00014}{2.9 \times 1.462 \times 548} (548^3 - 2 \times 548 \times 140^2 + 140^3)$$

$$= 0.192 \text{ in.}$$

Stresses:

At center -

$$\sigma_c = \pm \frac{M_c}{I_c} \pm \frac{V}{2\pi Rt}$$

$$= \pm \frac{35.9077 \times 77.5}{1.462} \pm 0$$

$$= 1900 \text{ psi}$$

At joints -

$$\sigma_j = \pm \frac{M_c}{I} \pm \frac{V}{2\pi Rt}$$

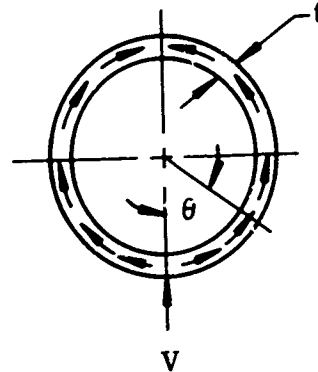
$$= \pm \frac{27.3196 \times 77.5}{1.462} \pm \frac{128,183}{2\pi 77.5 \times 1}$$

$$= 1,711 \text{ psi}$$

Shear Stress:

At joints -

$$\begin{aligned}\tau_{\max} &= \frac{VQ}{It} \\ &= \frac{V \sin \theta}{\pi R t} \\ &= \frac{128,123}{\pi 77.5 \times 1} \\ &= 526 \text{ psi}\end{aligned}$$



Load: (dynamic)

Maximum moment -

$$M = Wj^2 (1 - \operatorname{sech} \frac{1}{2} U)$$

Where:

$$j = \sqrt{\frac{EI}{P}} \quad U = \frac{L}{j}$$

$$w = \frac{W}{L} \text{ lb/in.}$$

$$\begin{aligned}P &= P_i \pi \left[R (1 + \epsilon) \right]^2 - T_N \\ &= 960 \times 3.1416 (77.5 \times 1.022)^2 - 1,280,000 \\ &= 17,640,269 \text{ lb} \\ j &= \sqrt{\frac{2.9 \times 10^3 \times 1.462}{17.64027}} \\ &= 490.25 \text{ in.}\end{aligned}$$

$$W = 957 \text{ lb/in.}$$

$$U = 1.119$$

Then:

$$\begin{aligned} M &= 957 \times 490.25^2 (1 - \operatorname{sech} 0.559) \\ &= 5,352,535 \text{ in. /lb} \end{aligned}$$

Deflection: (dynamic)

$$\begin{aligned} Y &= -\frac{W}{P} \left[\frac{1}{8} L^2 - j^2 (1 - \operatorname{sech} \frac{1}{2} U) \right] \\ &= -\frac{957}{17.64027 \times 10^6} \left[\frac{1}{8} 548^2 - 490.25^2 (0.13863) \right] \\ &= 0.229 \text{ in.} \end{aligned}$$

Stress (at center)

$$\begin{aligned} \sigma &= + \frac{M_c}{I} \\ &= \frac{5.353 \times 77.5 (1 + 0.022)}{1.462} \\ &= 290 \text{ psi} \end{aligned}$$

Shear Stress (handling rings)

$$\begin{aligned} \tau_{\max} &= \frac{VQ}{It} \\ &= \frac{262,100}{\pi 77.5 \times 0.602} \\ &= 1,788 \text{ psi} \end{aligned}$$

Only moderate stresses will be developed at the center of the assembled motor both prior to and during the firing. Prior to motor operation, a compressive stress of 1,900 psi will be developed at the center of the motor and 1,710 psi at the joints. A maximum deflection of 0.265 in. will be experienced midway between the end supports. During motor operation, the compressive stress at the case center due to motor weight only (pressure loads ignored) will be approximately 290 psi

with a deflection of 0.229 inch. These stress levels are very small and are well within the structural capabilities of the case segments.

The critical buckling stress for the center segment is P_{CR} 14,000 psi.

$$\begin{aligned} \text{F.S.} &= \frac{P_{CR}}{\sigma_{\max}} \\ &= \frac{14,300}{1,900} \\ &= +7.5 \end{aligned}$$

B. CASE REPAIR

1. REPAIR CONSIDERATIONS

The original bladder in the TU-312 motor case was found to be inadequately bonded to the basic wall structure of the segments. This condition was attributed to a lack of resin in the initial fiberglass layers at the segment inside diameters. A good bond must be maintained between the segment walls and bladder to support the propellant, which will adhere to the bladder when cast and cured.

A series of peel tests and visual inspections were made of each segment to determine the number of dry glass layers that existed and to find surfaces that would be adequate to meet structural bond requirements.

The removal of fiberglass material from segment walls results in lower factors of safety than indicated in the TU-312 case design report; however, the case was designed for an ultimate pressure of 1,200 psig with a minimum factor of safety of 1.2. Therefore, at the TU-312 maximum expected operating pressure (MEOP) of 880 psig adequate factors of safety will exist after case repair and the strength level of the segments, although reduced, will meet design requirements.

2. CASE REPAIR

The bladder was completely removed from the cylinder and domes of each of the three case segments except for a 14 in. strip at the joint ends of each segment. The original bladder was not removed in the joint areas to avoid disturbing the internal hoop rings in the segments. These rings provide the required hoop strength in the

joint areas and are also the mating surfaces of the segments. Therefore, it is essential that the hoop rings are not disturbed.

The 14 in. strip of original bladder was bonded back to the case wall by injecting UF-3119 between the bladder and case wall. The UF-3119 was then cured under vacuum at ambient temperature.

After bladder material was removed, the loose (unbonded) fiberglass in each segment was removed until a sound laminate was evident. The amount of glass requiring removal was different in each segment. In the forward segment, one layer of circumferential (hoop) windings and one layer of polar windings were removed from the cylinder. Two and one half layers of polar windings were removed from the forward segment dome, from the edge of the forward boss to the beginning of the cylinder.

One half layer of hoop windings and one layer of polar windings were removed from the center segment. In the helically wound aft segment, one half layer of hoop windings and two helical layers were removed from the cylinder. Two and one half layers of helical windings were removed from the aft dome, from the edge of the polar boss to the beginning of the cylinder.

To determine the bond strength to the fiberglass laminate following dry glass removal, four test plates (2 by 4 in.) were bonded in the cylindrical areas of each segment using UF-3119 and UF-3177 for tensile adhesion tests. Both formulations were cured under vacuum at ambient temperature. One sample plate of each formulation in each segment was step pulled as shown below.

<u>Step</u>	<u>Time (min)</u>	<u>Pressure (psi)</u>
1	1.0	10
2	1.0	20
3	1.0	30
4	1.0	40
5	1.0	50
6	1.0	60
7	1.0	70

The other test plate of each formulation was pulled for 1 min at 70 psi. All test plates passed the tensile adhesion test except the UF-3177 full load test plate in the center segment which failed after 57 sec at 70 psi. Inspection of the failed plate showed an actual bond area of approximately 4 square inches, indicating that failure had actually occurred above 100 psi. The tensile adhesion tests demonstrated that either UF-3119 or UF-3177 were adequate for bonding the replacement bladder into the segments. UF-3119 was selected because of superior working qualities.

Upon the successful demonstration of a sound fiberglass laminate to which a new bladder could be bonded with assurance of sufficient bond strength to support the propellant grain, bladder installation was initiated. The new bladder material, (General Tire and Rubber Co silica filled NBR (V-45) procured in 36 in. wide rolls) was wound onto a large (44 in. diameter) drum with Trevanno film between layers and autoclave cured.

The material was then cut into strips that extended the full length of the segments (Figure 8). The strips were bonded into the segments with UF-3119 by drawing a vacuum on both the inside of the segment over the bladder strip and on the outside of the segment behind the strip of bladder being installed (Figure 9). The configuration of the repaired case segments is shown in Figures 10, 11, and 12.

To verify that the required bond strength was obtained between the new case bladder and fiberglass laminate, two 2 by 4 in. test plates were bonded into the cylindrical section of each case segment after the bladder was installed. All test plates passed the tensile adhesion test of 70 psi for 1.0 min.

3. EFFECTS OF REPAIR ON CASE DESIGN STRENGTH

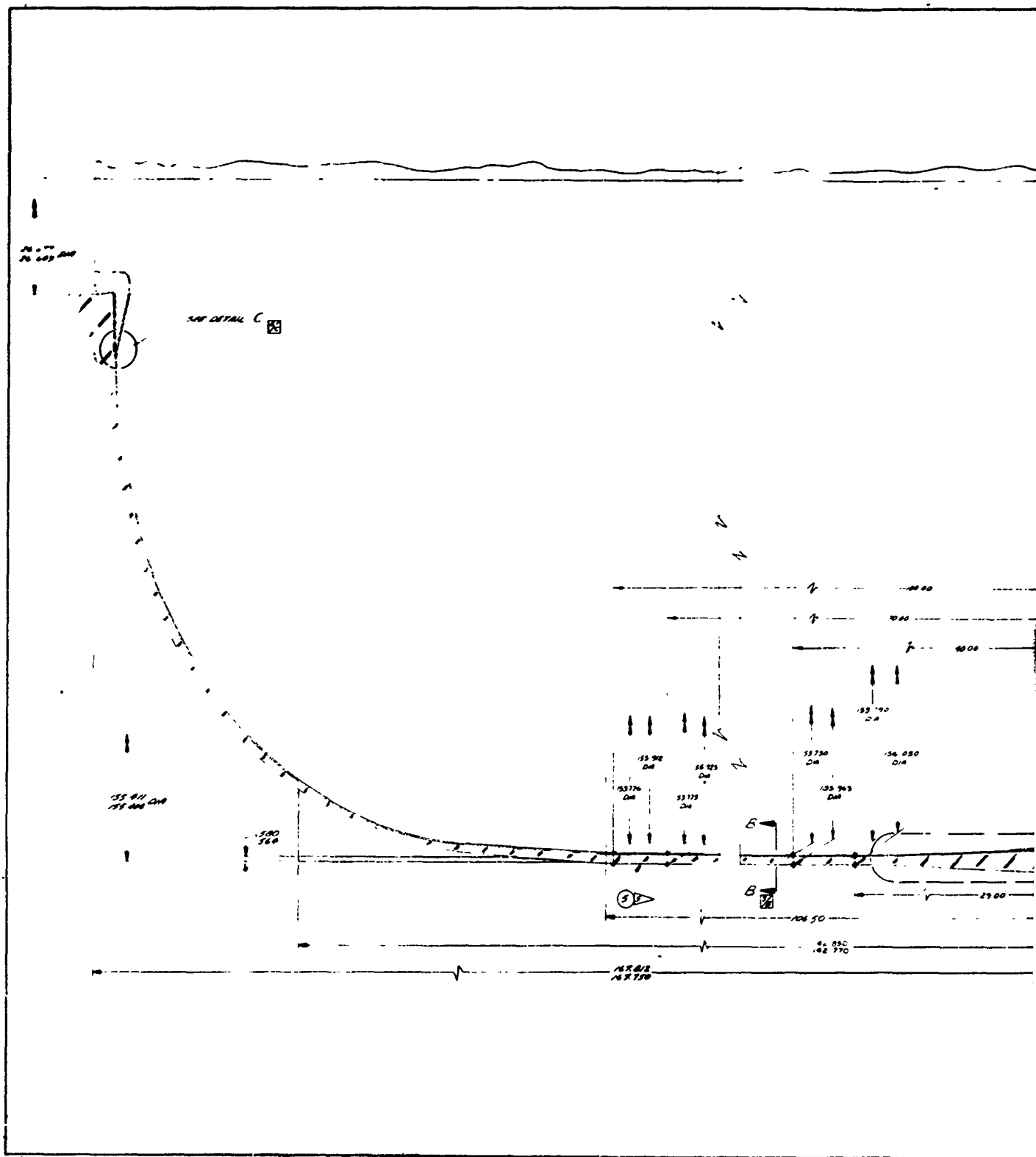
In addition to the case strength reduction resulting from the glass removal, other deviations occurred in handling and testing the case segments. The factors that caused degradation in the case strength are explained as follows.

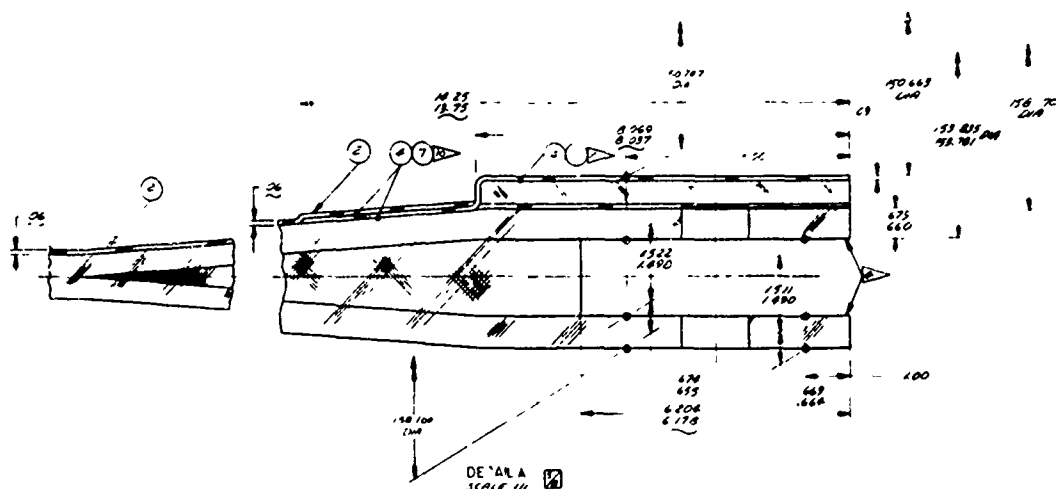
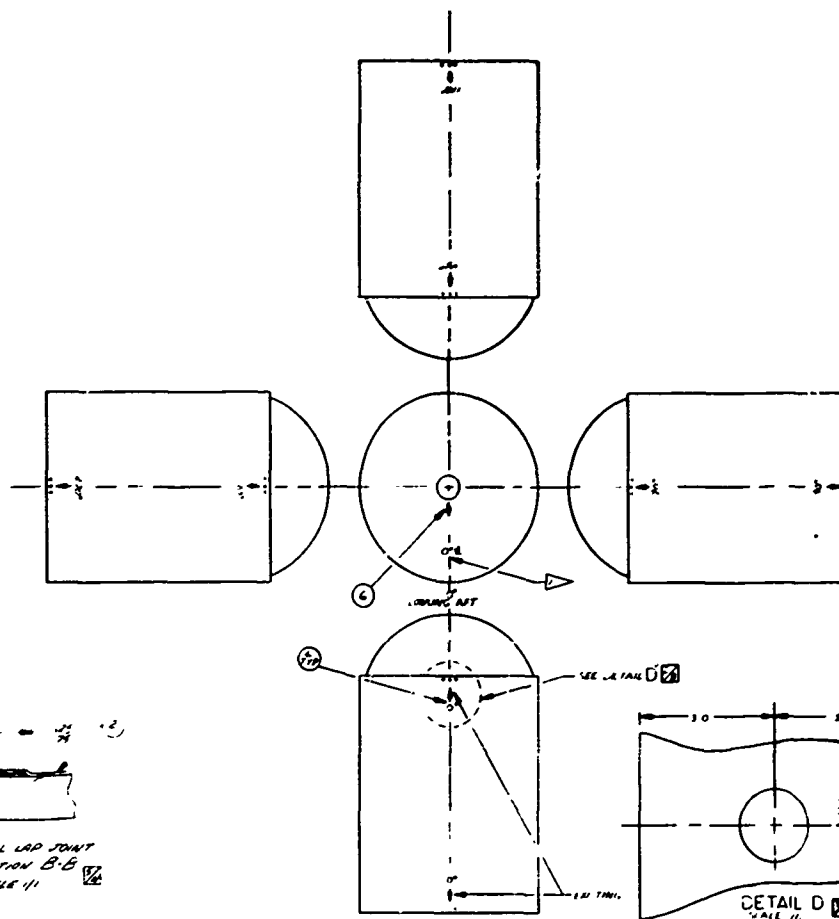


Figure 8. Replacement Bladder Partially Installed



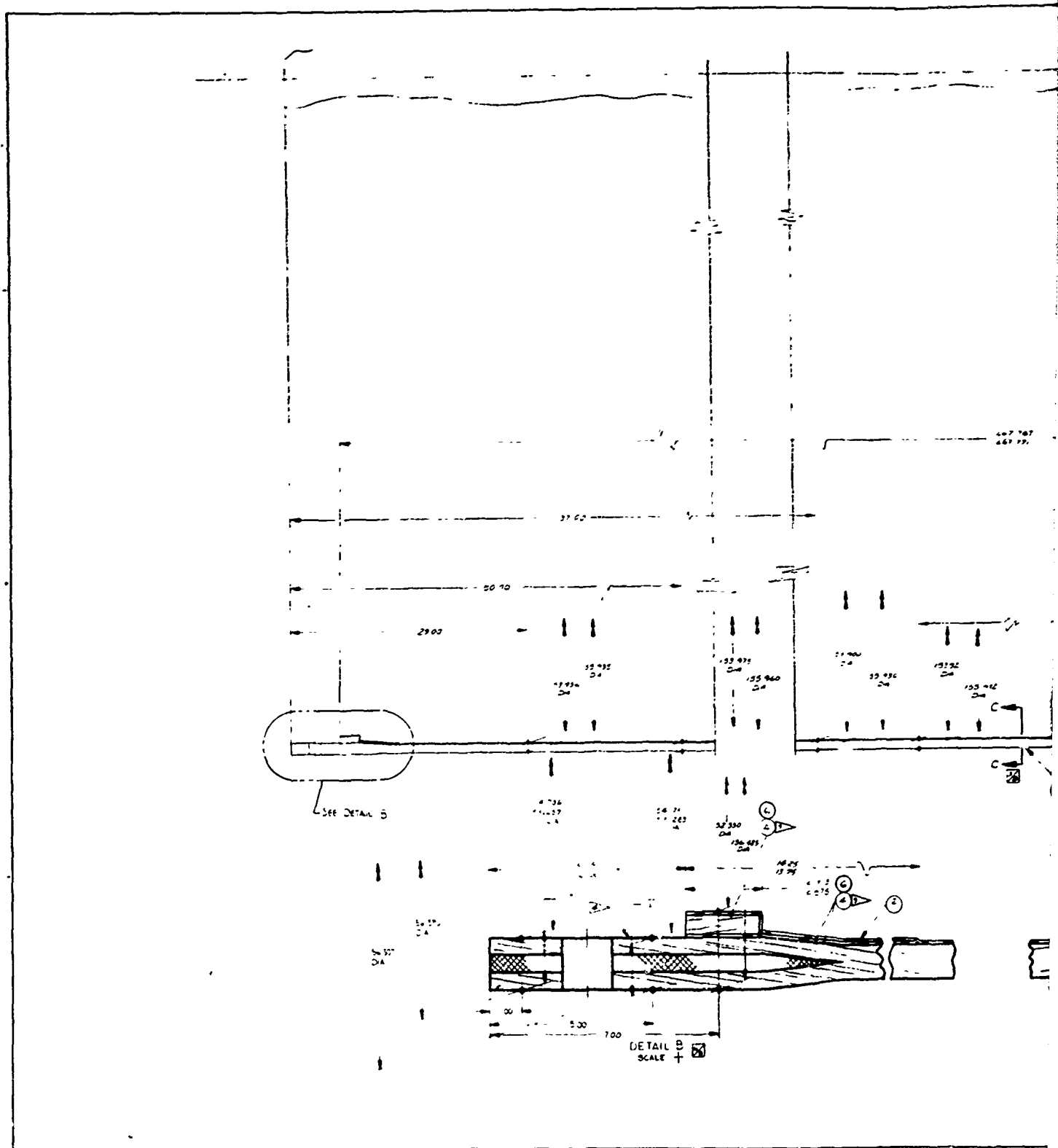
Figure 9. Vacuum Bag Installation Over Bladder

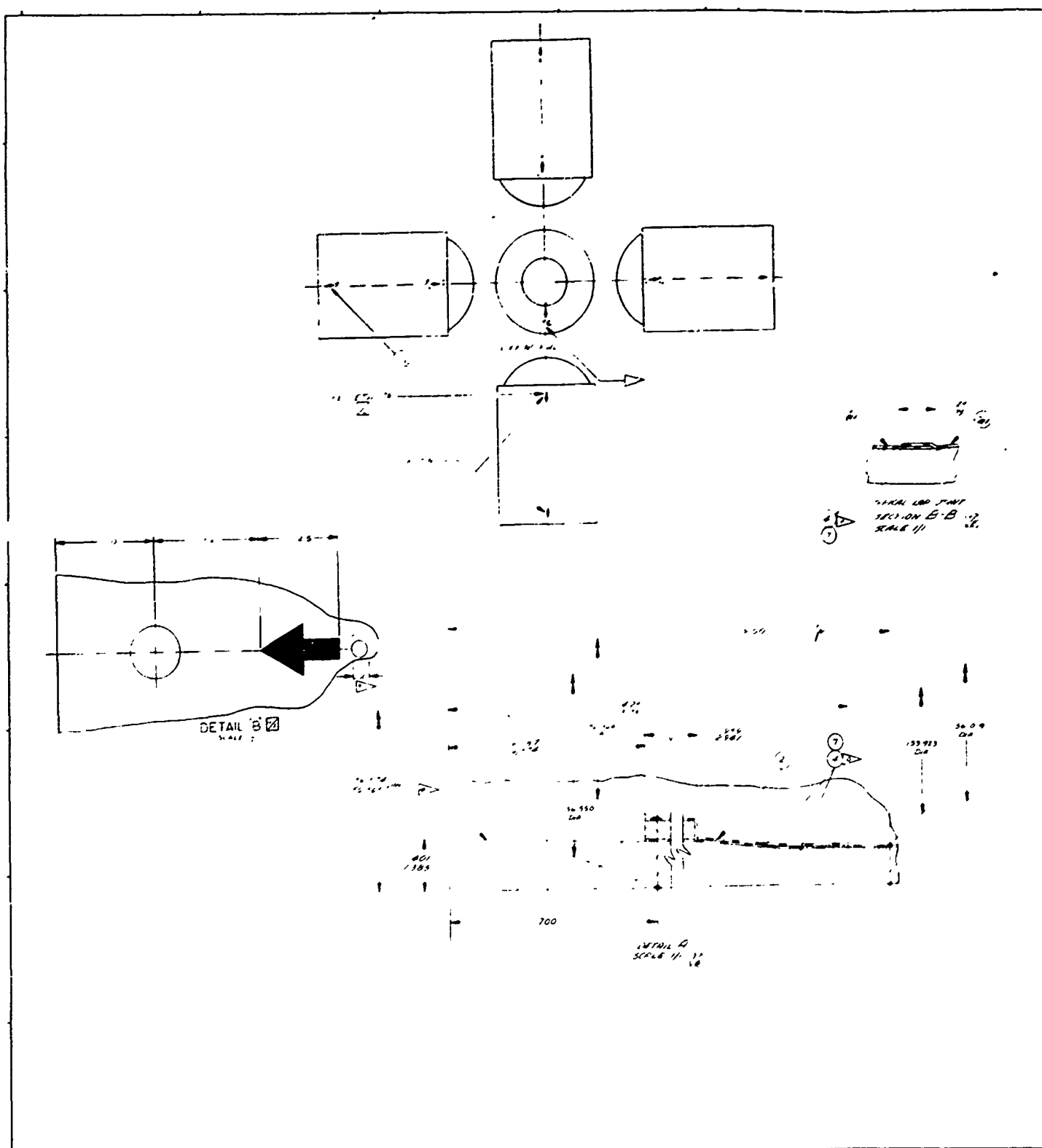


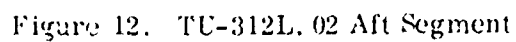


7037330

2







1. Glass removal because of bladder unbondedness.
2. Loss of 4 of the 3,200 center segment clevis joint shims during assembly of the case for the second hydrotest under Contract AF 33(657)-11303.
3. The local cutting of 1 1/2 helical layers adjacent to the aft polar boss after bladder removal.
4. Scratches on the forward segment, occurring during skirt repair under Contract AF 33(657)-11303, which locally cut 2 1/2 layers of hoop windings.

The combined effect of the above discrepancies was a reduction of the predicted burst strength of the case from above 1,500 psig to 1,440 psig. The analysis of the effects of each of the above discrepancies is presented in the following sections.

a. Glass Removal--The number of polar or helical and hoop layer of fiberglass required by the original design and the number remaining after bladder and glass removal are shown in Table I. In the following analysis of case strength after glass removal, Thiokol assumed that the maximum amount of glass removed from any one segment was removed from the entire segment; that is, in the forward segment where 2 1/2 layers of polar windings were removed from the dome area and only one polar layer was removed from the cylinder. 2 1/2 layers were assumed to be removed from the entire segment.

TABLE I
FIBERGLASS DESIGN REQUIREMENTS

	<u>Original</u>		<u>Rework</u>	
	<u>Polar/Helical Layers</u>	<u>Hoop Layers</u>	<u>Polar/Helical Layers</u>	<u>Hoop Layers</u>
Forward Segment	34	47.5	31.5	46.5
Center Segment	28	48	27	47.5
Aft Segment	40	38	37.5	37.5

The glass thickness required to carry the loads induced at an internal pressure of 880 psig (MEOP) are as follows.

(1) Forward Segment

(a) Polar Glass

$$\begin{aligned} t'_{G\varphi} &= \frac{PR (1 + \epsilon\varphi)}{2F_{G\varphi} \cos^2 \alpha} \\ &= \frac{880 \times 77.685 (1 + 0.014)}{2 \times 301,500 \times \cos^2 9^\circ} \\ &= 0.118 \text{ in.} \end{aligned}$$

(b) Hoop Glass

$$\begin{aligned} t'_{G\theta} &= \frac{PR (1 + \epsilon\theta)}{F_{G\theta}} \\ &= \frac{880 \times 77.685 (1 + 0.016)}{335,000} \\ &= 0.207 \text{ in.} \end{aligned}$$

(2) Center Segment

(a) Polar Glass

$$\begin{aligned} t'_{G\varphi} &= \frac{PR (1 + \epsilon\varphi)}{2F_{G\varphi} \cos^2 \alpha} \\ &= \frac{880 \times 77.683 (1 + 0.017)}{2 \times 301,500 \times \cos^2 5^\circ} \\ &= 0.116 \text{ in.} \end{aligned}$$

(b) Hoop Glass

$$\begin{aligned} t'_{G\theta} &= \frac{PR (1 + \epsilon\theta)}{F_{G\theta}} \\ &= \frac{880 \times 77.683 (1 + 0.017)}{335,000} \\ &= 0.207 \text{ in.} \end{aligned}$$

(3) Aft Segment

(a) Helical Glass

$$\begin{aligned} t'_{G\phi} &= \frac{PR(1 + \epsilon\phi)}{2F_{G\phi} \cos^2 \bar{\alpha}} \\ &= \frac{880 \times 77.685 (1 + 0.014)}{2 \times 301,500 \cos^2 30^\circ 25'} \\ &= 0.155 \text{ in.} \end{aligned}$$

(b) Hoop Glass

$$\begin{aligned} t'_{G\theta} &= \frac{PR(1 + \epsilon\theta)}{F_{G\theta}} \\ &= \frac{880 \times 77.685 (1 + 0.017)}{335,000} \\ &= 0.207 \text{ in.} \end{aligned}$$

The effective glass thicknesses for the original design (where the thickness of one layer is 0.00706 inch) are as follows.

(1) Forward Segment

(a) Polar Glass

$$\begin{aligned} t_{G\phi} &= n_{\phi} \times t_{GL} \\ &= 34 \times 0.00706 \\ &= 0.240 \text{ in.} \end{aligned}$$

(b) Hoop Glass

$$\begin{aligned} t_{G\theta} &= n_{\theta} \times t_{GL} + t_{G\phi} \sin^2 \bar{\alpha} \\ &= 47.5 \times 0.00706 + 0.240 \sin^2 9^\circ \\ &= 0.341 \text{ in.} \end{aligned}$$

(2) Cent. - Segment

(a) Polar Glass

$$\begin{aligned} t_{G\phi} &= n_{\phi} \times t_{GL} \\ &= 28 \times 0.00706 \\ &= 0.198 \text{ in.} \end{aligned}$$

(b) Hoop Glass

$$\begin{aligned} t_{G\theta} &= n_{\theta} \times t_{GL} + t_{G\phi} \sin^2 \bar{\alpha} \\ &= 48 \times 0.00706 + 0.198 \sin^2 5^\circ \\ &= 0.341 \text{ in.} \end{aligned}$$

(3) Aft Segment

(a) Helical Glass

$$\begin{aligned} t_{G\phi} &= n_{\phi} \times t_{GL} \\ &= 40 \times 0.00706 \\ &= 0.282 \text{ in.} \end{aligned}$$

(b) Hoop Glass

$$\begin{aligned} t_{G\theta} &= n_{\theta} \times t_{GL} + t_{G\phi} \sin^2 \bar{\alpha} \\ &= 38 \times 0.00706 + 0.282 \sin^2 30^\circ 25' \\ &= 0.340 \text{ in.} \end{aligned}$$

Using the same thickness per layer, but different numbers of layers for the reworked condition, the effective thicknesses remaining after bladder removal were as follows.

(1) Forward Segment

(a) Polar Glass

$$\begin{aligned} t_{G\phi} &= n_{\phi} \times t_{GL} \\ &= 31.5 \times 0.00706 \\ &= 0.222 \text{ in.} \end{aligned}$$

(b) Hoop Glass

$$\begin{aligned} t_{G\theta} &= n_{\theta} \times t_{G\phi} \sin^2 \bar{\alpha} \\ &= 46.5 \times 0.00706 + 0.222 \sin^2 9^\circ \\ &= 0.334 \text{ in.} \end{aligned}$$

(2) Center Segment

(a) Polar Glass

$$\begin{aligned} t_{G\phi} &= n_{\phi} \times t_{GL} \\ &= 27 \times 0.00706 \\ &= 0.191 \text{ in.} \end{aligned}$$

(b) Hoop Glass

$$\begin{aligned} t_{G\theta} &= n_{\theta} \times t_{GL} + t_{G\phi} \sin^2 \bar{\alpha} \\ &= 47.5 \times 0.00706 + 0.191 \sin^2 5^\circ \\ &= 0.336 \text{ in.} \end{aligned}$$

(3) Aft Segment

(a) Helical Glass

$$\begin{aligned}t_{G\phi} &= n_{\phi} \times t_{GL} \\&= 37.5 \times 0.00706 \\&= 0.265 \text{ in.}\end{aligned}$$

(b) Hoop Glass

$$\begin{aligned}t_{G\theta} &= n_{\theta} \times t_{GL} + t_{G\phi} \sin^2 \bar{\alpha} \\&= 37.5 \times 0.00706 + 0.265 \sin^2 30^\circ 25' \\&= 0.333 \text{ in.}\end{aligned}$$

The above calculations of required, original, and remaining glass thicknesses for each case segment are summarized in Table II. The resulting safety factors are also shown in this table.

TABLE II
REQUIRED, ORIGINAL, AND REMAINING GLASS
THICKNESSES AND SAFETY FACTORS PER SEGMENT

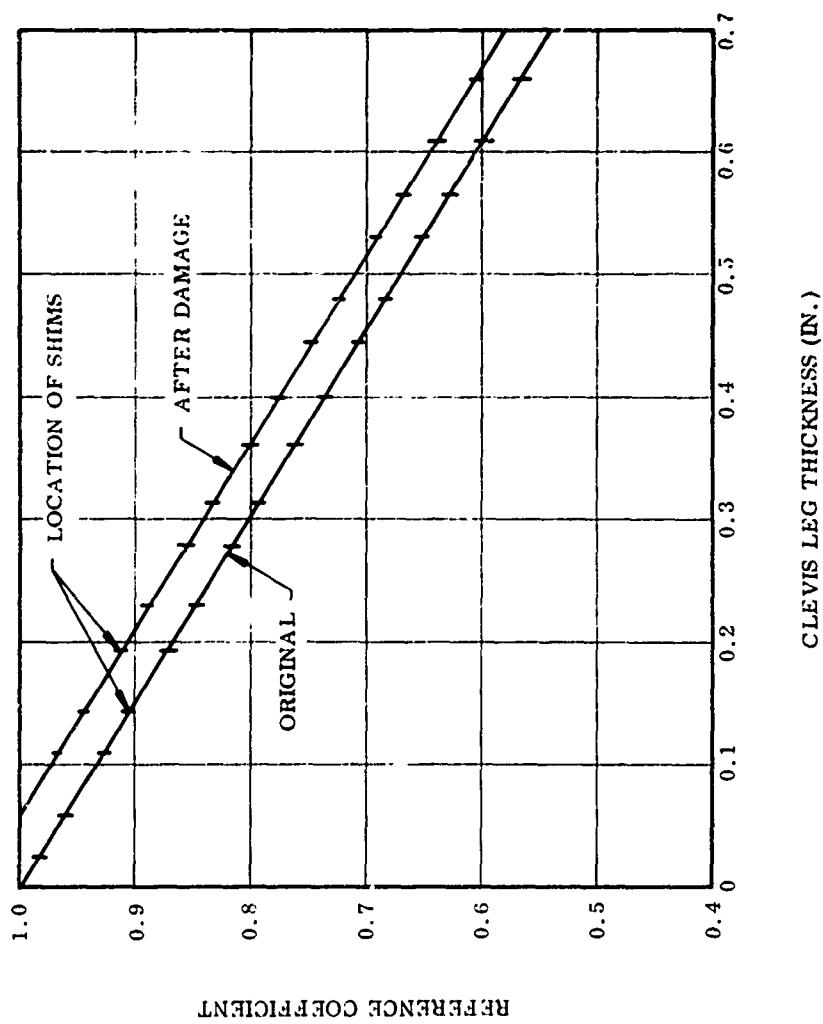
<u>Segment</u>	<u>Segment Glass Thicknesses (in.)</u>					
	<u>Required</u>		<u>As Fabricated</u>		<u>After Bladder Removal</u>	
	<u>Polar/Helical</u>	<u>Hoop</u>	<u>Polar/Helical</u>	<u>Hoop</u>	<u>Polar/Helical</u>	<u>Hoop</u>
Forward	0.118	0.207	0.240	0.341	0.222	0.334
Center	0.116	0.207	0.198	0.341	0.191	0.336
Aft	0.155	0.207	0.282	0.340	0.265	0.333

Safety Factors at MEOP (880 psig)

<u>Segment</u>	<u>Original</u>		<u>Reworked</u>	
	<u>Polar/Helical</u>	<u>Hoop</u>	<u>Polar/Helical</u>	<u>Hoop</u>
Forward	+2.03	+1.64	+1.91	+1.61
Center	+1.70	+1.64	+1.64	+1.62
Aft	+1.81	+1.64	+1.70	+1.60

b. Shim Damage--During the assembly of the case for the second hydrotest under Contract AF 33(657)-11303, interference between the center and aft segments resulted in the loss of four shims from the outside diameter of the inner clevis leg of the center segment. The four damaged shim stacks, which were reduced in total number of shims from 16 to 15, were randomly spaced around the segment (i.e., no two shim stacks incurring damage were adjacent to one another). For the purpose of analysis, it was assumed that the 16th shim (the outer shim of the inner leg) from all 100 shim stacks was damaged. Since there will be some distribution of load from the damaged shim stacks to the adjacent undamaged stacks, the analysis of the effect of the damage is conservative.

The clevis joint was originally designed for an ultimate strength of 153,875 lb per clevis leg per pin. The shims next to the clevis gap (the No. 16 and 17 shims) are the most highly loaded shims in each stack, thus the loss of the No. 16 shims shifts the influence coefficient curve (Figure 13) and reduces the ultimate strength to 146,891 lb per leg per pin.



12163-15

Figure 13. Relative Deflections For a Clevis Leg

Based on Figure 13, the ultimate load capability after the loss of the No. 16 shim is as follows.

$$\begin{aligned} & \sum \text{influence coefficients } (K_{br}) (F_{tu}) (D_p) (t_s) \\ & (0.984 + 0.960 + 0.927 + 0.905 + 0.872 + 0.847 + \\ & 0.794 + 0.761 + 0.738 + 0.705 + 0.684 + 0.650 + \\ & 0.628 + 0.600) (1.65) (250,000) (1.60) (0.020) \\ & = 146,891 \text{ lb.} \end{aligned}$$

The calculated load per pin per clevis leg at an internal pressure of 880 psig (lb.) 9,825 lb. Based upon the reduced ultimate strength resulting from the assumption of loss of all No. 16 shims, the factor of safety at MEOP is:

$$\begin{aligned} FS &= \frac{R_A' \text{ (ult)}}{R_A \text{ (MEOP)}} = \frac{146,891}{89,825} \\ &= 1.64 \end{aligned}$$

The safety factor of 1.64 represents a predicted failure pressure of the damaged joint of 1,440 psig. As stated previously, this predicted pressure is conservative because of the assumption that all No. 16 shims were damaged.

c. Local Cutting on Aft Dome--During the removal of the helical glass in the aft segment, 1 1/2 helical layers, over and above the 2 1/2 layers removed, were cut in a local area next to the aft polar boss. The cut was 1 1/2 layers deep by 3/16 in. wide by 2 in. long. Assuming the cut renders the complete 1 1/2 layers ineffective, the effective glass thickness is reduced four percent. The resultant factor of safety at MEOP after bladder removal, considering the local cut, is then:

$$\begin{aligned} FS &= \frac{t_{G\phi} (1 - 0.04)}{t'_{G\phi}} = \frac{0.265 (0.96)}{0.155} \\ &= 1.64 \end{aligned}$$

where:

$t_{G\phi}$ = Effective helical glass thickness after bladder removal.

$t'_{G\phi}$ = Effective helical glass thickness required to carry loads induced at 880 psig.

d. Local Scratches on Forward Segment--During the installation of the replacement skirt on the forward segment under Contract AF 33(657)-11303, the locking knob on a drill clamping fixture loosened from the attaching bolt, allowing the fixture to drop. When the fixture dropped, it hit the segment in four places and caused local abrasion of the outer 2 1/2 layers of hoop fibers. Based upon the assumption that the 2 1/2 locally damaged hoop layers are ineffective in carrying hoop loading, the resultant factor of safety at MEOP is:

$$\begin{aligned} FS &= \frac{t_{G\theta} - 2.5 \times 0.00706}{t'_{G\theta}} = \frac{0.334 - 0.018}{0.027} \\ &= 1.52 \end{aligned}$$

where:

$t_{G\theta}$ = Effective hoop glass thickness after bladder removal.

$t'_{G\theta}$ = Effective hoop glass thickness required to carry induced load at 880 psig.

The safety factor of 1.52 represents a predicted hoop glass failure in the forward segment at 1,340 psig. However, because of the conservatism of the calculated effect of damage and the original case design, a hoop glass failure in the forward segment is not expected.

The ultimate strength of S-994 fiberglass used in the case design was 335,000 psi. In the POLARIS Program, it has been found that 335,000 psi is the lower strength limit of S-994 fiberglass. Present fiberglass case designs are

based upon a design glass strength for S-994 of 350 to 370,000 psi. A more realistic ultimate strength for the TU-312L.02 fiberglass would be 350,000 psi based upon the present test values.

The scratches on the forward segment are local; therefore, it is expected that under pressurization, circumferential bands of hoop glass (2 1/2 layers thick and as wide as the width of the cut [1 in.]) will be shucked from the forward segment. The failure of the fiberglass bands will cause a higher loading in the unfailed hoop glass adjacent to the bands. However, as demonstrated in other programs, hoop load can be bridged across a gap by the polar or helical fibers. The TU-312L.02 case was fabricated with interspersed hoop and polar winding, thus increasing the capability of assuming the load of the hoop bands that failed.

For the above reasons, although the conservative calculations show that the predicted mode of failure is in the hoop fibers of the forward segment, failure would actually be expected in the damaged aft segment joint at a pressure of 1,440 psig.

SECTION III

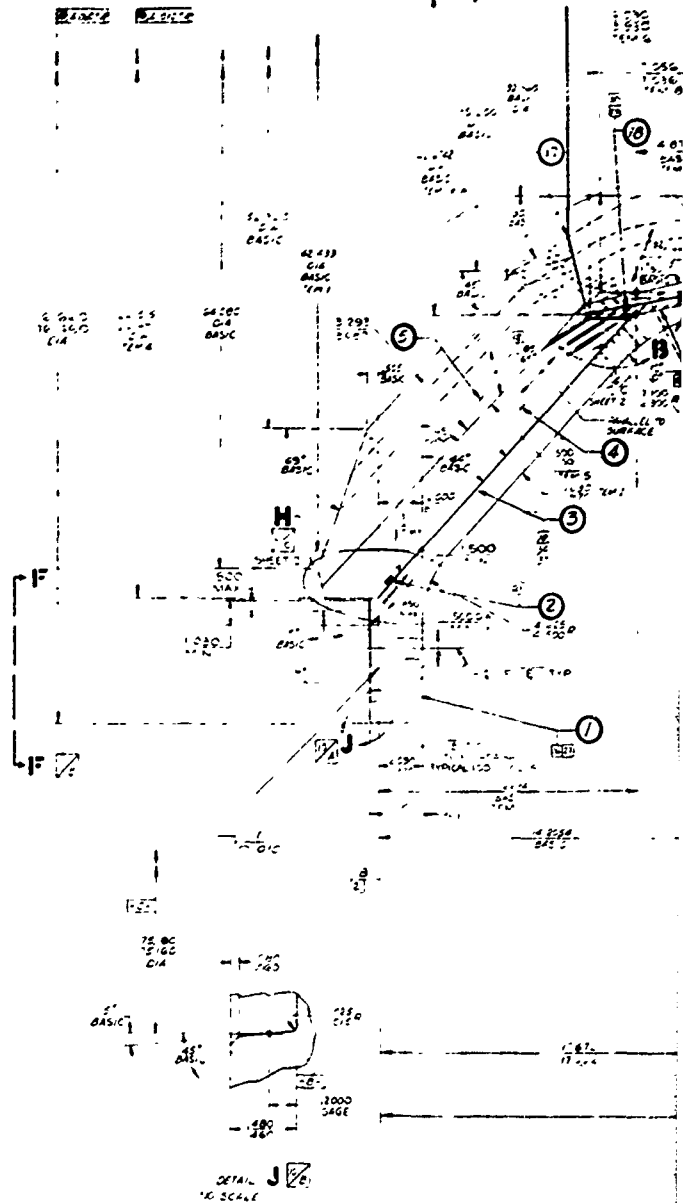
NOZZLE

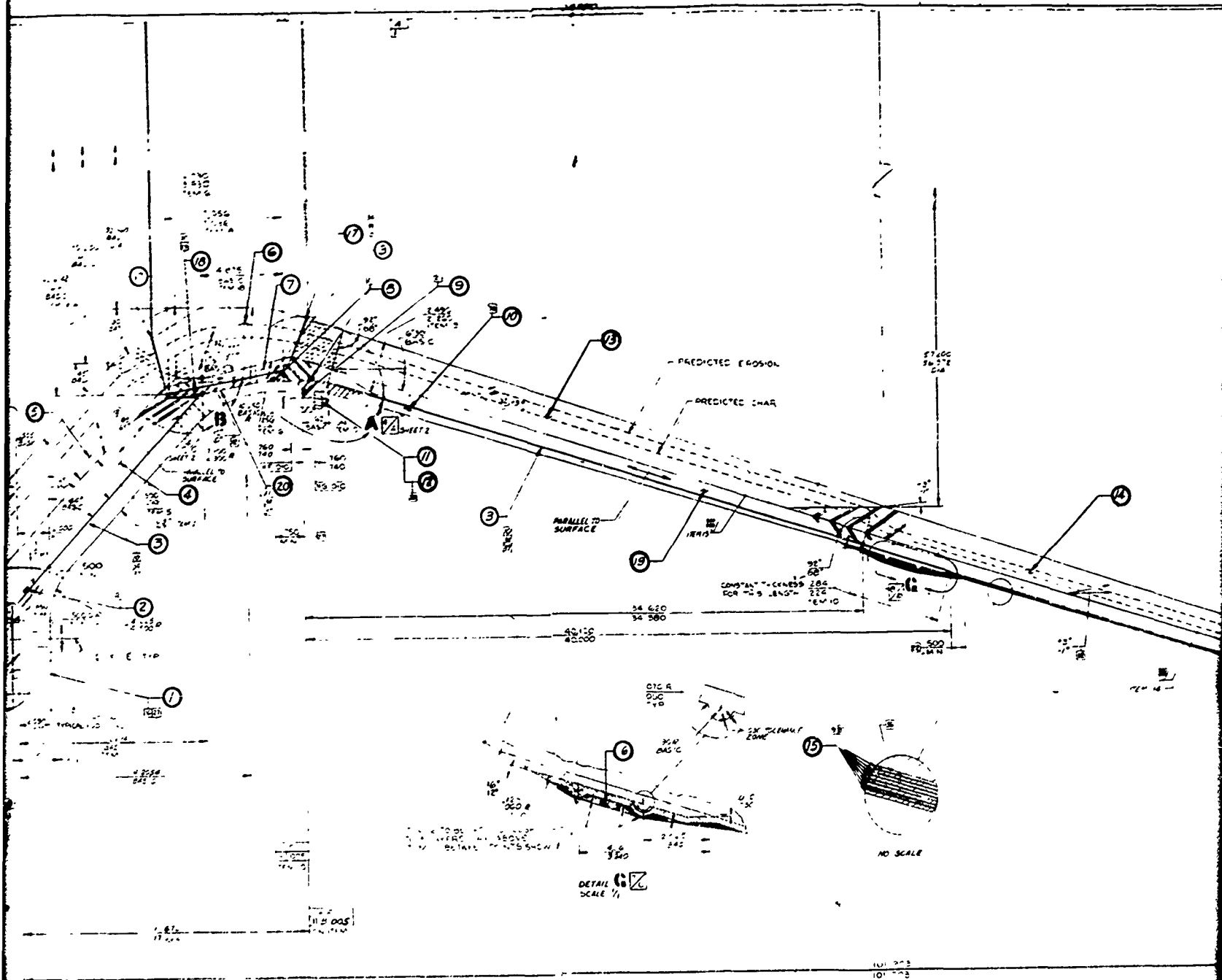
The nozzle for the TU-312L.02 motor is a fixed, external, ablative, plastic nozzle of the convergent-divergent type (Figure 14). The nozzle was fabricated by Thompson Ramo-Wooldridge Co (TRW) under Contract AF 33(657)-11301 (Development of Manufacturing Processes for Reinforced Plastic Solid Propellant Rocket Nozzles). The materials used in the fabrication of the nozzle are listed in Table III. A summary of the physical property test results reported by TRW on the nozzle components is given in Table IV.

The fabrication of the TU-312L.02 nozzle was accomplished in two modules: a throat module and an exit cone module. The two modules were bonded and bolted together to form the nozzle assembly.

A. NOZZLE DESIGN SUMMARY

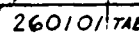
A review of the nozzle design report, presented in program final report AFML-TR-65-345, was made during this quarter and all aspects of the design were satisfactory. The structural review consisted of checking the base design parameters and loadings, the various materials properties, and methods and equations used in the analyses performed by TRW. Stress levels in critical areas were below the allowable levels for the materials used and adequate margins of safety exist in the nozzle design. These margins of safety were achieved based on an expected maximum operating pressure of 1,200 psi, which is approximately 1.5 times the predicted maximum pressure during motor burn time. The design is quite conservative.





26010 TAB

2



43

TABLE III
NOZZLE INSULATION MATERIALS

<u>Material</u>	<u>Location</u>	<u>Designation</u>
Graphite cloth phenolic	Throat approach Throat insert	U. S. Polymeric FM5014G U. S. Polymeric FM5014G
Carbon cloth phenolic	Throat extension	Fiberite MX 4926
Silica cloth phenolic	Throat approach insulator Throat insert insulator Exit cone extension Exit cone overwrap	U. S. Polymeric FM5131 U. S. Polymeric FM5131 U. S. Polymeric FM5131 184 Glass Cloth (epoxy impregnated)
Bonding materials		
Narmco 2034	Fabrication adhesive (cured components to uncured wraps)	
Steel Epon 913 and 919 Adhesives	Bonding (cured plastic components to each other and to steel)	
RTV Silicon Rubber	(throat module to exit cone module)	
Potting material		
RTV Silicon Rubber	(between inlet and throat insert)	

TABLE IV
PHYSICAL PROPERTY TEST RESULTS FOR
FULL SCALE NOZZLE COMPONENTS

<u>Nozzle Component</u>	<u>Material</u>	<u>Specific Gravity</u>	<u>Percent Acetone</u>	<u>Percent Volatile</u>	<u>Edgewise Compression</u>
Throat insert	FM5014G* with Basic Carbon graphite fabric	1.43 1.44	0.05 0.16	2.17 2.58	14,493 22,700
Throat insert insulator	FM5131* silica phenolic	1.73 1.76	0.14 0.24	2.89 4.00	-- --
Throat approach	FM5014G* with Basic Carbon graphite fabric	1.43	0.01 0.09	2.37 2.39	16,470 17,990
Throat approach insulation	FM5131* silica phenolic	1.74	0.24 0.29	0.22 0.41	-- --
Throat extension	Fiberite MX4926 carbon phenolic	1.415 1.417	0.26 0.27	1.37 1.54	46,200 49,600
Exit cone extension	FM5131* silica phenolic	1.69 1.74	0.37 0.55	2.20 2.37	23,400 23,900
Exit cone insulator	FM5131* silica phenolic	1.69 1.74	0.50 0.65	3.11 5.30	13,700 14,480

*U.S. Polymeric

In addition to the basic pressure and thrust loadings, "G" loadings from handling and/or assumed flight accelerations were considered. These analyses were reviewed and found to be acceptable.

The thermal stress analysis in the throat section (made by TRW) could not be reviewed because these stresses were computed by a computerized program, and calculations and equations were not included in the design report. From the TRW description of the methods and parameters used, however, the analysis is comparable to that normally used by Thiokol and the results are considered valid and within design limits.

A review of nozzle fabrication and processing showed no problem areas and only minor deviations or discrepancies to design requirements and engineering drawings. These minor deviations will have no effect on nozzle performance.

B. NOZZLE INSPECTION

Upon receipt at Thiokol, the nozzle shipping container was opened and the nozzle exterior was visually inspected. No discrepancies or damage were found.

Internal visual inspection and dimensional checks have not been made because the lifting and handling equipment and fixtures were not available. Fixtures and equipment to accomplish the removal and lifting of the nozzle from the shipping container and for breakover to horizontal position are in process.

Instrumentation tests and continuity checks also have not been conducted. These were postponed until after the availability of handling fixtures and equipment.

C. NOZZLE PERFORMANCE ANALYSIS

In reviewing previous analyses of case and nozzle insulation at the motor nozzle interface, Thiokol decided that the case insulation thickness at this point was marginal; consequently, additional thickness was added. This resulted in a hump

or sharper change in contour of the flow surface at the case nozzle interface. A flow analysis was then made of the aft case to nozzle throat section using the computerized flow net program to obtain convective heat transfer coefficients, predicted erosion profiles, and local wall Mach number profiles.

Runs were made for zero burn time and 100 percent burn time. The results are shown in Figures 15 and 16. These figures show some variation in the heat transfer coefficient and wall Mach number for 0 percent burn time and reflect the flow acceleration-decelerations and change in boundary layer thickness along the changing contour. The 100 percent burn time plots show a smoothing or reduction in variation, which reflects the eroding away of abrupt surface contour changes into a smoother contour form. No discontinuities are evident in the plots, which shows that flow separation and reattachment do not occur and that satisfactory flow conditions have been maintained. The erosion profile predicted from the flow net results is shown superimposed on the figures.

Erosion and char depths throughout the nozzle were calculated using methods developed by Thiokol from the study and analysis of a large number of materials and nozzle tests. The Thiokol erosion predictions vary somewhat from those of TRW but are generally in good agreement. The TRW values and Thiokol calculated values are tabulated below for comparison.

PREDICTED EROSION COMPARISON

Thiokol Analysis			TRW Report		
Area Ratio	Depth (in.)	Rate (mils/sec)	Area Ratio	Depth (in.)	Rate (mils/sec)
-2.52	0.433	3.61	-1.80	0.665	5.54
-1.4	0.72	6.0	-1.13	0.809	6.74
1.0	0.91	7.57	1.00	0.998	8.42
1.26	0.734	6.12	1.059	0.746	6.22
2.03	0.432	3.6	1.20	0.606	5.05
3.0 (carbon)	0.252	2.1	2.30	0.504	4.20
3.0 (silica)	1.00	8.4	3.48	0.760	6.34
3.215	0.89	7.4	4.00	0.600	5.00
4.9	0.34	2.8	7.00	0.276	2.30
7.0	0.02	0.15			

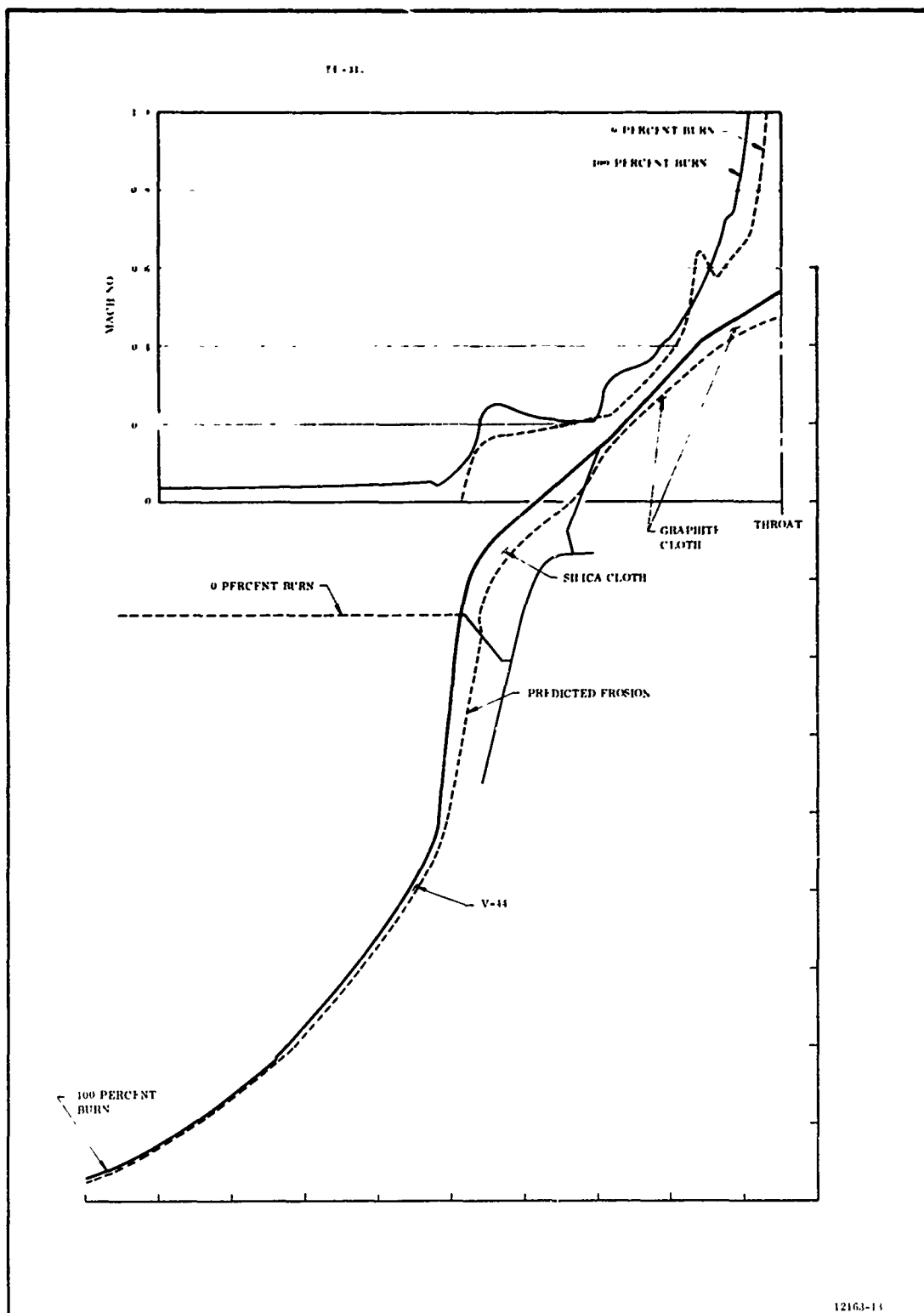


Figure 15. Wall Mach Number vs Axial Position, Aft Case and Nozzle Inlet

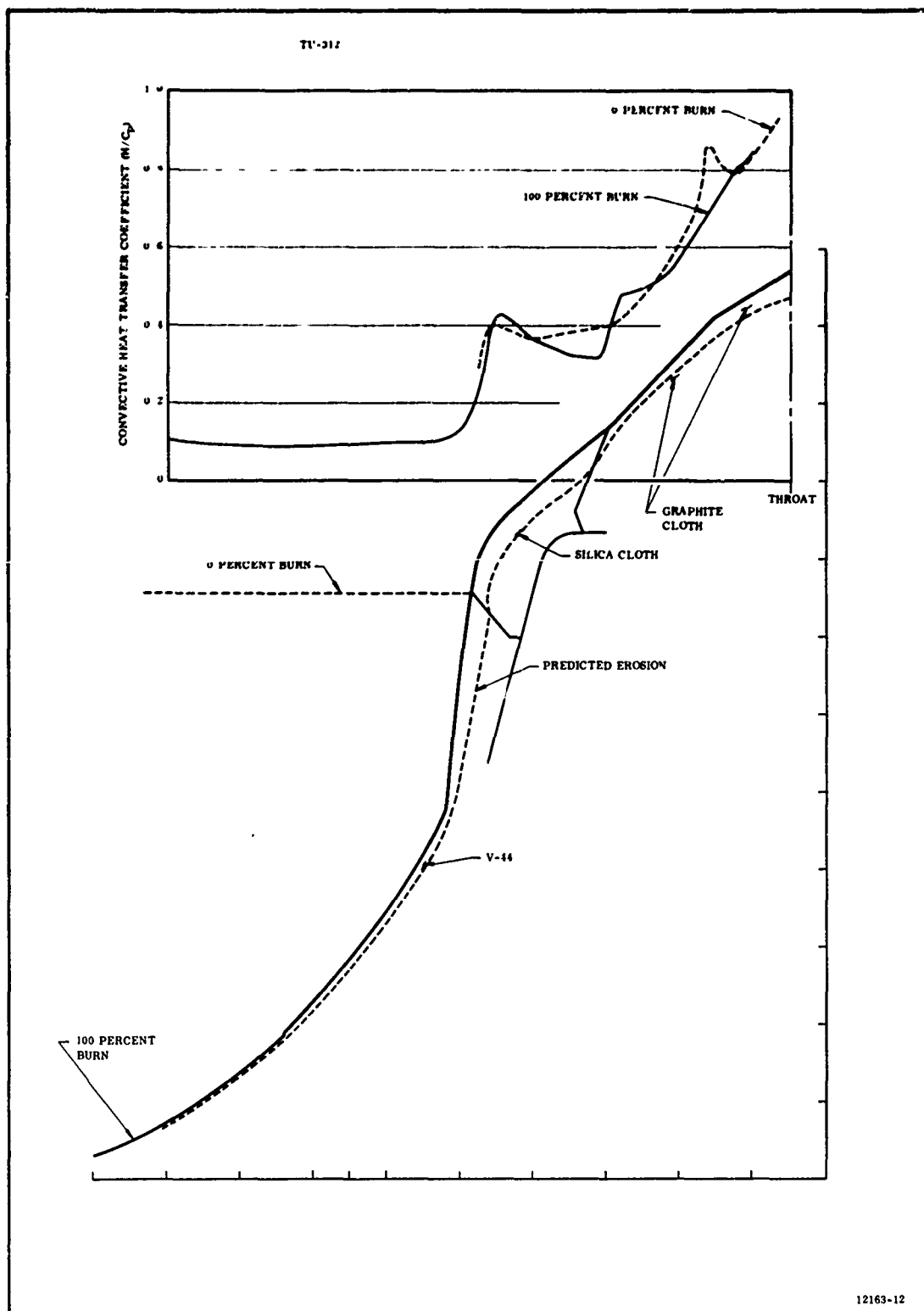
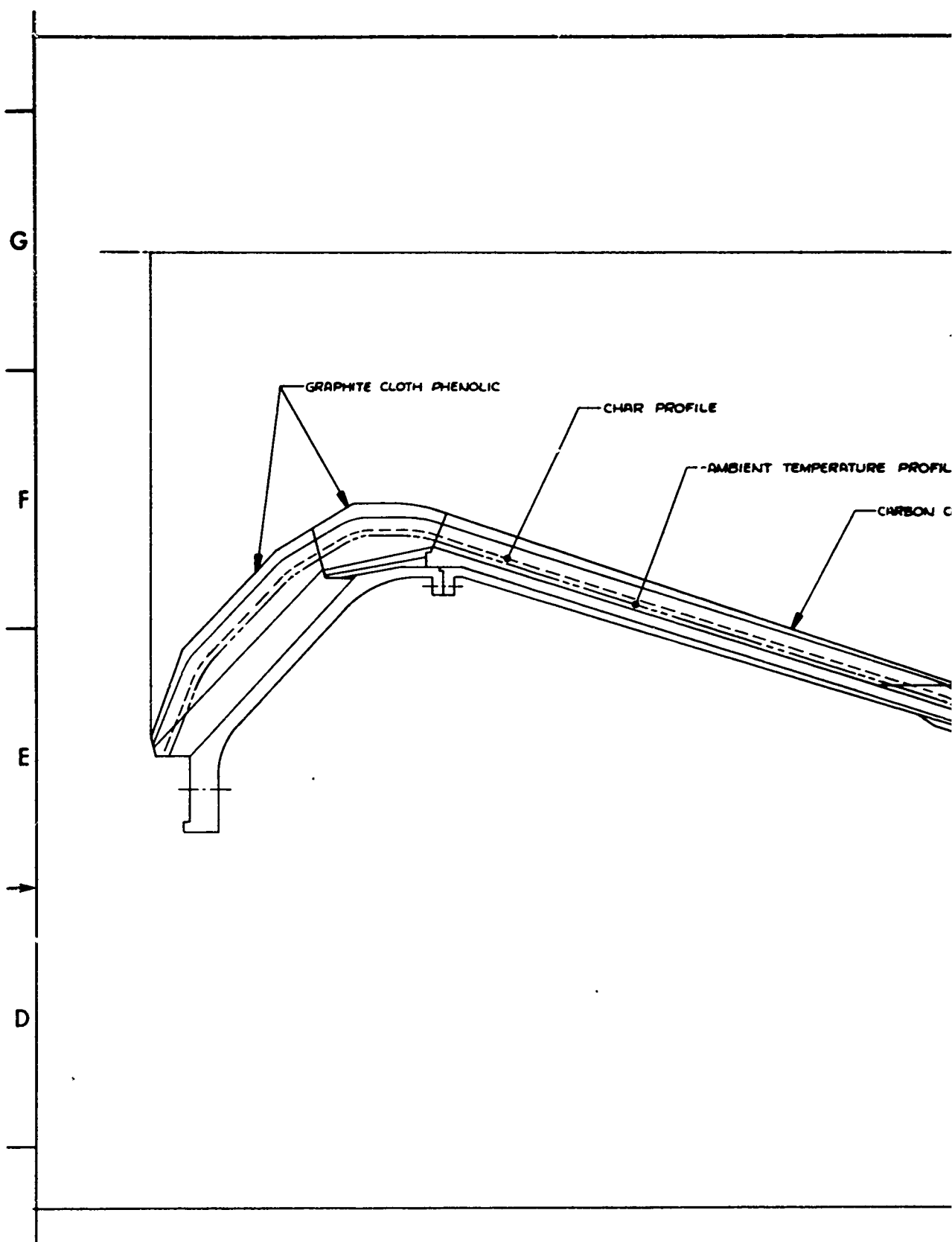


Figure 16. Convective Heat Transfer Coefficient vs Axial Position, Nozzle Inlet

The depth of char into the liner material and the depth below char to ambient temperature point were also calculated and profiles drawn. These are shown in Figure 17. As can be seen, adequate material thicknesses to withstand the erosion and thermal environment exist in the design with ample margins of safety.

The analysis showed that no heating should be experienced on the exterior of the nozzle exit cone through the transfer of heat from the exhaust gases; therefore, temperatures registered by the exterior thermocouples along the cone should remain at or very near ambient levels throughout the firing time.



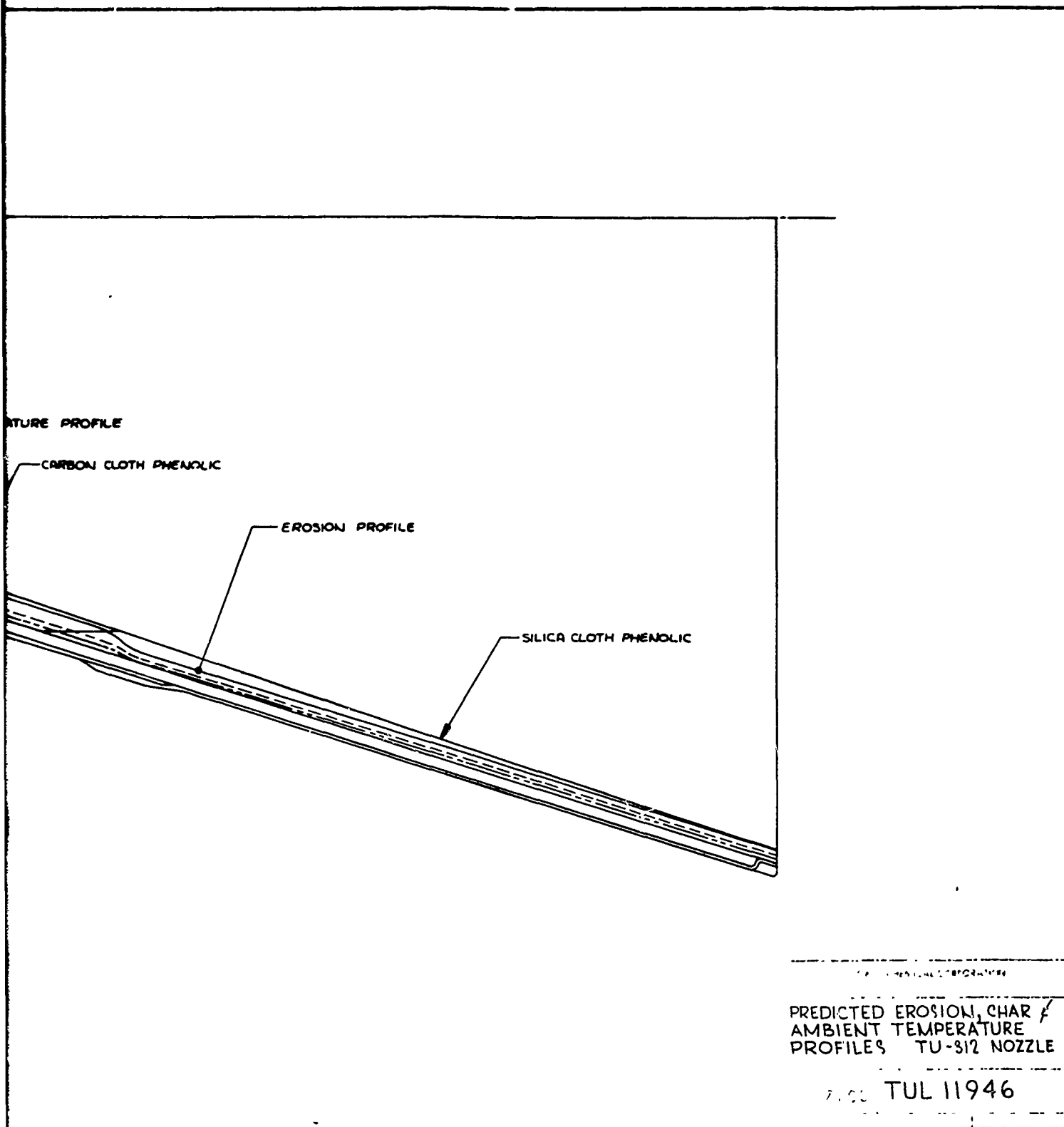


Figure 17. Predicted Erosion, Char, and Ambient Temperature Profiles for TU-312 Nozzle

SECTION IV

JOINT SEAL

A. DESIGN CRITERIA

The case segment joint seal must seal the case at MEOP of 880 psig. Moreover, it must be designed so that it can be manufactured by conventional methods.

The seal must be embedded in the insulation since the fiberglass case surfaces are pervious. The seal must be designed to withstand 1.4 in. case deflection and the 0.015 in. longitudinal movement in the joint areas demonstrated in the two hydrotests under Contract AF 33(657)-11303.

B. STRUCTURAL AND THERMAL ANALYSIS AND SUMMARY

The design of the joint seal has a "U" configuration as shown in Figure 18. The seal is extruded with Neoprene per MIL-R-417, and has a vulcanized splice that joins the ends to form a ring.

Thiokol places a high confidence in the seal and general design because of a small silicone rubber seal of the approximate configuration successfully used in the MINUTEMAN motor adjacent to case-closure threads.

The 156-8 seal is designed to be pressure actuated; however, to insure sealing at initial low pressures and to compensate for necessary wide tolerance in the

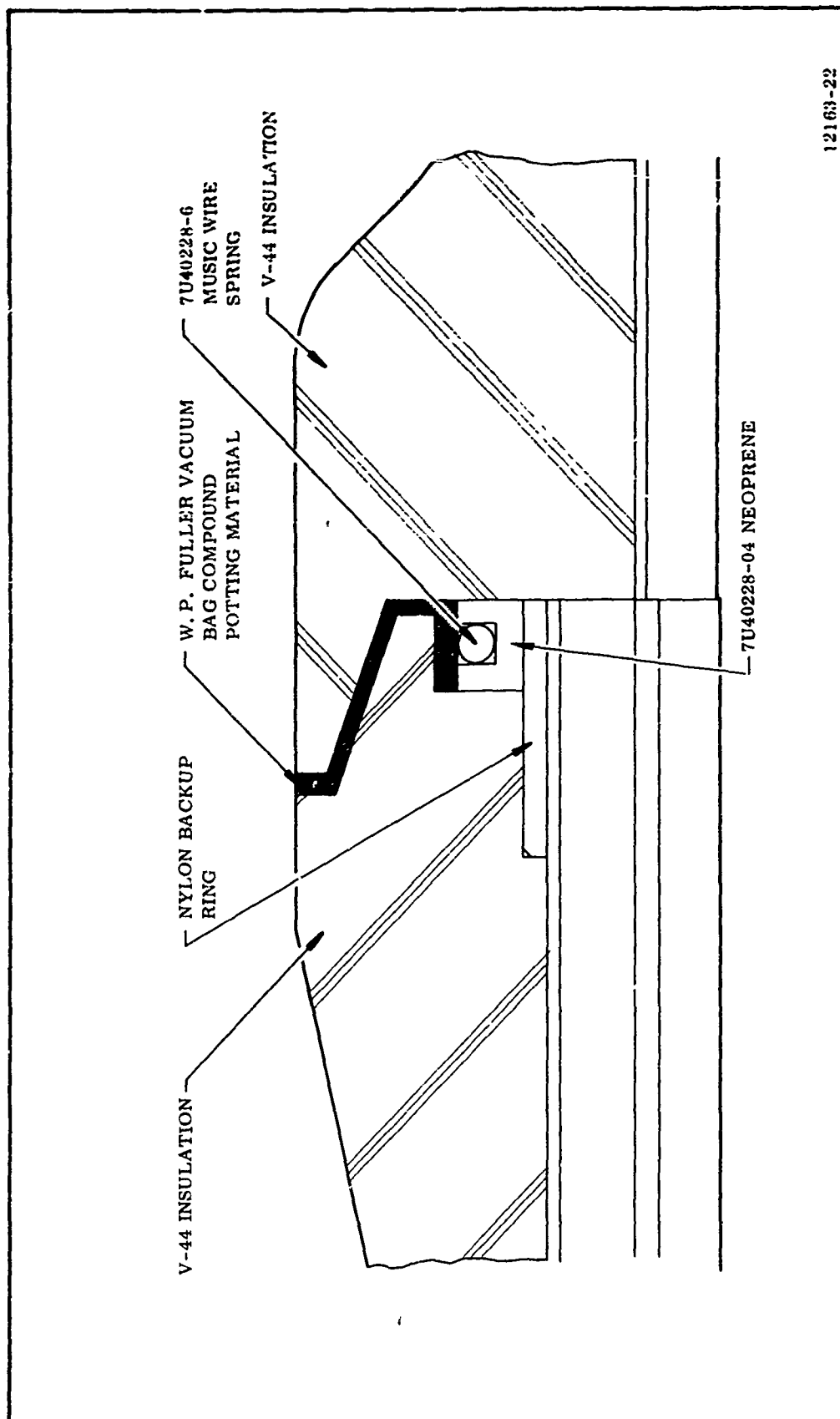


Figure 18. 156-8 Motor Joint Seal

neoprene seal and insulation. The seal was designed to be in a state of compression. A wire spring placed within the seal ring insures that in the nonpressurized state the seal leg surfaces are in contact with the insulation surfaces. The seal ring and spring when assembled have an axial width between 0.674 and 0.770 inch. The cavity in the insulation has an axial depth between 0.592 and 0.637 inch. Therefore, the ring-spring combination is between 0.037 and 0.178 in. larger than the cavity.

A computer program capable of calculating the stresses, strains, and displacements in any three dimensional axisymmetric body of revolution was used to calculate the displacements in the vicinity of the seal ring. Since steel shims were embedded in the clevis and tongue of each segment joint, the axial growth was negligible in the 156-8 case near the joints. However, a separation of the segments may be noted during case pressurization due to the tolerance of the connecting pins.

An analysis was conducted to determine the effect of a 0.015 in. separation of two segments. The insulation was nearly in a hydrostatic compression stress field. Since the pressure in the void between insulation segments resulting from case segment separation was negligible as compared to the 1,110 psi compressive stress field in the insulation, the insulation fills the void a short distance from the case. Thus, the effect of case axial movement is dissipated before reaching the insulation in the neighborhood of the seal ring.

The insulation is asbestos filled NBR (V-44) which has a shore A hardness of approximately 80 and a minimum elongation of 200 percent. This indicates a modulus of approximately 750 psi. Since the insulation is nearly incompressible, a Poisson's ratio of 0.5 was used. The seal ring is made of a neoprene rubber which has a modulus and Poisson's ratio approximately the same as the insulation (shore A hardness of 80).

Figure 19 indicates the change in shape of the seal ring and surrounding insulation in the 156-8 case. The solid line represents the original geometry; the broken line is the superimposed geometry after pressurization with the case used as a zero displacement reference point. The apparent decrease in volume of the insulation after pressurization is not experienced since the radii of the case and insulation increase with pressure. The aft portion of the seal ring (point 1) is displaced 0.022 in. aft while the forward portion (point 2) is displaced 0.010 in. in the opposite direction. Thus the maximum axial expansion of the seal ring is 0.032 inch.

The maximum strains within the seal ring are as follows: radial strain, -6 percent (compressive); hoop strain, +2 percent (tensile); and axial strain, +4 percent (tensile). These are well within the capability limits of the seal. The minimum compressive strain appearing within the seal is 1,056 psi. This is a 44 psi (4 percent) decrease in axial stress and appears near the nylon ring. This loss is attributed to the fact that the insulation is bonded to the case, which prevents axial movement of the insulation.

The joint insulation is designed so that in the most severe erosive conditions the seal will not experience temperatures above ambient nor will the gases at any time have a direct radiation path through the potting material to the seal.

The seal is embedded in the asbestos filled NBR case insulation as shown in Figure 18. The exposure time of the insulation in this area will be 120 sec maximum. An erosion rate based on the maximum experienced in the 156-1 (TU-412.01) of 0.0032 in./sec is used.

Based on the above, the maximum predicted material loss is 0.384 inch. The minimum asbestos filled NBR remaining between the hot chamber gases and the seal at web burnout will be 0.5 inch. In addition, the joint potting material (W. P. Fuller compound 3992) will provide protection.

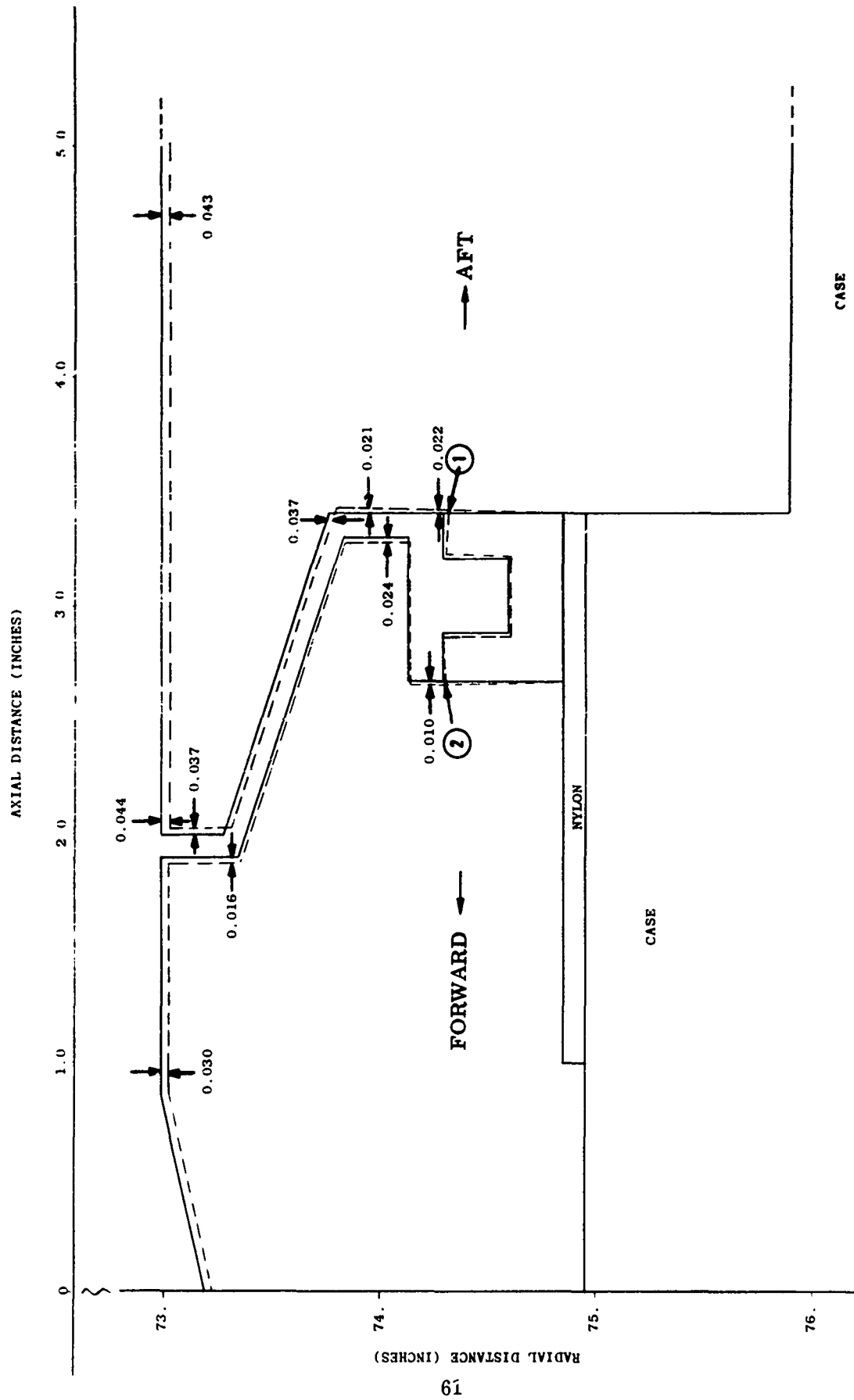


Figure 19. Displacements for the 156-8 Motor Seal

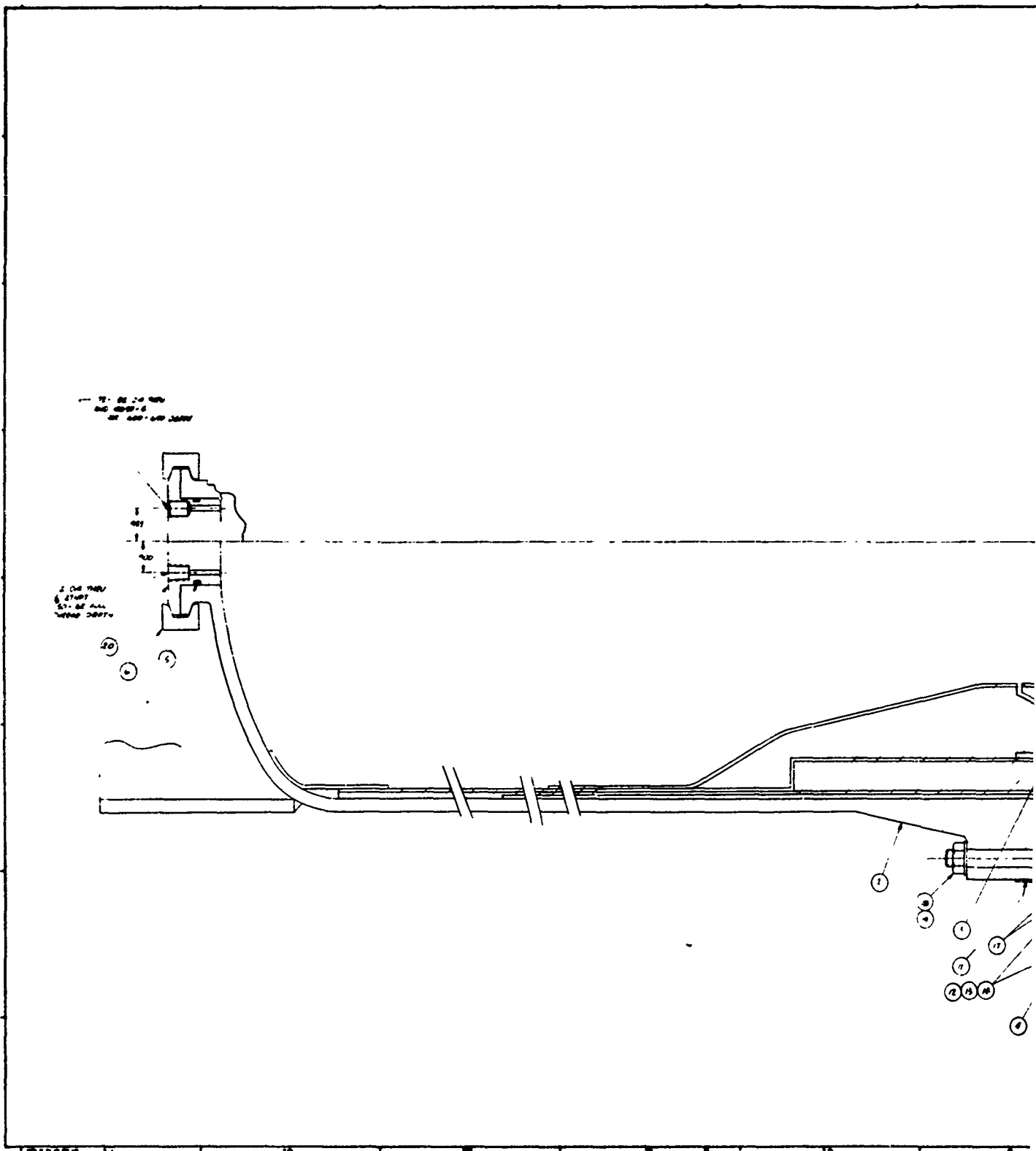
C. SUBSCALE JOINT SEAL DEVELOPMENT

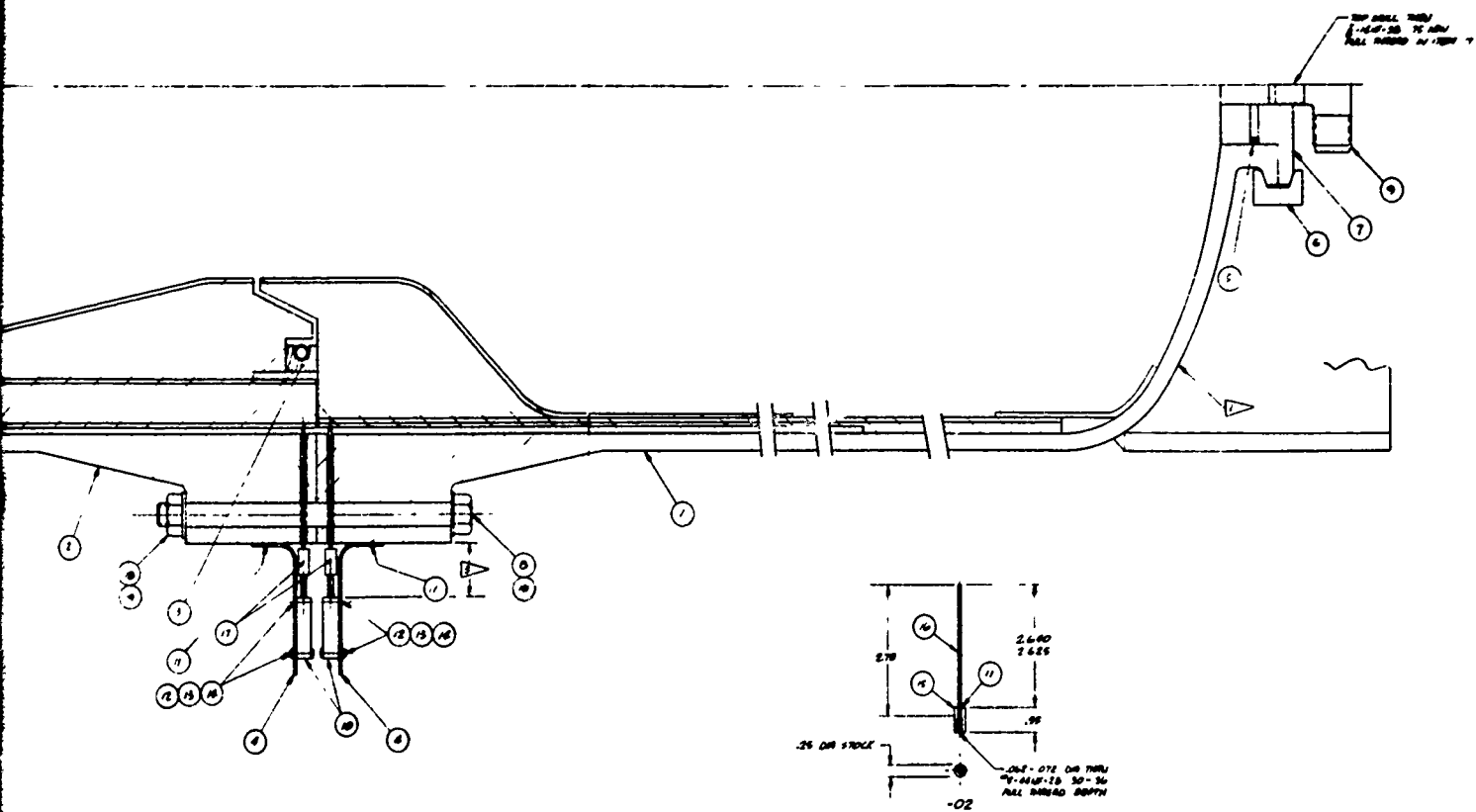
1. SUBSCALE DESIGN

The purpose of the subscale test was to demonstrate the capability of the seal; consequently, the subscale test vessel was such that the circumferential strain in the seal would duplicate as close as possible that of the full scale case. Other displacements are considered insignificant. A preliminary stress analysis was made to (1) determine the radial deflection of the subscale model which would simulate the circumferential strain of the 156 in. case (this was calculated to be 0.14 in. on the subscale vessel) and (2) calculate rotational displacements in the vicinity of the seal to see if they were tolerable.

The subscale test assembly design (Figure 20) consisted of two segments of a fiberglass cylinder fitted at the joining ends with an insulation joint of the same general cross sectional configuration as the 156 in. motor. Each fiberglass segment was mounted in a DU 1020-01 case and then the two sections bolted together at the center. The DU 1020-01 cases were purposely not sealed so that the seal in the insulation joint only would be tested. The fiberglass cylinder was supported and sealed at each end only, leaving the test joint free to move radially 0.14 in. before being restrained by the relatively rigid steel DU 1020-01 case, thus insuring that the maximum hoop strain in the joint seal area would be that of the full scale joint. Extensometers were installed to indicate the radial movement of the joint.

The seal used in the 156-8 is made of neoprene rubber with a channel shaped cross section to receive a music wire spring which holds the seal in place and initially in contact with the insulation. A nylon backup ring is installed in the outside perimeter of the joint to prevent the seal from extruding into the joint space. To demonstrate the feasibility of insulation joints in this area, the insulation was designed to be cut longitudinally on the bias and the resulting space filled with potting compound.





7U40225

Of particular importance in this analysis was the effect of radial growth on the deflections within the insulation. Because of the decreased radius of this test vessel having insulation with the same cross sectional dimensions as the 156-8, the effect of radial expansion was greatly magnified. The total calculated longitudinal expansion of the subscale seal is 0.059 in. (Figure 21), as compared to 0.032 in. in the 156-8 motor (Figure 19). Therefore, Thiokol concluded that after a successful demonstration of the seal in the subscale motor, no difficulty would be experienced in the full scale motor.

The maximum strains in the subscale seal ring are as follows: radial strain, -8.8 percent (compressive); hoop strain, 3 percent (tensile); and axial strain, 6.1 percent (compressive). The minimum compressive stress appearing within the seal is 1,056 psi.

2. SUBSCALE FABRICATION AND TEST

a. Mandrel Fabrication--The mandrel for insulation layup and fiberglass sleeve winding consisted of a 2 in. steel shaft, plywood bulkheads, conduit filler, wire mesh, and plaster. The plywood bulkheads were installed on the shaft and the conduit installed in the necked down area of the joint to provide extra strength against high winding and shrinkage loads. Wire mesh was then installed and plaster was applied to the mesh and screeded to the desired configuration and oven dried.

b. Insulation Fabrication--The outside surface of the mandrel was covered with Teflon tape. A 30 percent MEK and 70 percent Caram 216 mixture was applied to the Teflon tape to provide a sticky surface for the first layer of V-44 insulation.

A flat pattern was developed for cutout of the V-44 sheet stock allowing 1/2 and 3/4 in. overlap between sheets. The lap edges of the V-44 were skived at 45 deg and the first insulation layer was installed on the mandrel with the overlap

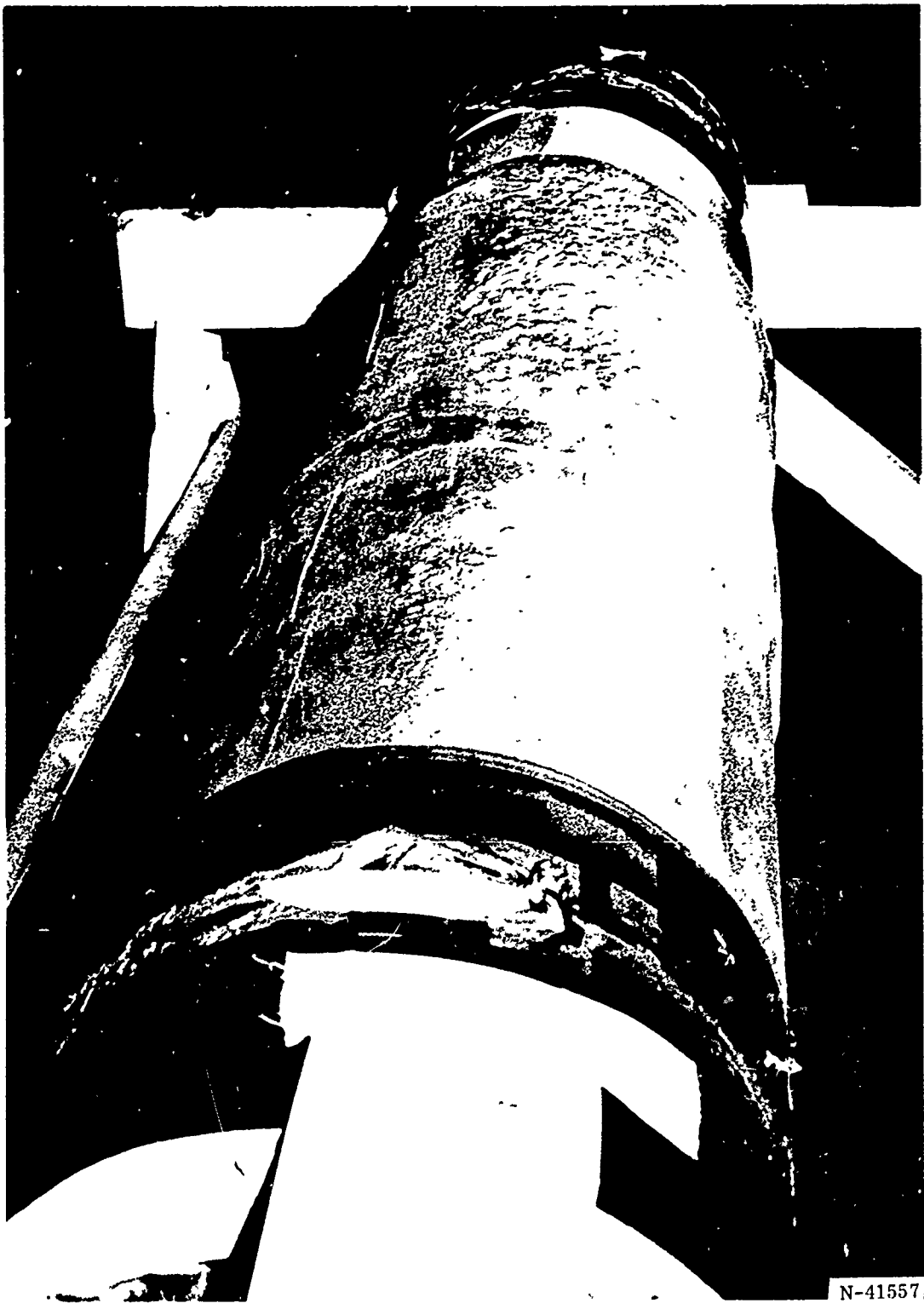
edges activated with MEK. For subsequent insulation layers, the entire insulation surface was activated with MEK and allowed to dry 15 min before the next insulation layer was installed.

After the insulation was positioned on the mandrel, the "seams" and "overlaps" were stitched with rollers and the layer was rolled down onto the mandrel. Air bubbles were localized with a smooth roller and removed with a hypodermic needle injected in the edge of the bubble.

After the insulation was installed, the assembly was covered with a 1/4 in. thick felt pad and nylon sheeting. Vacuum was then applied and the insulation was cured for 3 hr at 290 to 310°F in an atmosphere of CO₂ at 140 to 160 psi. After the vacuum bag was removed, it was discovered that a strip on the bottom of the mandrel, as it was positioned in the autoclave, was not fully cured (Figure 22). Investigation revealed that full circulation of heat around the mandrel in the autoclave was not achieved during the vulcanizing cycle.

The defective material was cut out and removed, and uncured V-44 insulation was installed using UF-3196 as bonding material between the uncured insulation and cured insulation. The uncured to uncured surfaces were then activated with MEK as the original layup. A vacuum bag was installed and the reworked mandrel was autoclave cured for 6 hr at 290 to 310°F in an atmosphere of CO₂ at 140 to 160 psi.

After removal of the vacuum bag, excess material was machined off the OD of the insulated mandrel. The grooves for the nylon and Epocast 31D rings were machined in the thick section of the insulation. To simulate the joints in the large motor insulation, a slit was made across the thick section of the insulation with sharp knives and the slit was filled with UF-3195 and cured 5 hr at 135°F.



N-41557

Figure 22. Subscale Insulation Showing Uncured Area

The nylon ring was grit blasted to roughen the surfaces and bonded in place with UF-3195.

The Epocast 31D ring was cast in place by installing a piece of rolled aluminum sheet over the groove. The rolled sheet overlapped the groove edges one inch and lacked one inch from completely wrapping around the mandrel, thereby forming a slot to pour the Epocast 31D. The surface of the sheet next to the mandrel was covered with Teflon tape for a mold release and the edges of the sheet were sealed with vacuum tape to prevent leakage. The Epocast 31D was cured for 16 hr at $80 \pm 20^\circ\text{F}$. The Epocast 31D ring was then machined to required dimensions and 16 equally spaced slits cut. The 16 slits were filled with UF-3194 and cured for 20 hr at 170°F . A layer of uncured V-45 was bonded over the entire outside surface of the mandrel with UF-3195.

c. Fiberglass Sleeve Fabrication--The glass was applied to the mandrel in the following sequence.

<u>Ply</u>	<u>Material</u>	<u>Method of Application</u>
1	Fiberglass cloth style 143 with E717 resin	Hand layup
2	Same as 1	
3	Same as 1	
4	Preimpregnated roving	Wound
5	Same as 4	
6	Same as 1	
7	Same as 1	
8	Same as 4	
9	Same as 4	

Following completion of winding, the wrap was cured in the following sequence.

2 hr at 190 to 210°F

4 hr at 240 to 260°F

8 hr at 290 to 310°F

4 hr at 340 to 360°F

Following the cure, the sleeves on the shaft were parted by machining and saw cut. The mandrel was then removed.

The insulated fiberglass cylinders were then installed in the steel cases and centered in the aft end of the case with a centering tool. A strip of V-45 was bonded over the inside forward end of the cylinder and to the case with UF-1149. The UF-1149 was cured for 16 hr at $80 \pm 20^\circ\text{F}$. With the cases in the vertical position, UF-3177 was poured between the OD of the cylinder and the case inside wall to the required level to bond the forward end of the fiberglass cylinder to the case wall.

The joint seal configuration was rough machined leaving 0.125 ± 0.060 in. excess material. Voids in the bonding material in the slit were filled with UF-3177 and cured for 8 hr at $80 \pm 20^\circ\text{F}$. The joint seal configuration was then finish machined with form cutters.

d. Testing--The assembly was submitted to three tests. Each test consisted of the following.

1. Assembling the vessel.
2. Pressurizing to 100 psig.
3. Checking for leaks.
4. Pressurizing to 1,100 psig and holding for 120 sec.
5. Depressurizing.

6. Pressurizing to 1,100 psig and holding for 120 sec.
7. Depressurizing.
8. Disassembling.
9. Inspecting.

In the assembly for the first test (Figures 23, 24, and 25), the seal was lubricated with PBAA. In assembly for the second two tests, the PBAA lubricant was used in the same manner; however, the joint gap was also potted with W. P. Fuller vacuum bag compound No. 3992 in the same manner which the 156-8 joint will be potted for static test (Figure 26).

3. SUBSCALE TEST DATA AND ANALYSIS

The test was an unqualified success. No leakage whatsoever was experienced during the hydrotest. As can be seen in Figures 27 through 32, the extensometers did measure a radial displacement of up to 0.14 in., representing a circumferential strain of $0.14/7.3 = 0.0192$ in./in. An earlier test of the full size case measured a maximum radial deflection in the joint of 1.34 in., representing a circumferential strain of $(1.34/78) (1,100/1,000) = 0.0188$ in./in., thus the subscale test may be considered as successfully and closely duplicating the actual full scale case strains. A difference existed in the indicated growth at D001 (female joint) and D002 (male joint). This difference was actually found to be due to the gap between the fiberglass sleeve and the DU-1020 case variation. Calling attention to the compressive marks near the outside perimeter of the insulation (Figure 33), the pattern qualitatively substantiates the results of the stress analysis.

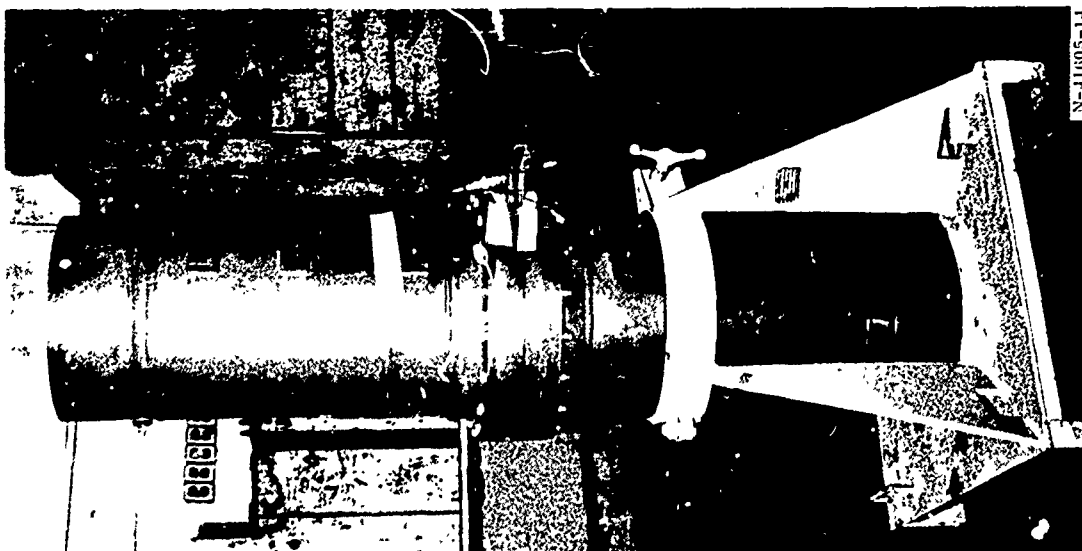


Figure 23. Test Assembly

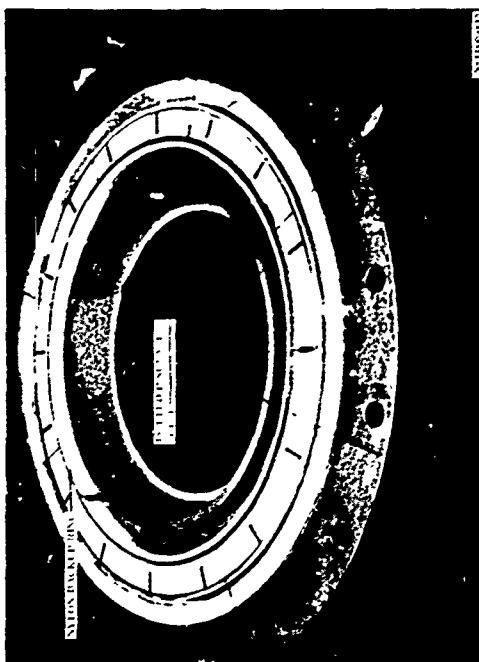


Figure 24. Female Joint Insulation

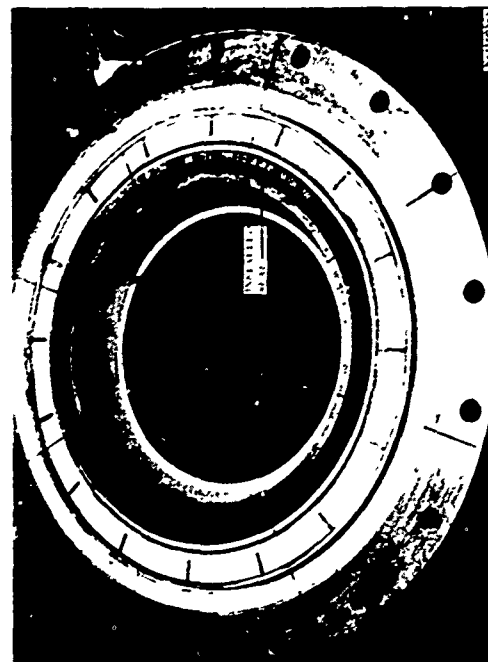
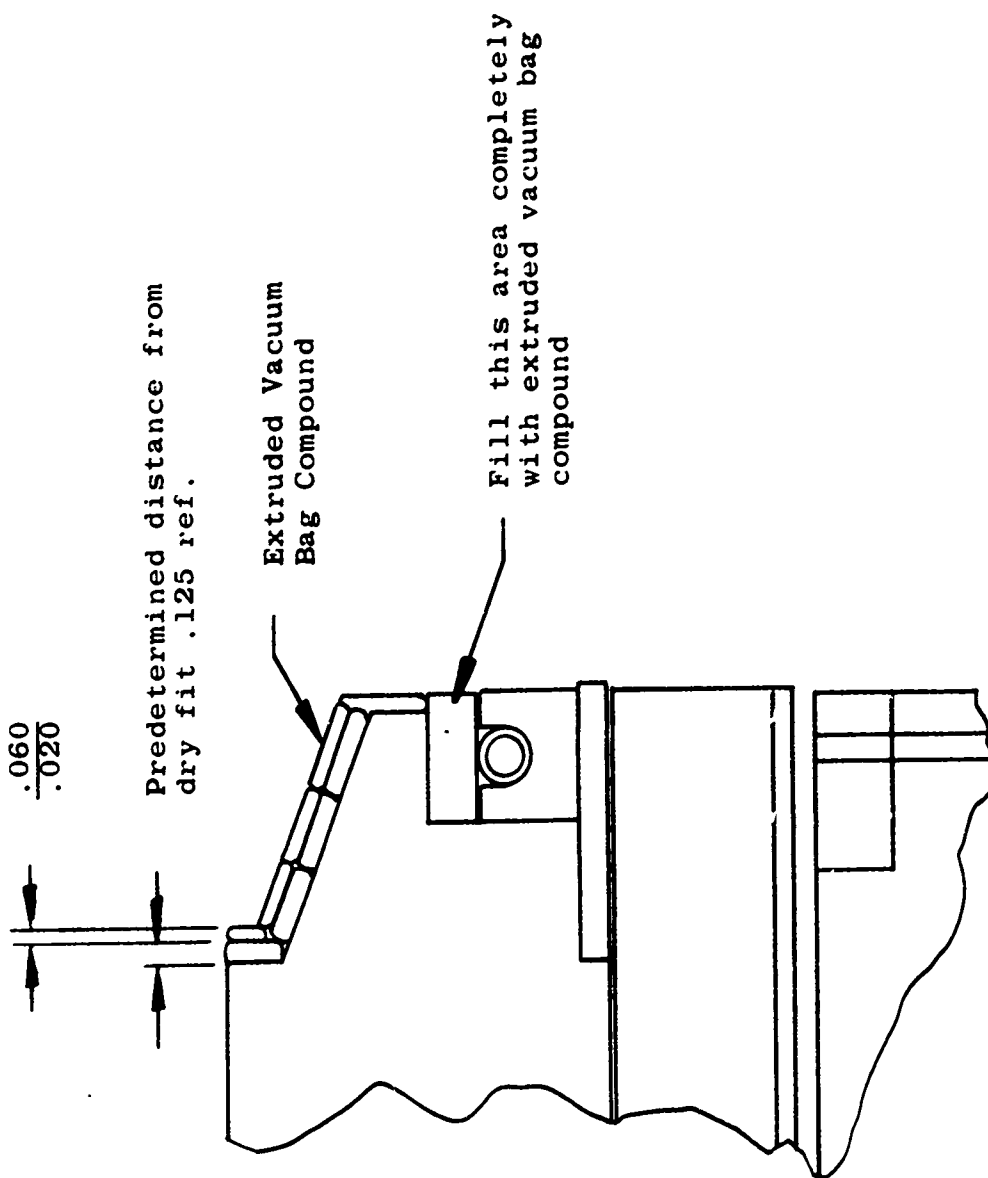


Figure 25. Female Joint with Seal Installed



-01 Detail

Figure 26. Vacuum Bag Compound Fill

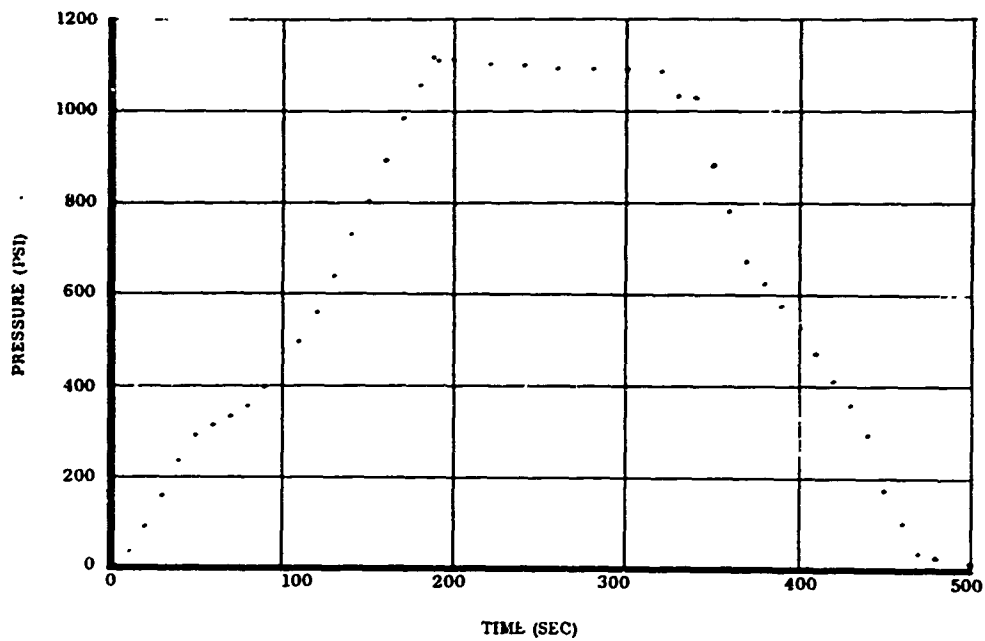


Figure 27. Pressure Trace, Test No. 1, First Pressurization

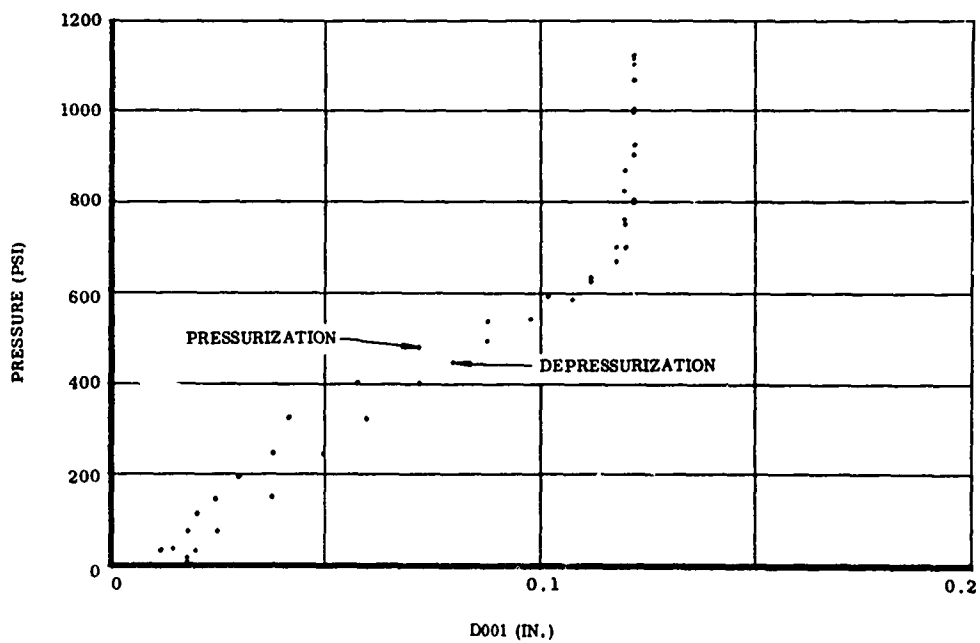


Figure 28. Extensometer Trace, Test No. 1

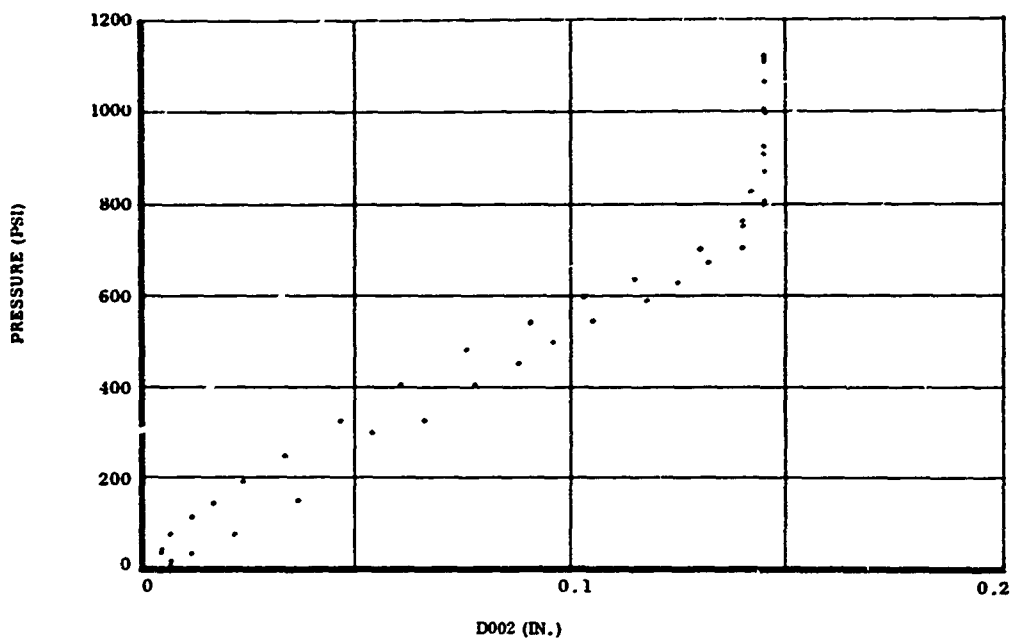


Figure 29. Extensometer Trace, Test No. 1, First Pressurization

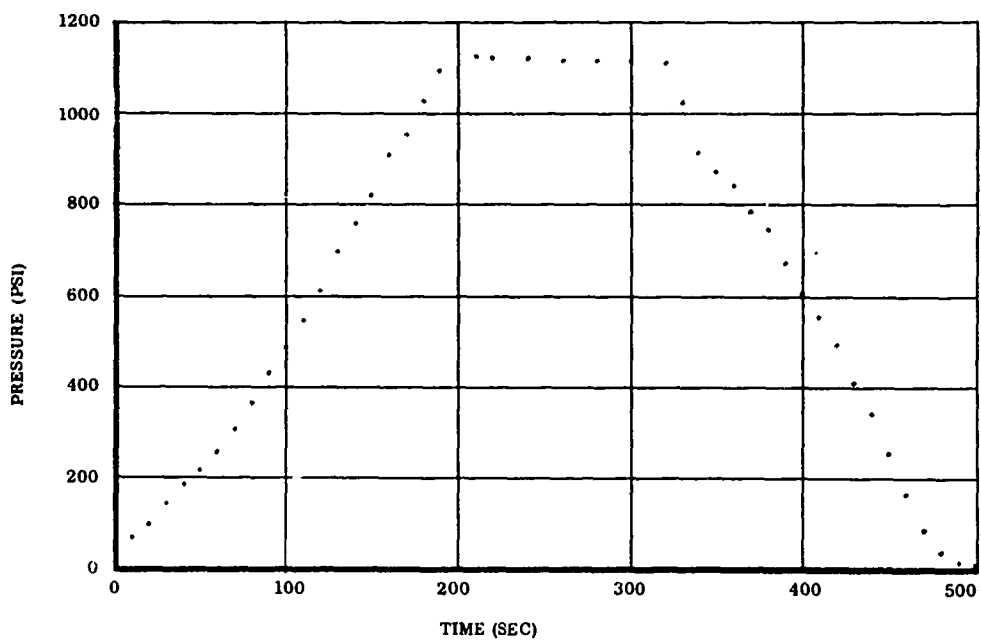


Figure 30. Pressure Trace, Test No. 1, Second Pressurization

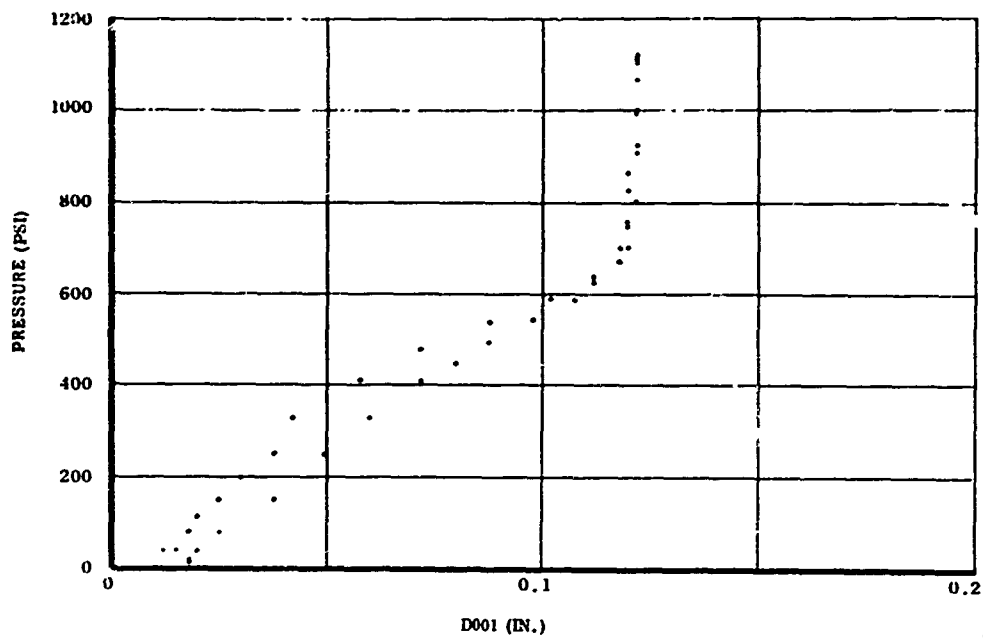


Figure 31. Extensometer Trace, Test No. 1, Second Pressurization

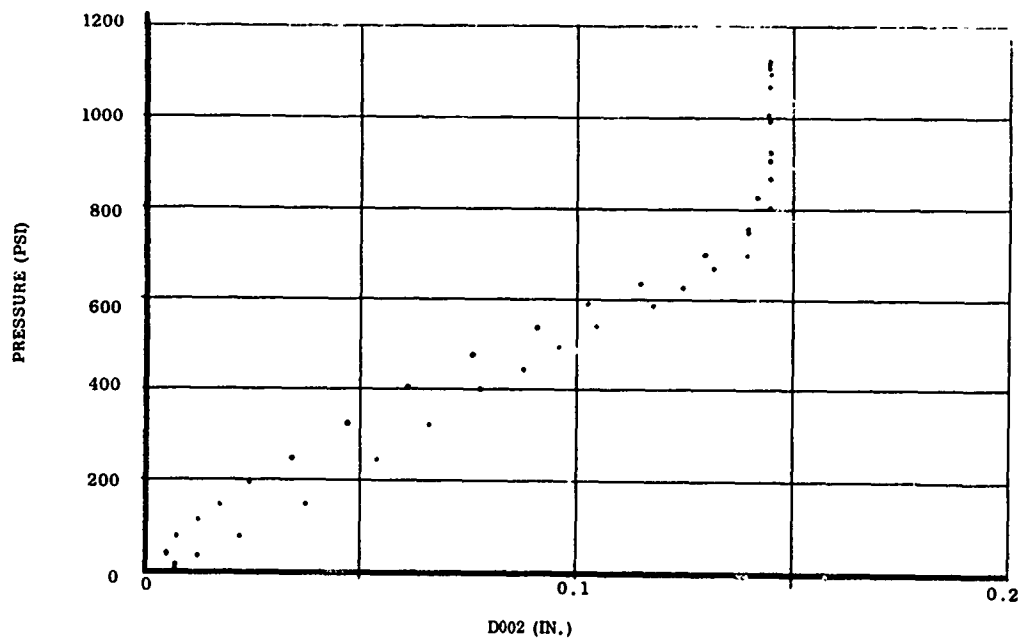


Figure 32. Extensometer Trace, Test No. 1, Second Pressurization

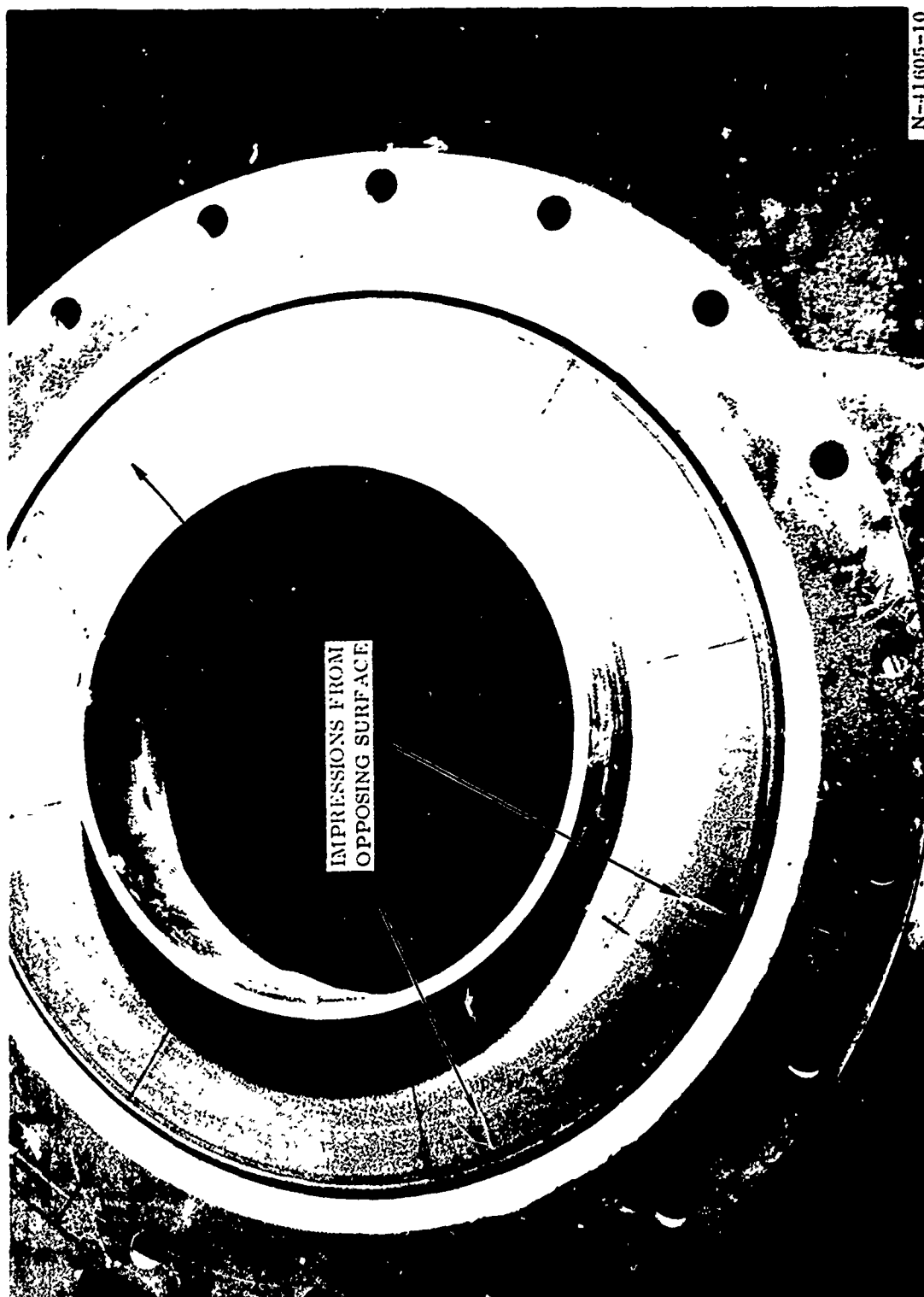


Figure 33. Male Joint

SECTION V

INSULATION AND LINER

A. DESIGN CRITERIA

The internal case insulation was designed to assure that the structural integrity of the case is not degraded by thermal effects throughout the motor operation.

B. MATERIAL SELECTION

1. INSULATION

Insulation materials selected during this quarter for the TU-312L.02 motor were silica cloth phenolic, asbestos-filled NBR (Gen Gard V-44), and silica filled NBR (Gen Gard V-45). The application of these materials is shown in Figure 1. Tables V thru VII present data pertaining to these materials. The selection of these materials was based on the following considerations.

1. Proven performance in solid propellant rocket motors.
2. Proven fabrication techniques.
3. Proven installation techniques.
4. Compatibility with the joint seal design.

The V-45 material was selected as the bladder material to insure that no gas leakage occurs through the fiberglass case wall. It also serves as an insulation for a short period of time (approximately 5 sec) during tailoff.

TABLE V

INSULATION RING

(Generic Name: Silica Cloth Phenolic, Fiberite MX 2600)

Physical Properties

Density (lb/cu ft)	108
Tensile Strength (psi)	14,000
Compressive Strength (psi)	18,000
Flexural Strength (psi)	20,000
Hardness (Barcol)	60

Thermal Properties

Thermal Conductivity @ 500° F (Btu/sq ft-hr-° F/ft)	0.208
Specific Heat @ 150° F (Btu/lb-° F)	0.22
Assumed Ablation Temperature (° F)	800

Method of Fabrication

Tape wrapped and hydroclave cured

Method of Installation

Bonded in place with UF-3195

TABLE VI

CASE INSULATION

(Generic Name: Asbestos Filled NBR, Gen Gard V-44)

Physical Properties

Density (lb/cu ft)	80
Tensile Strength (psi)	1,600
Elongation (%)	200
Hardness (Shore A)	80

Thermal Properties

Thermal Conductivity (Btu/sq ft-°F-hr/ft)	0.10
Specific Heat (Btu/lb °F)	0.42
Assumed Ablation Temperature (°F)	800

Method of Fabrication

0.100 in. sheet stock, hand laid up in mold and autoclave cured

Method of Installation

Bonded in place with UF-1149

TABLE VII

CASE BLADDER

(Generic Name: Silica Filled NBR Gen Gard V-45)

Physical Properties

Density (lb/cu ft)	75
Tensile Strength (psi)	2,000
Elongation (%)	400
Hardness (Shore A)	70

Thermal Properties

Thermal Conductivity (Btu/sq ft-hr-°F/ft)	0.13
Specific Heat (Btu/lb °F)	0.34
Assumed Ablation Temperature (°F)	800

Method of Fabrication

Autoclave cured as 0.060 in. sheet stock

Method of Installation

Bonded in place with UF-3119

The primary insulation materials are the V-44 and silica cloth phenolic. The V-44 is used in the forward dome, segment joints areas, and aft dome, while the silica cloth phenolic forms the transition between the aft dome V-44 and the nozzle inlet. The silica cloth phenolic is used in this higher erosion environment area because of its higher erosion resistance as compared to the V-44 material.

2. LINER

An asbestos filled polyhydrocarbon material (UF-2121) was chosen as the liner material. An epoxy primer (Koropon) was selected, based on past experience, to improve the reliability of the liner to insulation and case bladder bond. The properties of UF-2121 are listed on Table VIII. These materials were selected because of their extensive use with V-44 and V-45 insulation materials and the TP-H1011 propellant in this motor.

C. MATERIAL CONFIGURATION

1. INSULATION

The internal insulation was designed to insure structural integrity in the fiberglass case segments throughout the motor operation. The use of proven materials and manufacturing techniques influenced the insulation design. The insulation was also designed to assure that no undesirable high stresses would be induced in the propellant. The design of these insulation components are discussed relative to the particular area of usage as follows.

a. Forward and Center Case Segments--The insulation design thickness was based on the following factors which are a result of available empirical data and calculated analytical data.

1. Erosion rate of 3.2 mils/second.
2. Exposure time.

TABLE VIII
UF-2121 LINER

Usage

Propellant to Insulation Bond
Propellant to Bladder Bond

Composition (%)

HC Polymer	82.86
MAPO	2.42
ERLA-0500	1.67
Asbestos Floats	10.30
Unixin "E"	1.75
Iron Drier Catalyst	1.00

Cure

Precure: 19 hr at 135°F Full Cure: 96 hr at 135°F

Physical Properties

Density (lb/cu ft)	62.4
Tensile Strength (psi)	198
Elongation (%)	160

Thermal Properties

Thermal Conductivity (Btu/sq ft-hr-°F/ft)	0.10
-------------------------------------------	------

3. Safety factor of 1.5.

4. Thermal protection.

The exact material thickness requirements were obtained by the following relationship:

Design thickness = (erosion rate) x (exposure time) x (safety factor) + thermal protection

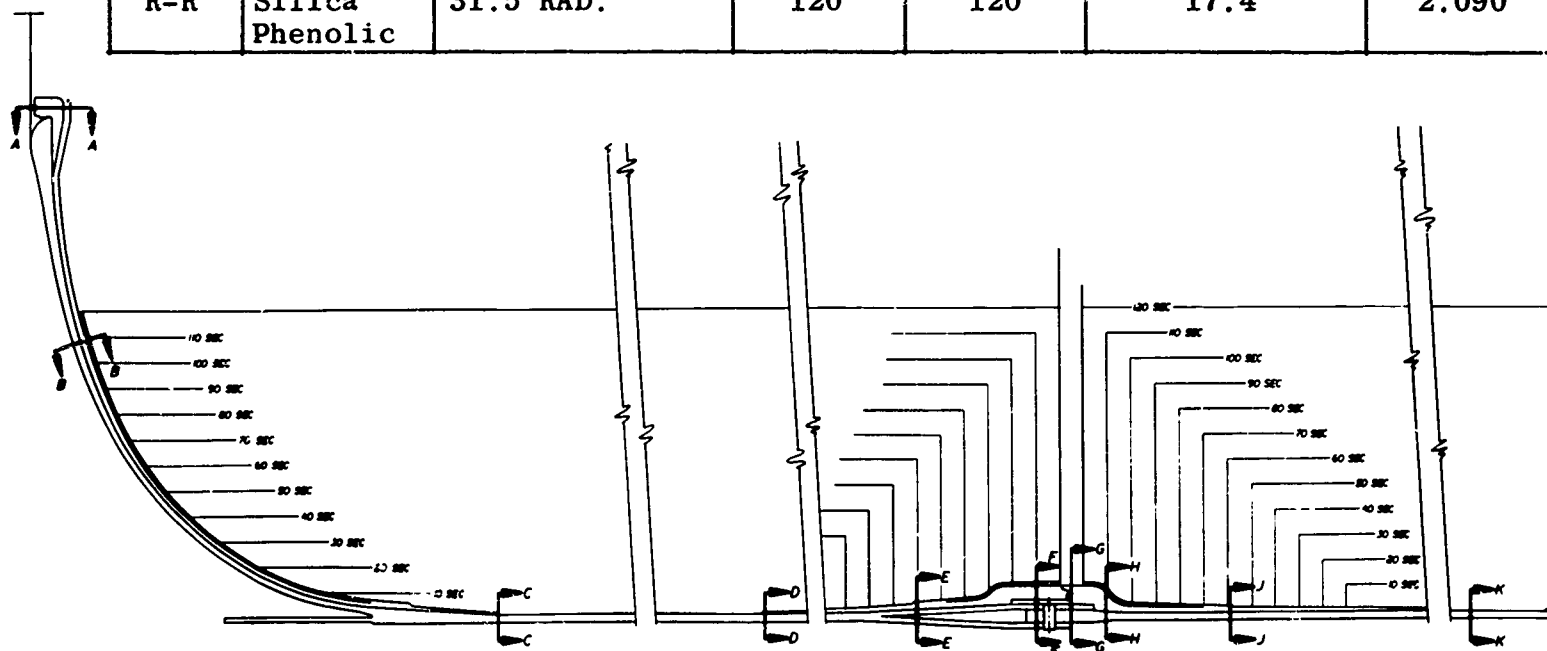
Since the components are fabricated by laying up 0.100 in. thick sheets of V-44 material, the insulation components will taper in 0.100 in. thickness intervals. Figure 34 shows the minimum design thickness requirements at pertinent stations. The forward and center segment insulation is defined on drawings 7U37320 and 7U37321, respectively.

b. Aft Case Segment--The design thickness of the silica cloth phenolic and V-44 in the aft case segment was calculated exactly as that in the previous paragraph with the exception of the erosion rate value. Since the erosion environment changes significantly between the case dome tangent point and the entrance to the nozzle, it was necessary to use a varying erosion rate. Previous motor tests have shown that the erosion rate of these materials correlate closely with various heat transfer and gas flow parameters which were used in the design calculations.

This insulation was designed using the following parameters: (1) erosion rate vs convective heat transfer coefficient (h/C_p) for the silica cloth phenolic, and (2) erosion rate vs Mach No. for V-44. Recent erosion studies indicated that the erosion rate of this silica cloth phenolic correlated closer to the total heat flux, q_t , while the erosion rate of V-44 correlated closer to h/C_p . Figures 35 thru 38 show these four relationships. Predictions of the parameters (heat transfer coefficient, total heat flux, Mach No.) vs location in the motor are given on Figures 39 thru 41.

From these relationships, the aft dome insulation design (described in drawing 7U37322) was obtained. Since the initial design was obtained from the earlier set of parameters mentioned, the design was re-evaluated using the better

SECTION	INSULATION MATERIAL	LOCATION, IN.	EXPOSURE TIME		PREDICTED MAT'L LOSS RATE MIL/SEC	PREDICTED MAT'L LOSS INCHES
			WEB BURN SEC	EFFECTIVE SEC		
A-A	V-44	13.0 RAD.	120		3.2	.384
B-B	V-44	41.48 RAD.	110	120	3.2	.384
C-C	V-44	Fwd dome line	Tailoff		3.2	
D-D	V-44	39.22 fwd of prop. face	Tailoff		3.2	
E-E	V-44	19.61 fwd of prop. face	60		3.2	.192
F-F	V-44	3.27 fwd of prop. face	110	120	3.2	.384
G-G	V-44	Center of slot	120		3.2	.384
H-H	V-44	3.27 aft of prop. face	110	120	3.2	.384
J-J	V-44	19.61 aft of prop. face	60		3.2	.192
K-K	V-45	Cyl. area liner & bladder only	Tailoff		3.2	
L-L	V-44	7.5 aft of aft dome datum	4.0		3.2	.013
M-M	V-44	50.93 RAD.	80	98.4	9.3	.915
N-N	V-44	40.00 RAD.	113	120	17.7	2.124
P-P	Silica Phenolic	37.00 RAD.	120	120	9.3	1.120
R-R	Silica Phenolic	31.5 RAD.	120	120	17.4	2.090



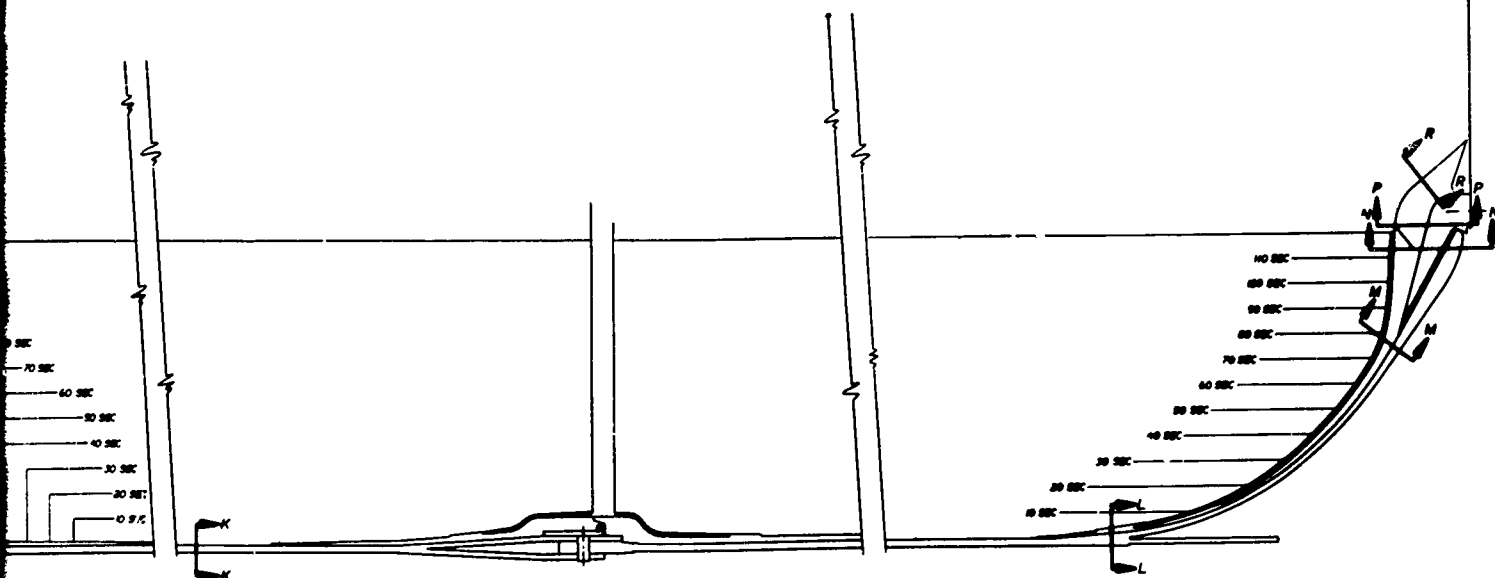
* Total thickness arrived at to meet desired contour and use of .1" st

** .06" thick bladder and .085" thick liner provide thermal protection-
all other areas these items not considered.

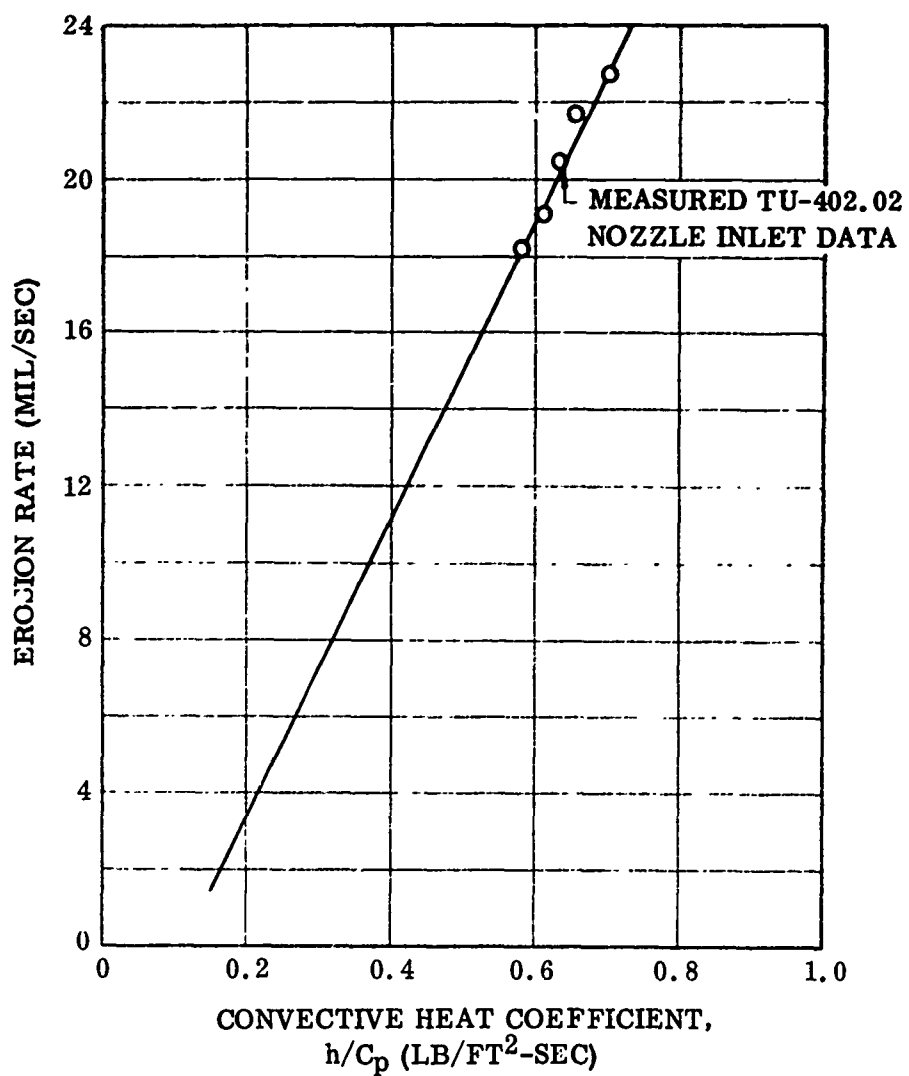
1

Figure 34. TU-312L.02 Insulation Des

MAT'L LOSS INCHES	PREDICTED MAT'L LOSS INCHES	ADDED FOR 1.5 SAFETY FACTOR INCHES	ADDED FOR THERM PROTECT INCHES	INSUL DESIGN THICKNESS INCHES	TOTAL INSUL DESIGN THK. * INCHES	COMBINED SAFETY FACTOR
	.384	.192	.20	.776	.80	2.08
	.384	.192	.20	.776	.80	2.08
			.10	.100	.10	
			.10	.100	.10	
	.192	.096	.145	.433	.50	2.60
	.384	.192	.20	.776	1.50	3.91
	.384	.192	.20	.776	2.10	5.47
	.384	.192	.20	.776	1.30	3.39
	.192	.096	.145	.433	.50	2.60
			.09	.090	** -	-
	.013	.007	.10	.120	.30	23.44
	.915	.458	.184	1.557	1.60	3.25
	2.124	1.062	.20	3.386	3.50	2.47
	1.120	.560	.365	2.045	4.00	3.66
	2.090	1.045	.365	3.500	3.55	2.57



and use of .1" stock.
thermal protection--



10315-36

Figure 35. Predicted Erosion Rate of Silica Cloth Phenolic as a Function of Heat Transfer Coefficient

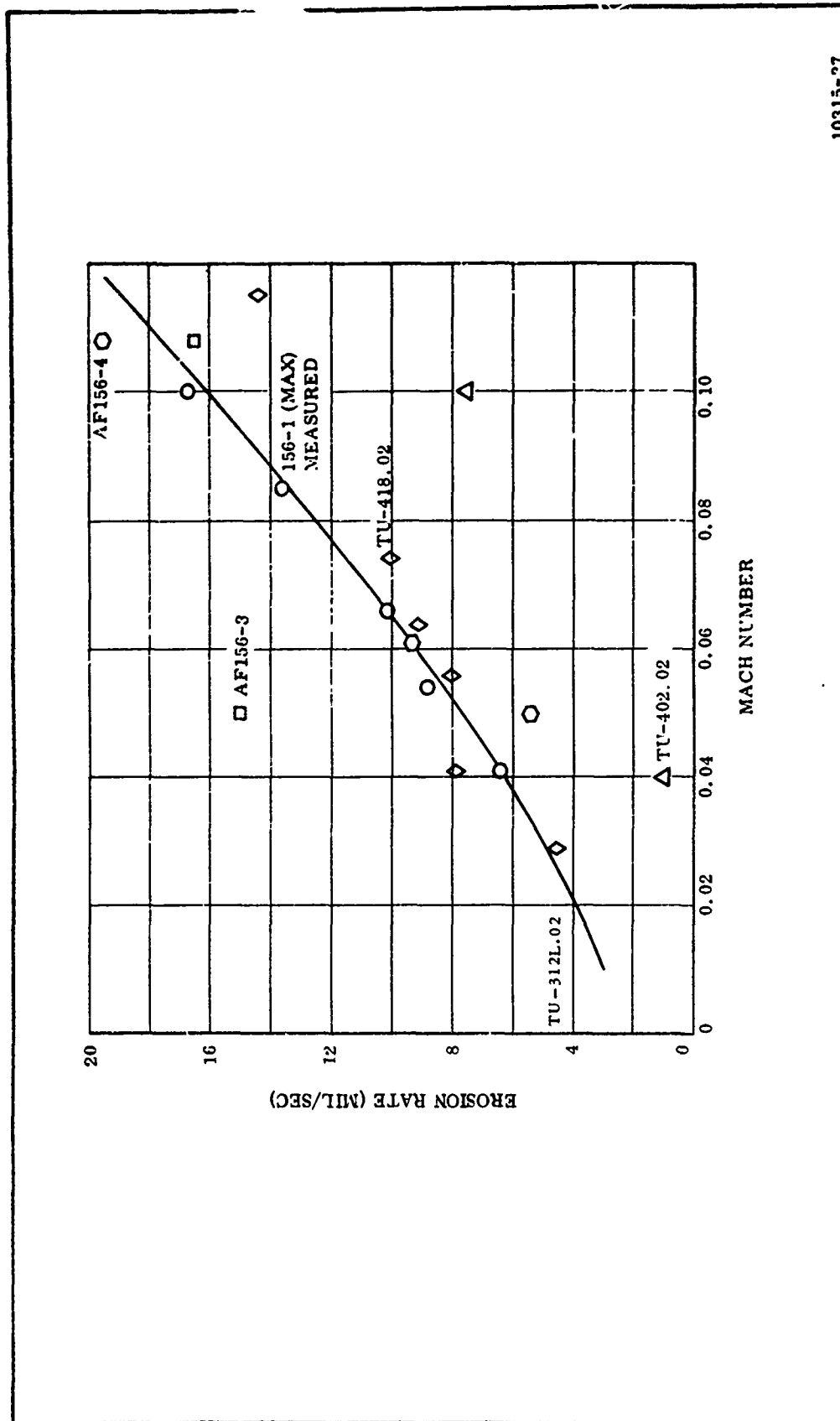
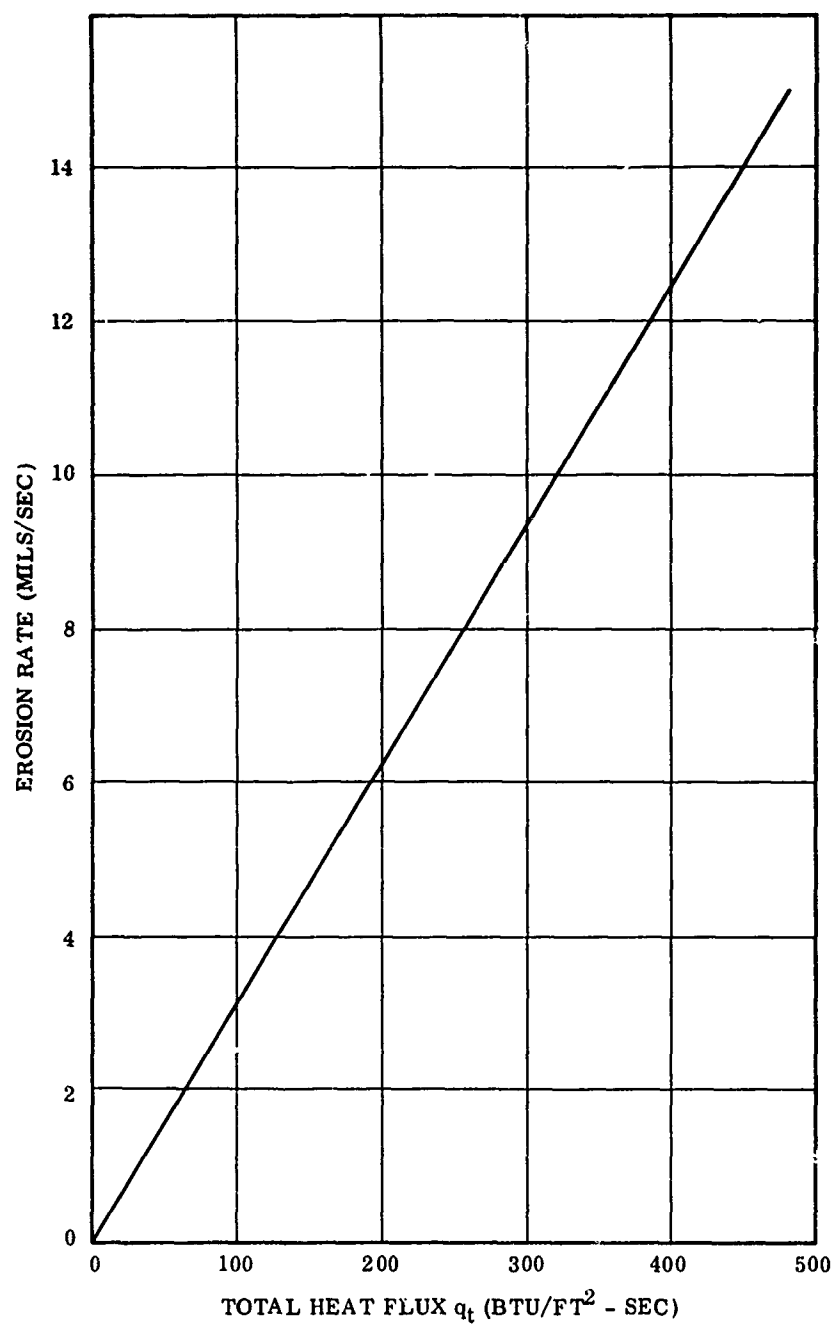
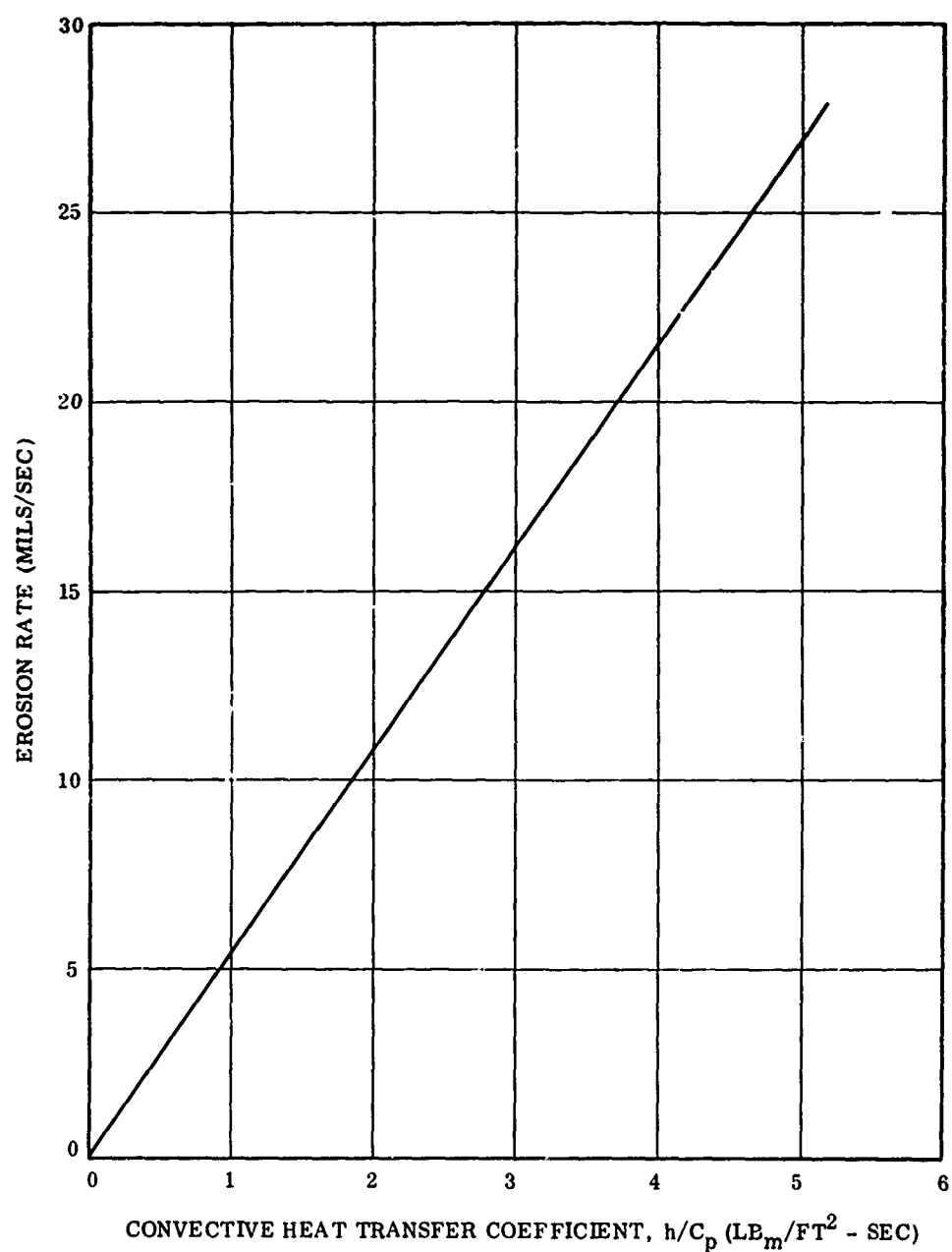


Figure 36. Predicted Erosion Rate of Asbestos Filled NBR vs MACH Number in TU-312L.02 Motor Compared with Measured Erosion in Other Large Motors



12163-28

Figure 37. Silica Cloth Erosion Rate vs Total Heat Flux



12163-29

Figure 38. V-44 Erosion Rate vs Convective Heat Transfer Coefficient

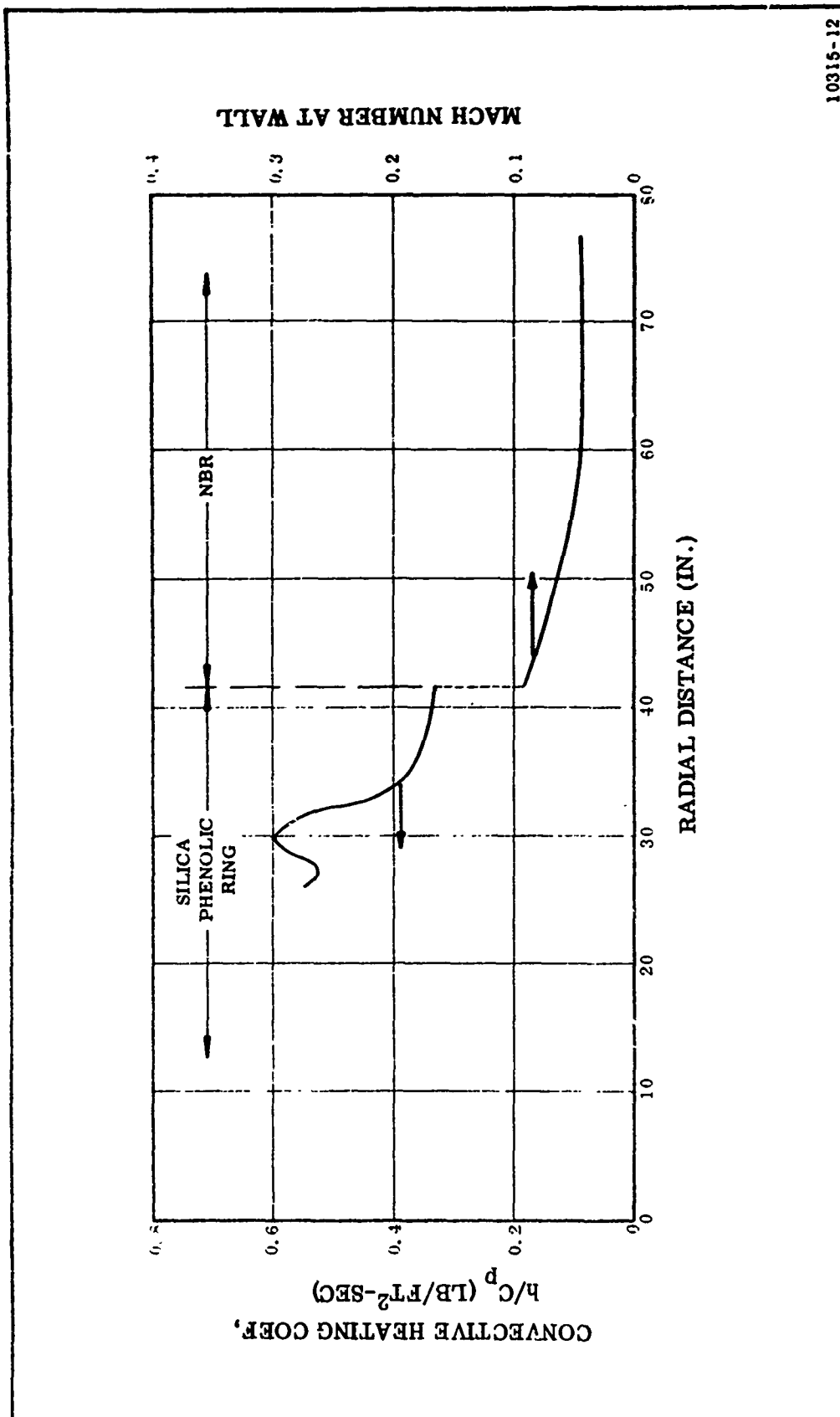


Figure 39. Predicted Mach Flow and Heat Coefficient Through Aft Closure

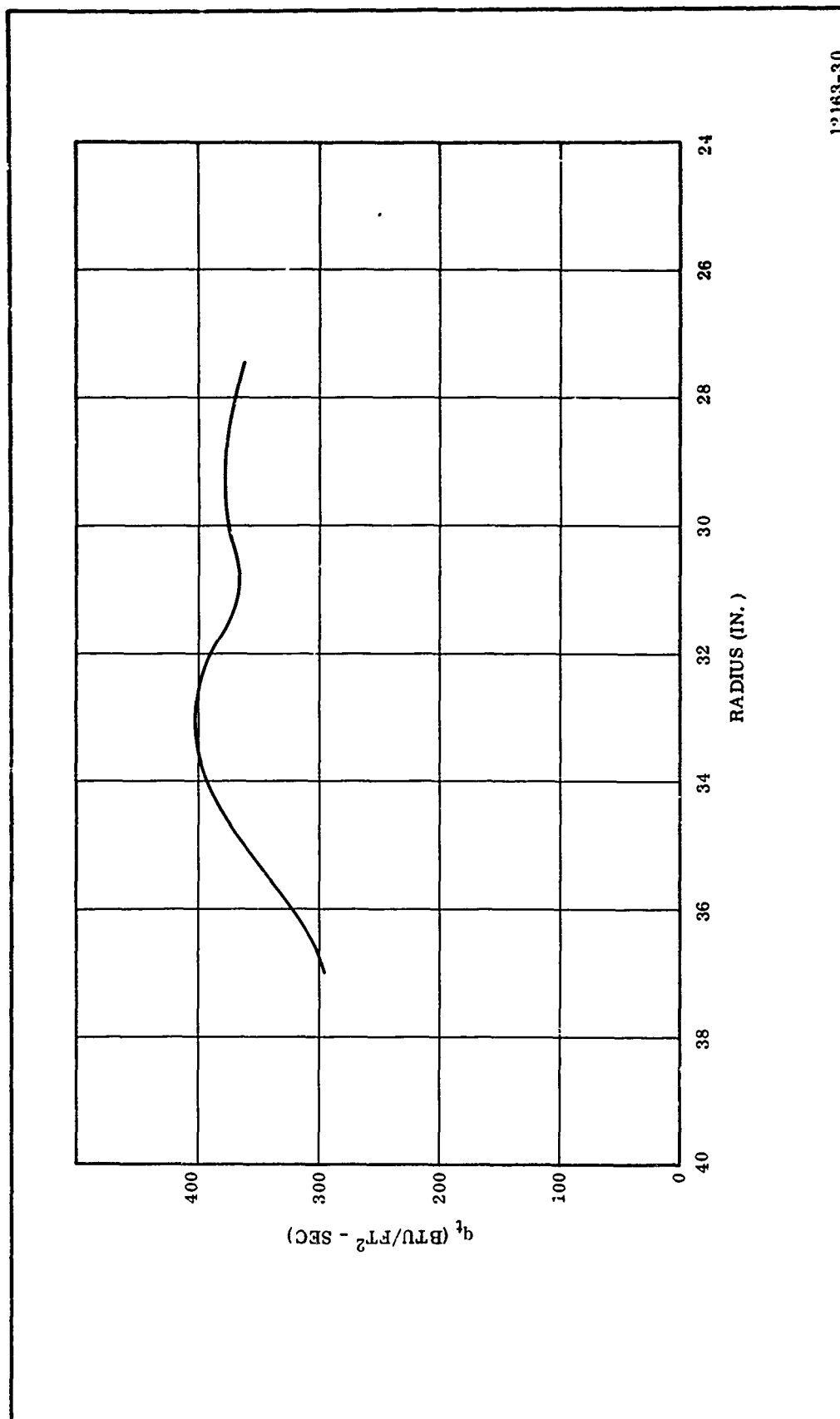
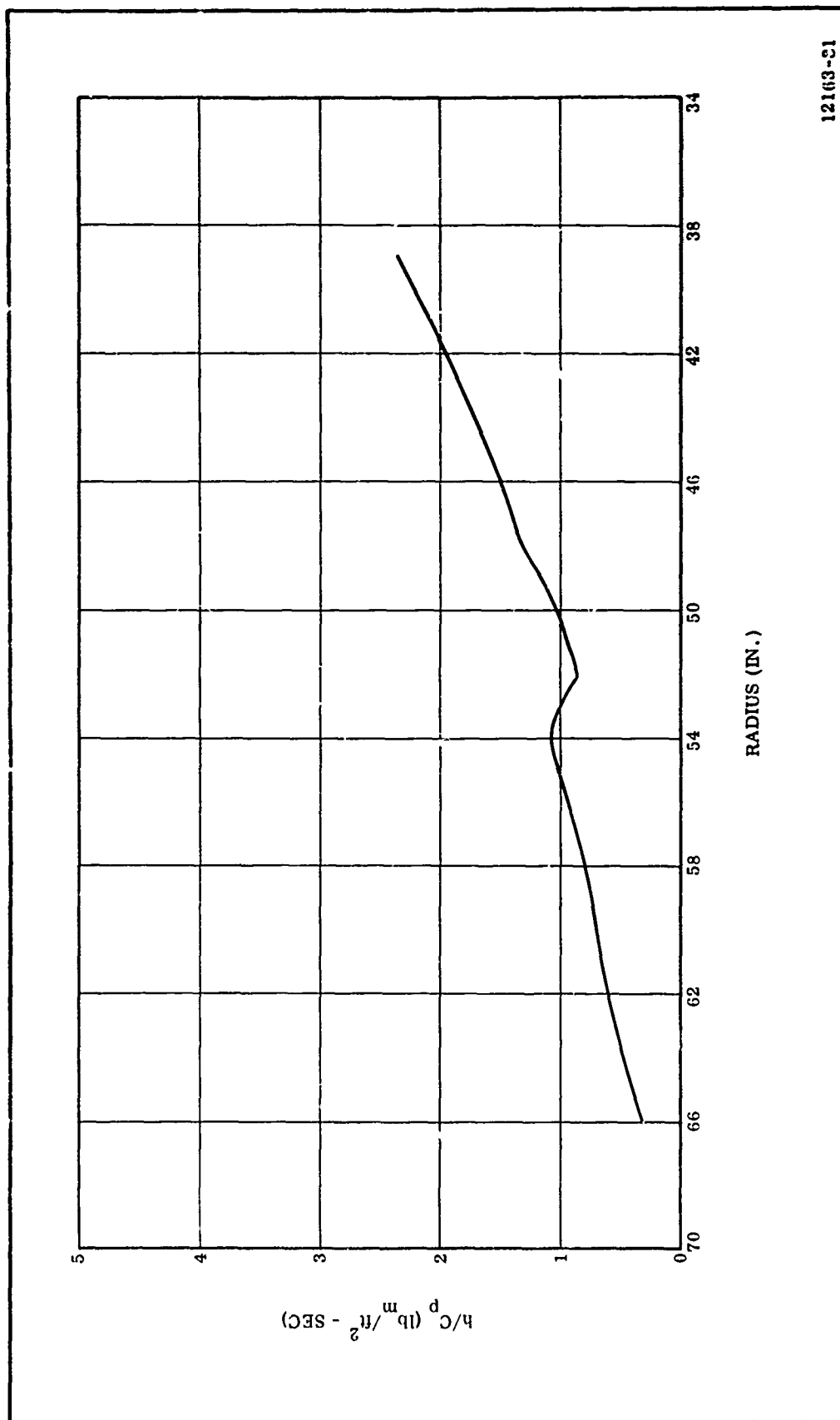


Figure 40. TU-312L.02 Motor Aft Dome Total Heat Flux Variation on Silica Cloth

12163-30



12163-31

Figure 41. TU-312L.02 Motor Aft Dome Heat Transfer Coefficient Variation on Asbestos Filled NBR

7

correlations obtained from the recent erosion studies. Figure 3-4 shows the location and design thicknesses throughout the motor with those thicknesses obtained from the early design parameters, while the resulting safety factor used the latter parameters. The design has an adequate margin of safety.

c. Stress Relief Flap--To prevent undesirable stress in the propellant grain which may cause separations and subsequent excessive propellant burning surface, stress relief flaps of V-44 are used at the end of each propellant grain. The relief flaps provide insulation that is bonded to the propellant and attaches to the primary insulation a given distance away from each end of the propellant grain. The unbonded length of the relief flap openings are one-half the propellant web thickness (20 in.) in the cylindrical portions of the segments and one propellant web thickness (40 in.) in the dome areas. The flap material thickness (0.2 in.) is sufficient to prevent the propellant adjacent to the gaps from burning.

d. Case Joints, Segment to Segment--A pressure-tight seal at the segment joints is provided by a spring loaded, U-shaped neoprene seal installed in a step joint. Design details are covered in Section IV, Joint Seal. Structural and thermal analysis as well as subscale testing has verified this joint design.

2. LINER

The liner system of UF-2121 liner and the Koropon epoxy primer is used over the entire case bladder and case insulation. The epoxy primer is applied in a thin coat to the insulation and bladder to prevent migration between the bladder and liner systems. The UF-2121 liner is then applied to a nominal 0.075 in. thick layer over the entire interior of the Koropon-coated case.

D. BONDING MATERIALS, SEALANTS, AND RELEASE AGENTS

The bonding materials, sealants, and release agents chosen and scheduled for use in the fabrication of the case are listed below.

<u>Material</u>	<u>Use</u>
UF-3119	Bladder (V-45) to case (fiberglass) bonding material.
UF-3195	1. Nylon to bladder bonding material. 2. Primary insulation (silica cloth phenolic) to bladder (V-45) bonding material.
UF-1149	Primary insulation (V-44) to bladder (V-45) bonding material
UF-3196	Pot thermocouples in primary insulation (V-44) during fabrication.
Teflon Tape	Release material to fabricate relief flaps.
Vacuum Bag Compound	1. Case segment to segment joint sealant. 2. Relief flap filler to hold flaps in position during motor manufacture.

The properties of the bonding materials are listed on Tables IX thru XI.

TABLE IX
UF-3119 BONDING MATERIAL

Usage

V-45 Bladder to Fiberglass Case

Composition (%)

Liquid Epoxy Resin (Type II)	35.00
Versamid 140	65.00

Cure

24 hr at 80° F

Physical Properties

Density (lb/cu ft)	658
Tensile Strength (psi)	65.8
Elongation (%)	106
Peel Strength, V-45 to Fiberglass (pli)	53
Tensile Adhesion, V-45 to Fiberglass (psi)	255

Thermal Properties

Thermal Conductivity (Btu/sq ft-hr-° F/ft)	0.10
--------------------------------------------	------

TABLE X
UF-3195 BONDING MATERIAL

Usage

Nylon Ring to V-45 Bladder
Silica Phenolic Ring to V-45 Bladder

Composition (%)

Liquid Epoxy Resin (Type II)	27.52
Versamid 140	51.09
Asbestos Floats	20.40
Cab-O-Sil	0.99

Cure

4 hr at 170° F or
24 hr at 80° F

Physical Properties

Density (lb/cu ft)	60.15
Tensile Strength (psi)	1,510
Elongation (%)	59
Modulus (psi x 10 ⁴)	4.7
Peel Strength 180° (pli)	63

TABLE XI
UF-1149 BONDING MATERIAL

Usage

V-44 Insulation to Bladder
V-44 Insulation to Silica Phenolic Insulation
V-44 Insulation to V-44 Insulation

Composition (%)

Epon 828	29.16
Versamid 140	33.33
Genamid 2000	16.66
M-Floats (asbestos)	20.85

Cure

24 hr at 80° F or
5 hr at 135° F or
3 hr at 170° F

Pot Life

2.5 hr in 100 gm quantities

Physical Properties

Density (lb/cu ft)	63.4
Tensile Strength (psi)	580
Elongation (%)	89
Tensile Adhesion (psi)	
NBR to Steel	630
Steel to Steel	1,160

E. BOND VERIFICATION TESTING

The test plan for the verification of liner and insulation bonds was compiled, submitted, and received subsequent Air Force approval. The tests planned are separated into eight phases: Phases IA, IB, IIA, IIB, III, IVA, IVB, and IVC. Each phase is discussed below.

1. PHASE IA

Tests under Phase IA were established to determine what material would be suitable to bond the replacement V-45 bladder into the case segments after the original bladder was removed and the case surface was cleaned of loose glass. Since it would be very difficult to duplicate the condition of the glass composite in the 156-8 case segments, it was decided to perform these tests directly on the interior of the segments. A conservative minimum acceptance limit of 70 psi tensile adhesion was established to test the bond to avoid further damage to the glass surface through specimen failure.

Two of Thiokol's most reliable bonding materials (UF-3119 and UF-3177) were chosen. Both materials have been used extensively in past programs.

A special test apparatus was designed and fabricated (Figures 42 and 43). This apparatus adapted an air piston to the conventional tenshear plate which is normally used on the Instron testing machine. The tenshear plate test uses a 7 to 8 sq in. bond area. The air piston was mounted in a frame which reacted the load back to the segment wall to apply direct tension to the specimen. Accurate loading was applied to the tenshear plate through accurately controlled air pressure. V-45 bladder material was bonded to the tenshear plate on one side with a standard adhesive. The other side of the V-45 was bonded to the case wall with the test materials where it was cured for 16 hr (min).

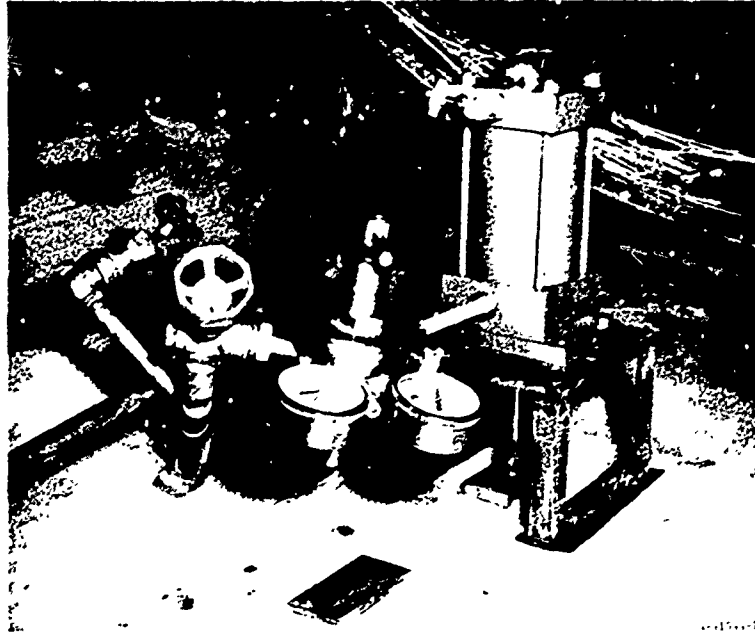


Figure 42. Bond Test Apparatus Connected to Specimen

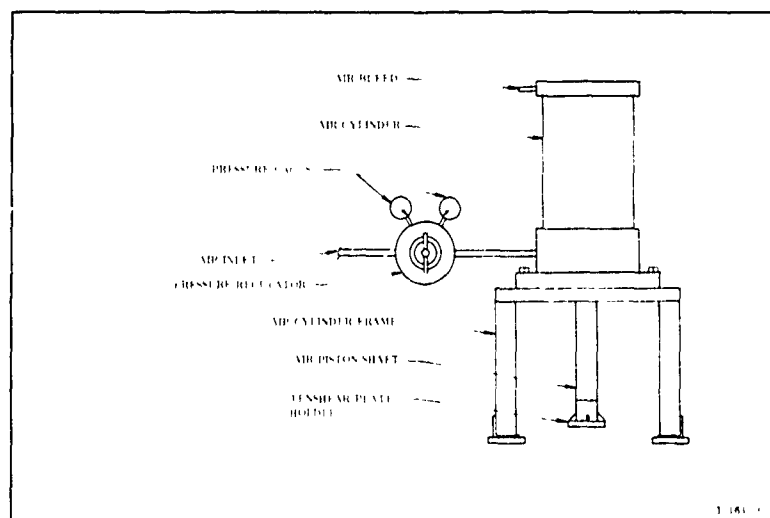


Figure 43. Apparatus for Testing Tenshear Plates Bonded in TU-12L.02 Case

Two UF-3119 samples and two UF-3177 samples were bonded to each of the aft and center segments and tested. Only UF-3119 samples were prepared and tested in the forward segment. The tensile force was applied to each bond in 10 lb increments. The load was held at each level for one minute.

Of the 10 samples tested, only one failed. This sample used UF-3177 as a bonding material and failed at the final loading. Examination of this specimen revealed that it had not seated properly and that a fraction of the area had been bonded. Measurement of the effective bond area and calculation of the load applied revealed that the actual bond stress was approximately 120 psi at failure.

Although both of the test materials met the bond requirements, UF-3119 was selected because of its better processibility due to longer pot life.

2. PHASE IB

Phase IB was designed to determine the effect of the silicone dioxide release agent from Trevarno cloth on bonds to the V-45 and possible methods of removing this release agent. In past programs, insulations and bladders have been cured with Trevarno cloth containing silicone dioxide release agent; however, these items have also been buffed on the surface following cure. Since buffing of the 0.060 in. thick bladder of the 156-8 would produce thin spots and possible holes, another method of cleaning required development.

Tenshear samples consisting of two tenshear plates bonded together with V-45 (cured with Trevarno cloth) between the plates were prepared. The surfaces of the V-45 used in the specimens were prepared by various test methods. The methods used are shown in Table XII. Three samples for each condition were prepared and tested.

The results of the test showed no effect of the release agent in that all samples failed at a minimum of seven times the established minimum acceptable bond to the case.

TABLE XII
V-45 (CURED WITH TREVARNO CLOTH) ADHESION TO UF-3119
(PHASE IB)

Sample	Steel						
Adhesive	UF-3195						
Insulation	V-45						
Cleaning Method	None	MEK Wipe	Soap and Water	Trichloro-ethylene Wipe	Soap and Water (H ₂ O) Rinse	Sanblast	Wire Brush
Adhesive	UF-3119	UF-3119	UF-3119	UF-3119	UF-3119	UF-3119	UF-3119
Number of Tensile Adhesion Samples	3	3	3	3	3	3	3
Tensile Adhesion Values (psi)	534	551	525	526	420	636	581
Failure Mode	All samples failed in th UF-3119.						

The MEK wipe method was chosen because this is necessary to remove any other contaminants.

3. PHASE IIA

Phase IIA was designed to verify the compatibility of the bond system between the insulation and propellant using actual raw materials and simulated processes planned for the manufacture of the TU-312L.02 motor. Samples will consist of V-44 insulation, Koropon primer, UF-2121 liner, and TP-H1011 propellant (Table XIII). Since this system historically has had a high reliability, these tests are designed to reveal any possible unnoticed deficiency in the raw materials or planned processes. These tests will be completed prior to applying the UF-2121 liners in the TU-312L.02 motor segments.

Two types of specimens will be prepared and tested. The tenshear specimen will be used to determine the tensile adhesion. The load will be applied with the Instron testing machine in direct tension. Figure 44 shows the apparatus and sample. The specimen will have a 7 to 8 sq in. bond area.

The 180 deg peel specimen is used qualitatively to determine the ability of the bond to withstand peeling action. The specimen is one inch wide. Figure 45 shows a typical specimen and the apparatus.

4. PHASE IIB

Phase IIB is designed to accomplish the same objectives as Phase IIA except with relation to the V-45 bladder. Since the bladder is in the center of the segment and the UF-2121 liner in this area receives an intermediate cure, time variations are not entered at this point. See Table XIV for test details.

Again these tests will be complete prior to applying the liner to the TU-312L.02 motor.

TABLE XIII
PHASE IIA COMPATIBILITY TEST
OF PROPELLANT TO INSULATION BOND

Insulation	V-44		
Barrier	Koropon		
Liner	UF-2121		
Liner Cure	Minimum 12 hr ambient 26 hr at 135° F	Maximum Forward and Aft Segment 48 hr at 135° F	Maximum Center Segment 66 hr at 135° F
Propellant	TP-H1011	TP-H1011	TP-H1011
ASTM 180 deg Peel pl ^h Samples	5	5	5
Tenshear Tensile Adhesion Samples	5	5	5

TABLE XIV
UF-2121 TO MEK WIPED V-45 BLADDER MATERIAL
(PHASE IIB)

Insulation	V-45
Clean	MEK Wipe
Barrier	Koropon
Liner	UF-2121
Propellant	TP-H1011
ASTM 180 deg Peel Samples	5
Tenshear Tensile Adhesion Samples	5

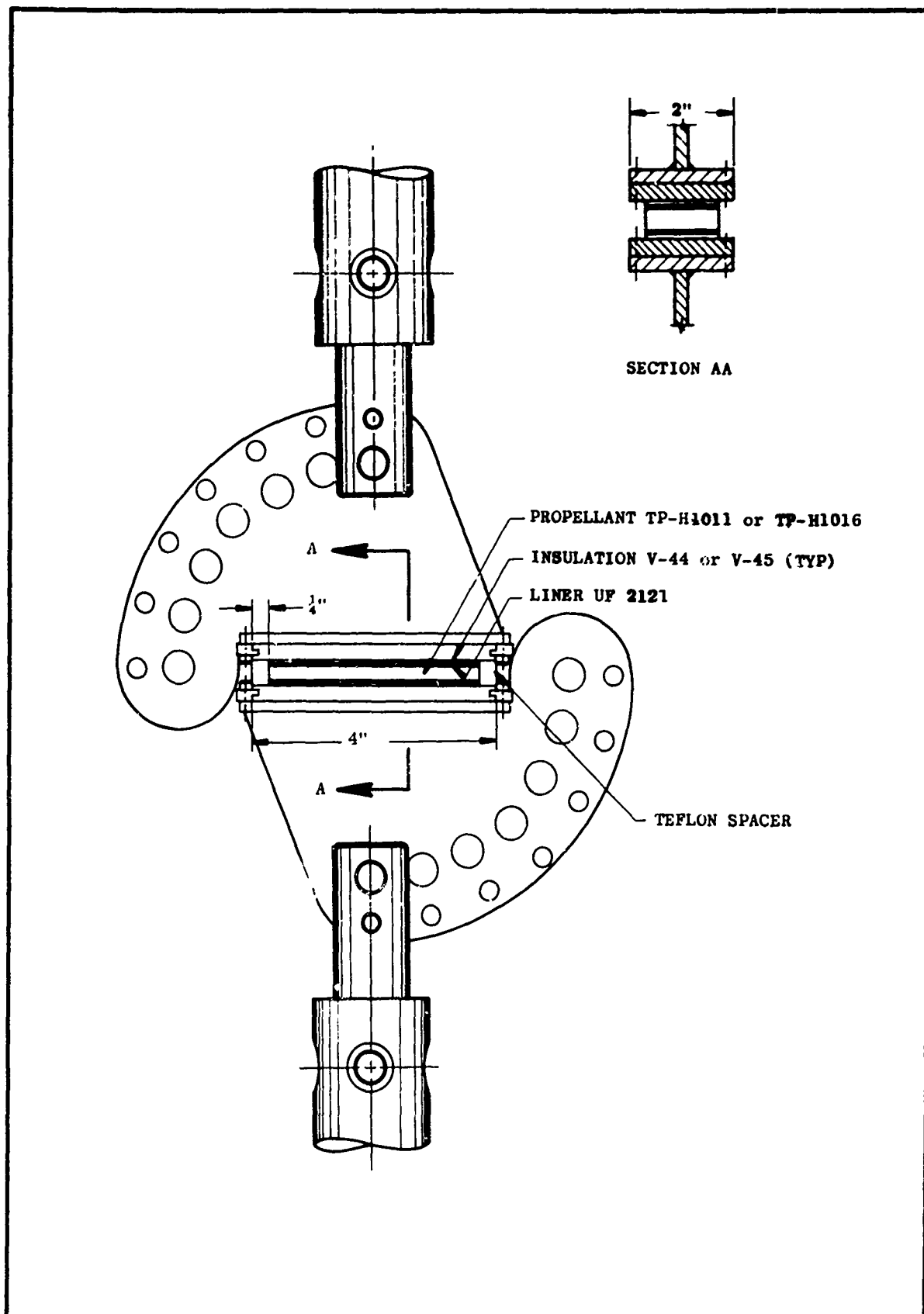


Figure 44. Tenshear Test Apparatus

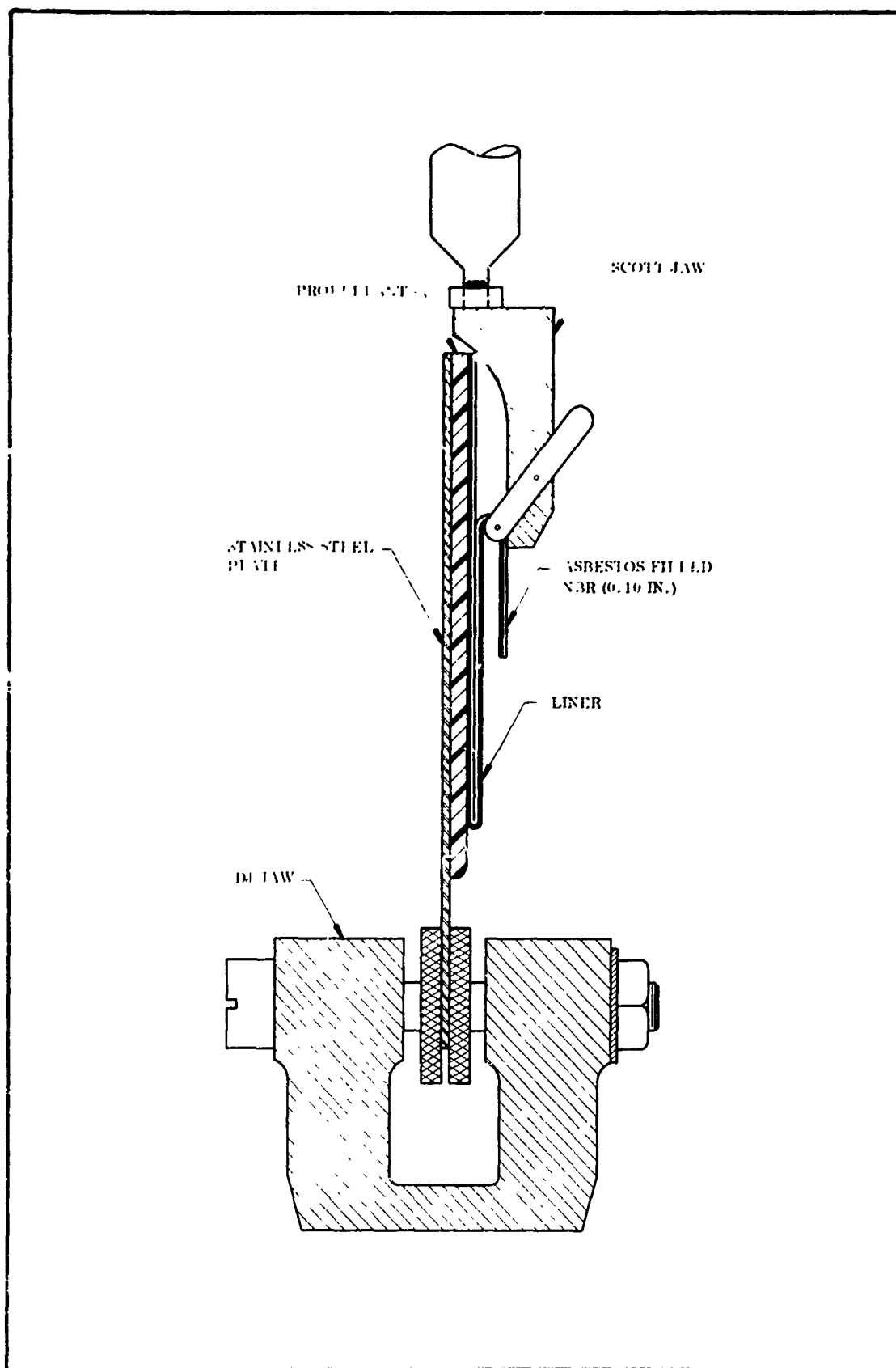


Figure 45. 180 Deg Peel Test Specimen and Arrangement

5. PHASE III

The Phase III tests are designed to verify the compatibility of the bond of the igniter propellant to the internal insulation of the igniter.

These test specimens will be prepared using actual planned raw materials and simulated processes for the igniter. The make-up of the test specimens and number are shown in Table XV.

6. PHASE IVA

Phase IVA testing was established to verify the integrity of the bonds achieved when installing the bladder in the TU-312L.02 case. Two tenshear plates were bonded to the installed bladder at random locations in each case segment. The specimens were then tested to 70 psi bond load using the apparatus described in Phase IA. All specimens successfully withstood the 70 psi bond load.

7. PHASE IVB

Phase IVB is designed to verify the bond strength between the TU-312L.02 insulation and propellant grain. These samples will be prepared from actual material batches from the motor and will be processed with the motor. Past history has reflected no appreciable difference in bonds to V-44 vs bonds to V-45; consequently, only V-44 will be used in this phase. Also, the V-44 bonds represent the processing extremes because the material is located in the ends of each segment. Table XVI depicts the test matrix.

TABLE XV
TU-312L.02 IGNITER COMPATIBILITY TESTS
(PHASE III)

Insulation	V-44
Barrier	Koropon
Liner	UF-2121
Propellant	TP-H1016
ASTM 180 deg Peel Samples	5
Tenshear Tensile Adhesion Samples	5

TABLE XVI
TU-312L. 02 INPROCESS TESTS
(PHASE IVB)

Motor Segment	Forward	Center	Aft
Insulation	V-44	V-44	V-44
Barrier	Korocon	Korocon	Korocon
Liner	UF-2121	UF-2121	UF-2121
Cure	Minimum 3 hr Ambient 26 hr at 135°F	Minimum Maximum	Minimum Maximum
		56 hr at 135°F	--
Propellant	TP-H1011	TP-H1011	TP-H1011
ASTM 180 deg Peel Samples	5	5	5
Tenshear Tensile Adhesion Samples	5	5	5

8. PHASE IVC

Phase IVC is designed to verify the bonds achieved in processing the 156-8 igniter motor. These samples will be prepared using material from the actual batches used in the 156-8 igniter and will accompany the igniter motor through all processing. The sample make-up and number are shown in Table XVII.

TABLE XVII
TU-312L.02 IGNITER INPROCESS TESTS
(PHASE IVC)

Insulation	V-44
Liner	UF-2121
Propellant	TP-H1016
ASTM 180 deg Peel Samples	5
Tenshear Tensile Adhesion Samples	5

SECTION VI
PROPELLANT AND GRAIN

A. GRAIN DESIGN SUMMARY

1. BALLISTIC DESIGN

The grain for the TU-312L.02 motor was designed during this first quarter. A three segment center perforated grain with two 4 in. slots separating the segments was selected for this motor. The bore diameter of the grain was sized by determining the propellant weight required to produce a nominal total impulse of 118,811,500 lbf-sec (sea level) at 100° F, based upon a 3 sigma variation of ± 1 percent in total impulse as determined from Stage I MINUTEMAN data. Compliance with the RFP requirement of 120,000,000 lbf-sec maximum (sea level) total impulse is assured at the maximum motor operating temperature.

The propellant weights were determined by using the following.

1. As many actual measurements as could be obtained from each of the three case segments.
2. Current insulation, liner, and Koropon primer designs.
3. Calculated uncured propellant volumes multiplied by a theoretical uncured density of 0.06405 lbm/in.³ corrected by a 0.991 factor to compensate for propellant curing shrinkage.

Refinements in the ballistic performance of the TU-312L.02 motor required a change in core diameter to compensate for corrected propellant weights and propellant weight variation resulting from minor modifications in insulation designs.

2. GRAIN STRESS ANALYSIS

A comprehensive stress analysis of the propellant structure of the 156-8 (Thiokol TU-312L.02) motor grains was accomplished. The analysis was based on an axisymmetric, elastic, stiffness matrix method developed at Thiokol and programmed for the IBM 7040 computer.

The calculated stress and strain patterns for conditions of cure, thermal shrinkage, and pressurization were calculated and compared to the failure criteria. The failure criteria used was the Smith failure boundary derived from biaxial and uniaxial propellant tests. The analysis showed satisfactory margins between the calculated imposed loads and the failure boundary in all cases.

The grain web thickness of all three segments is 52 percent, and from fore to aft, the length to diameter ratios are 0.714, 1.37, and 0.693. Since the forward and aft segments have nearly identical geometric constraints, only the former was analyzed. The TU-312 grains are of TP-H1011 propellant, which is also used in the Stage I MINUTEMAN. The loading conditions considered in this study were cure and thermal shrinkage, pressurization, and 1 g lateral slump.

In general, the TU-312 studies conducted during this first quarter have defined (1) deformations caused by stress inducing loads, and (2) worst stress-strain conditions in the motor compared to the capability limits.

The grid boundary and the actual grains are not precisely the same, as can be seen by comparing Figures 46 and 47 to Figure 1. From a structural standpoint, no significant differences will be found.

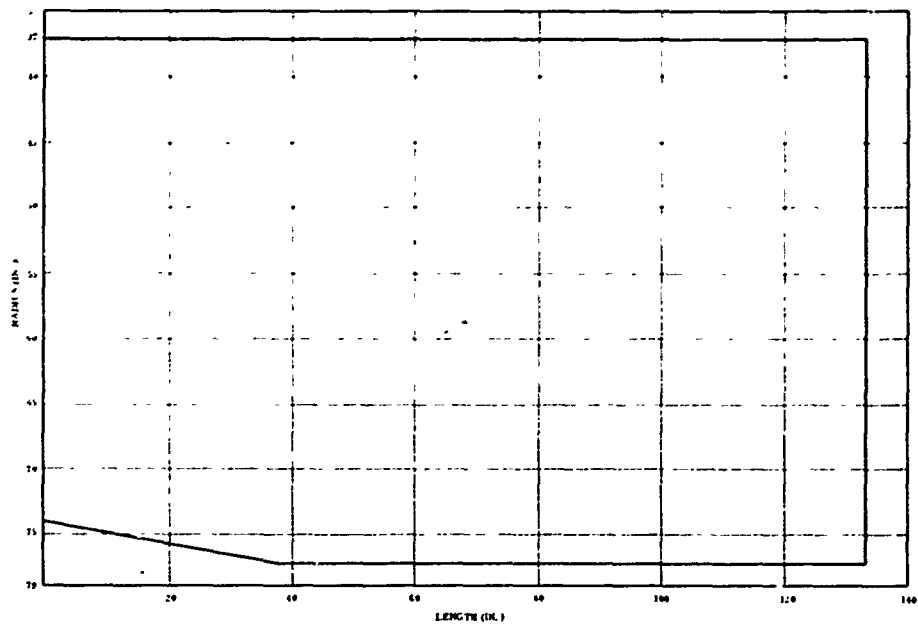


Figure 46. Schematic Sketch of Half of TU-312 Center Segment Grain (Stress Analysis Grid Boundary)

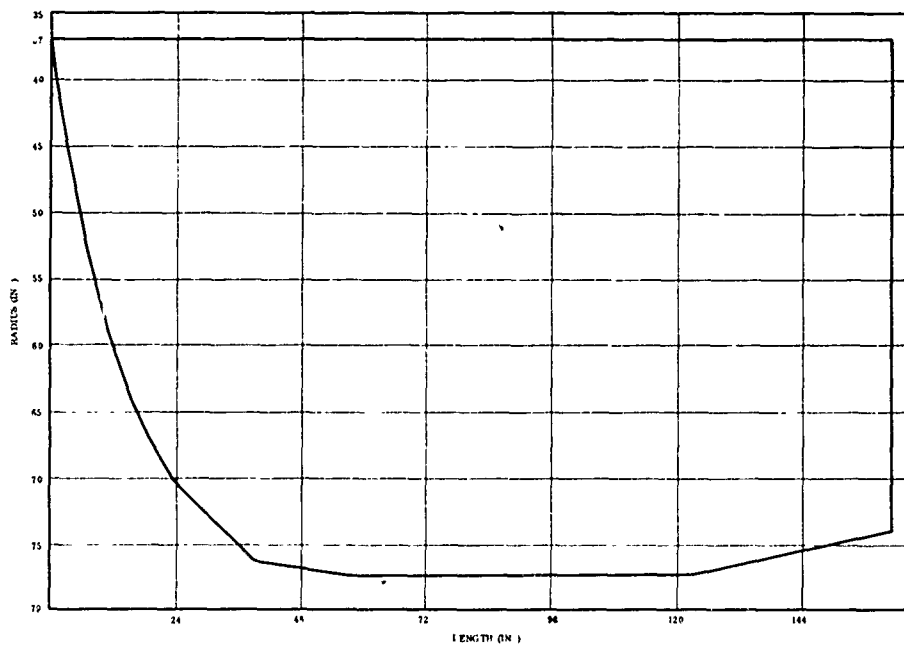


Figure 47. Schematic Sketch of TU-312 Dome Segment Grain (Stress Analysis Grid Boundary)

The cure and thermal shrinkage deformations of the center and dome segments at + 60° F are presented, respectively, in Figures 48 and 49. The worst stress-strain conditions for each of these grains due to the + 60° F soak temperature are tabulated in Table XVIII along with the 1 g lateral slump.

The deformation patterns due to pressure are not significantly different than those shown for the cure and thermal shrinkage as can be seen in Figures 50 and 51 . Note that the pressure case was superimposed on the cure and thermal shrinkage deformed grid. The worst stress-strain conditions for each grain pressurized condition are also tabulated in Table XVIII.

Computation of the failure criteria is very straight forward and requires only superposition of the above tabulated stresses and strains on the proper failure boundary. Figure 52 presents the dilatational failure boundary. Since the failure boundary is independent of path, only the end points for each case are shown. As can be seen in Figure 52 , dilatational load conditions do not approach the boundary limit. Figure 52 presents the distortional failure boundary, where pressure effects are considered independently of shrinkage effects. Again, no point reaches the boundary. Finally, the distortional and dilatational effects are accumulated and presented in Figure 52.

As has been seen above in Figure 52, the TU-312 grains do not approach the failure boundary for any specific loading conditions. Further, even the accumulated loading effects do not approach the boundary. To illustrate the excellent structural characteristics of the TU-312 grains, margins of safety were compiled for the various loads (Table XIX). As can be seen, the least margin is greater than 1.79; hence, it must be assumed that no deleterious propellant structural conditions will occur in the TU-312 motor.

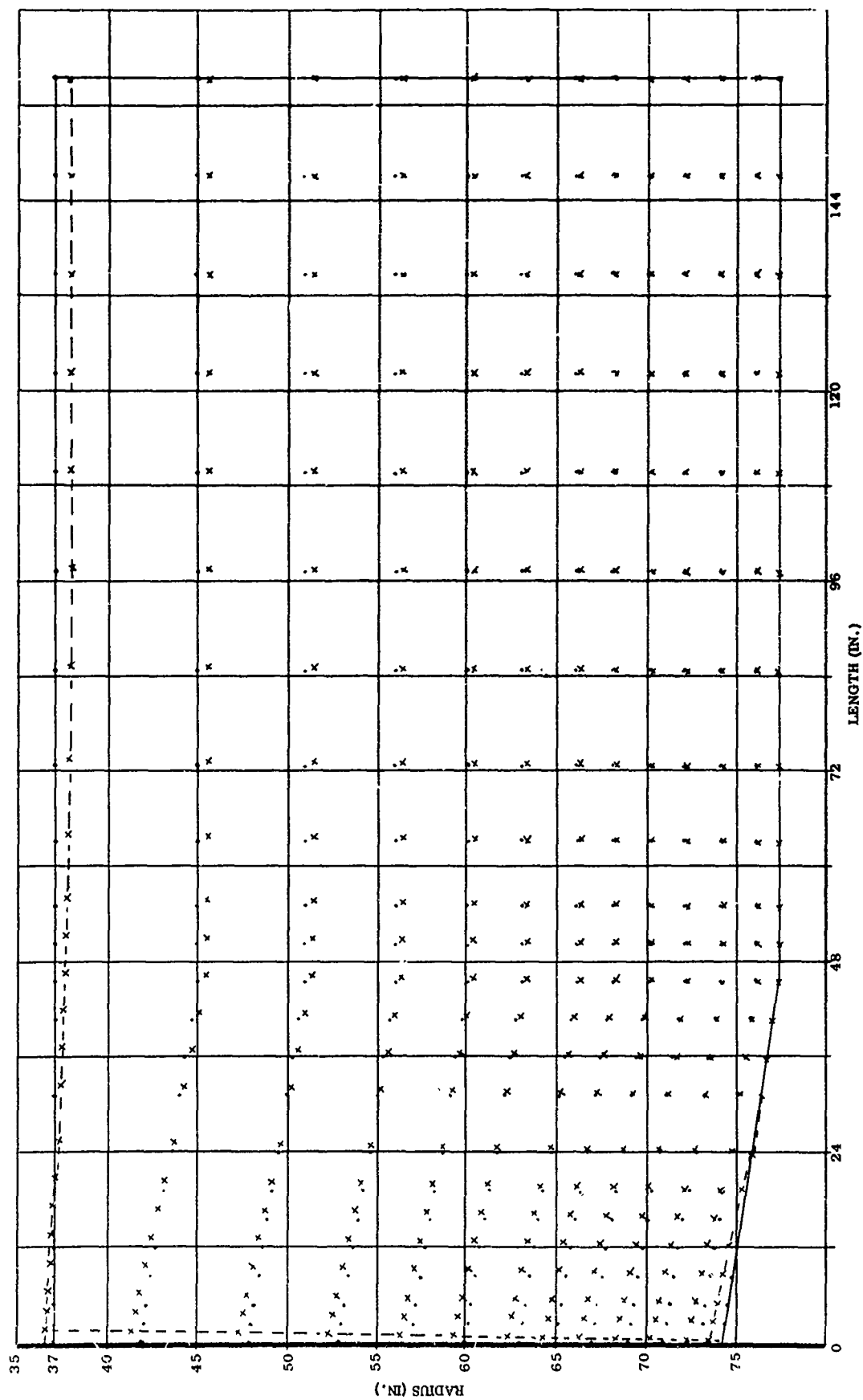


Figure 48. Deformation of the TU-312 Center Grain at 60° F

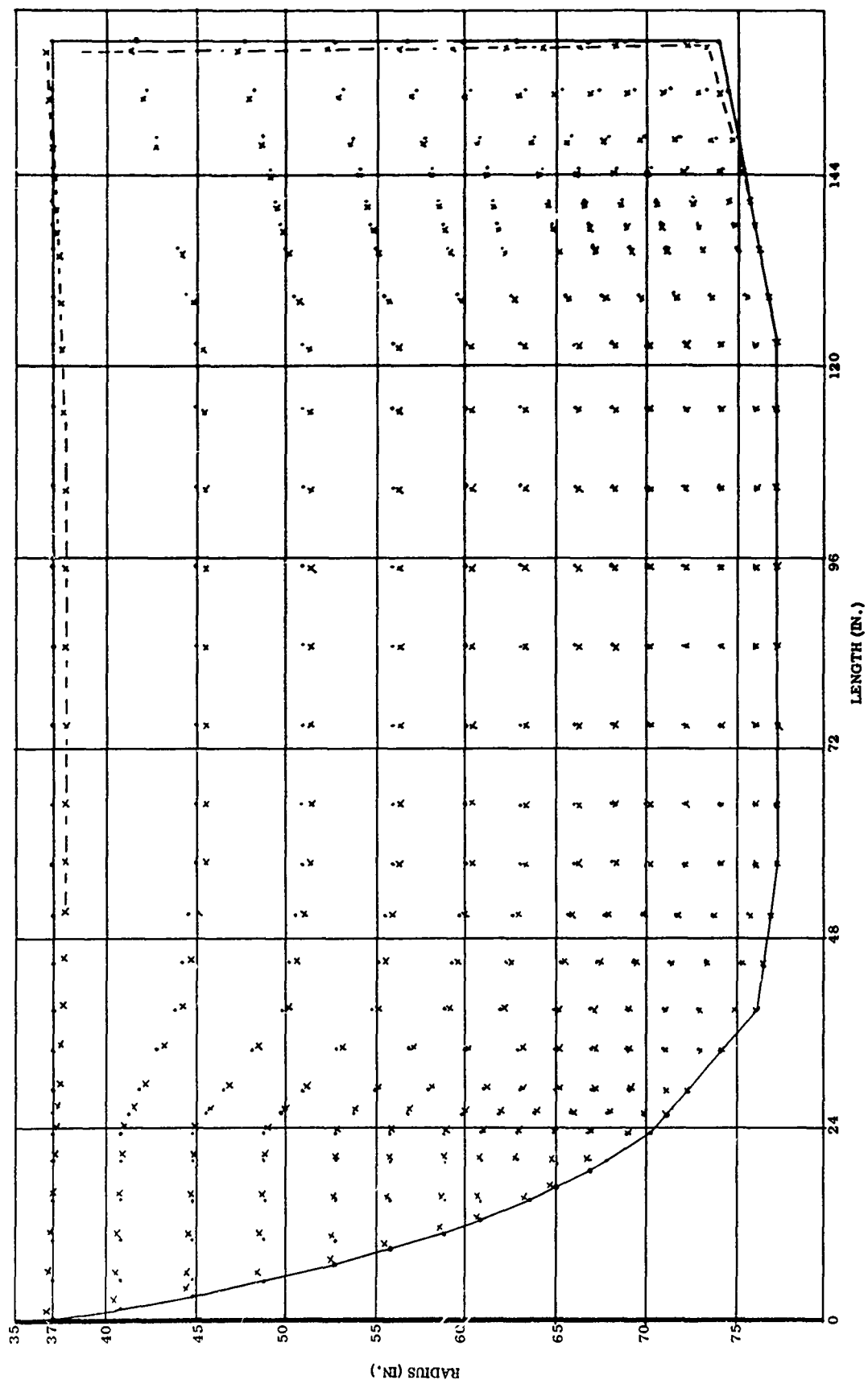


Figure 49. Deformation of the TU-312 Forward Dome Grain at 60° F

TABLE XVIII
STRESS-STRAIN CONDITIONS IN THE TU-312 GRAINS

A. Cure and Thermal Shrinkage (to + 60°F)		<u>Center Segment</u>	<u>Dome Segment</u>
Inner Bore Hoop Strain (in./in.)		0.027	0.021
Sum of Principal Stress (psi)		15.8	8.8
Maximum Principal Strain at Case Interface (in./in.)		0.033	0.031
Sum of Principal Stress at Case Interface (psi)		20.4	23.0
B. Horizontal Slump (1 g)			
inner Bore Hoop Strain (in./in.)		0.0222	0.0222
Sum of Principal Stress (psi)		6.16	6.16
Maximum Principal Strain at Case Interface (in./in.)		0.002	0.002
Sum of Principal Stress at Case Interface (psi)		6.66	6.66
C. Pressure (at 750 psi)			
Inner Bore Hoop Strain (in./in.)		0.0632	0.0542
Maximum Deviatoric Stress (psi)		17.0	14.0
Maximum Principal Strain at Case Interface (in./in.)		0.0565	0.096
Maximum Deviatoric Stress at Case Interface (psi)		17.5	34.0

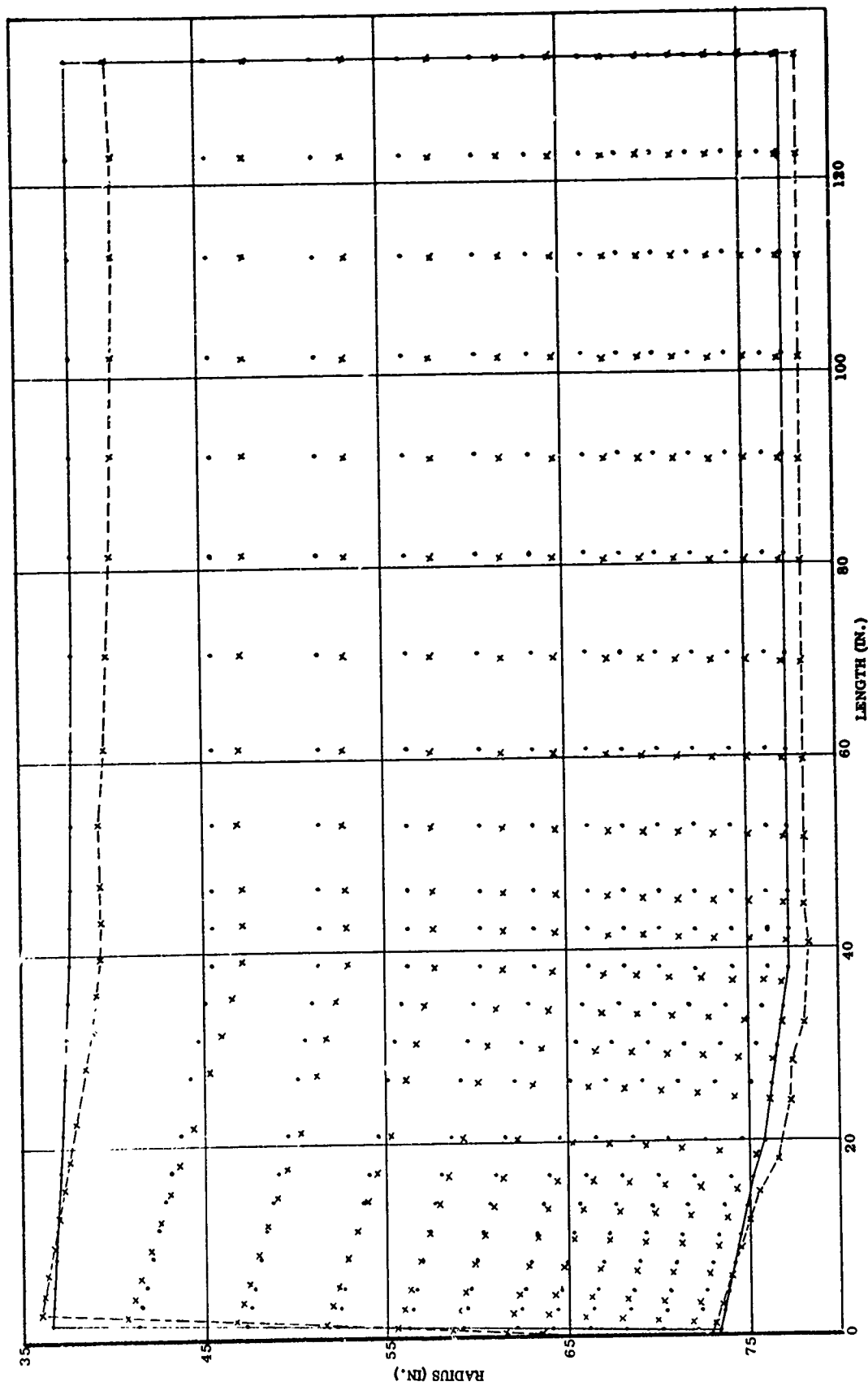


Figure 50. Deformation of the TU-312 Center Grain at 750 psi

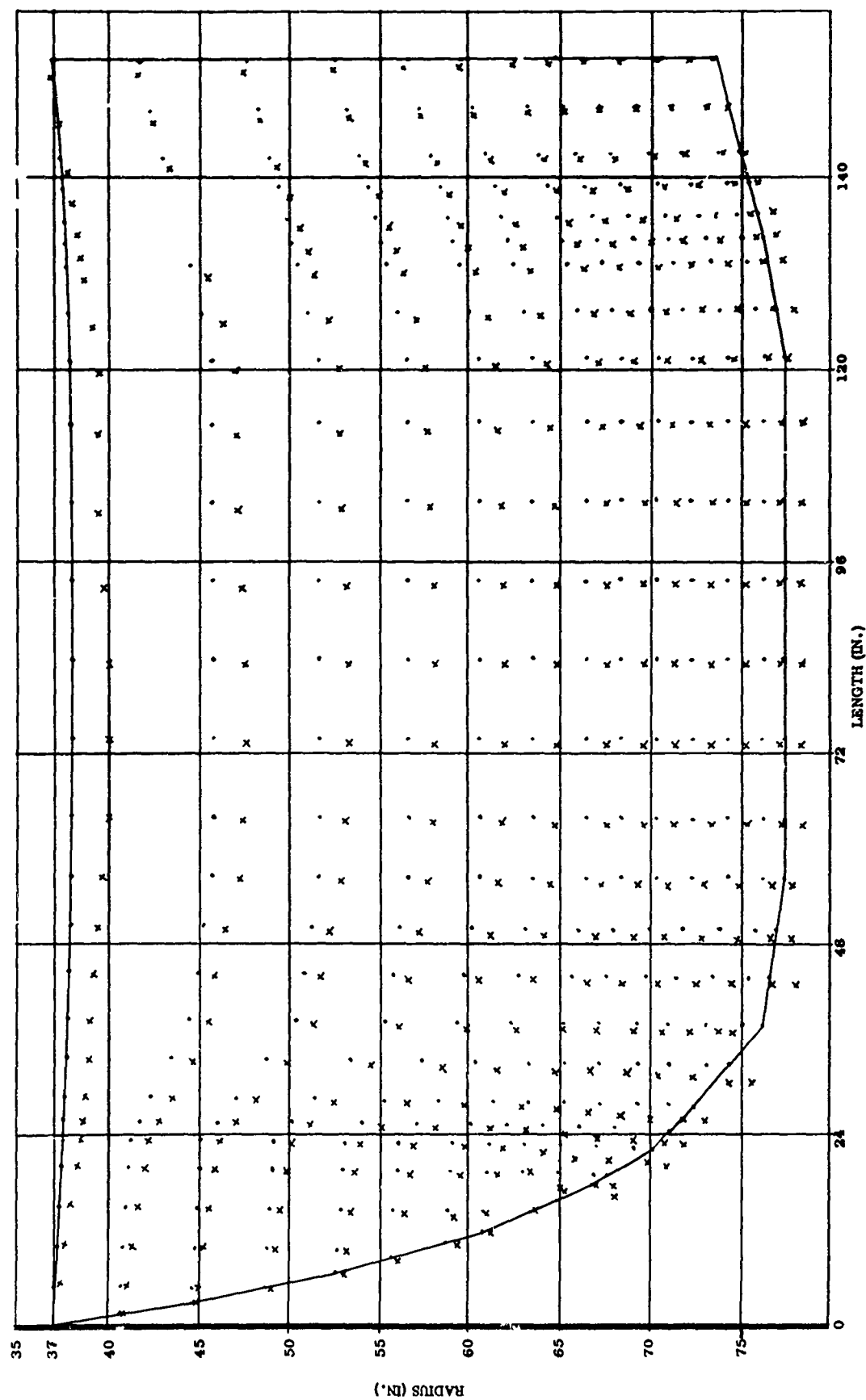


Figure 51. Deformation of the TU-312 Forward Dome Grain at 750 psia

Figure 52. Failure Criteria for TU-312 Grains

TABLE XIX
SAFETY MARGINS FOR THE TU-312 LOADING CONDITIONS
(WORST CONDITIONS ONLY)

<u>Load</u>	<u>Failure Criteria</u>	<u>Maximum Tensile Stress and/or Strain</u>	<u>Propellant Stress/Strain Capability*</u>	<u>Margin of Safety</u>
Cure and Thermal Shrinkage (60°F)	Sum of Principal Stress/psi	23.0	41.1	1.79
	Maximum Strain, in./in.	0.033	0.238	7.2
Slump	Sum of Principal Stress/psi	6.7	41.1	6.13
	Maximum Strain, in./in.	0.022	0.238	10.8
Cure and Thermal Shrinkage plus pressur- ization to 750 psi	Sum of Principal Stress/psi	34	476	14.0
	Maximum Strain, in./in.	0.127	0.238	1.875

*Propellant capability has been reduced by 17.6 and 21.8 percent for strain and stress, respectively. This represents the three sigma coefficient of variation for these parameters.

REFERENCES

- (1) Cook, W. A., "A Finite Element Formulation for Axisymmetric Bodies Having Incompressible and Near Incompressible Materials," TWR-1749, Thiokol Chemical Corporation, Brigham City, Utah. March 1966.
- (2) Becker, E. B. and Brisbane, J. J., "Application of the Finite Element Method to Stress Analysis of Solid Propellant Rocket Grains," Vol. I and II, Report No. S-76 Rohm and Haas Company, Huntsville, Alabama. November 1965.
- (3) Macbeth, A. W., "Stress Analysis of the TU-465 Propellant Grain Rev A," TWR-1577, Thiokol Chemical Corporation, Brigham City, Utah. 10 November 1965
- (4) Nelson, J. M., Special Report, "Improvement of the Elastic Analysis Method of Predicting Low Temperature Operation of Capability of Solid Propellant Motors (U)," Thiokol Chemical Corporation - Alpha Division, Huntsville Plant. 27 November 1963.

B. BALLISTIC PERFORMANCE

Predicted performance values for the selected grain design are listed in Table XX and illustrated in Figures 53 thru 63. The performance predictions were prepared using standard equations relating gas produced and exhausted. The TU-312L.02 propellant surface area (as a function of distance burned) was determined manually from a projected burning pattern. The calculated surface area is shown in Figure 62. Throat area vs time was determined using empirical throat erosion predictions based upon test data from other static tested motors. Motor throat area vs time is shown in Figure 63.

The composition of the propellant for the TU-312L.02 motor is shown in Table XXI. Propellant ballistic properties were obtained from a chemical equilibrium computer program and test data from other Wasatch Division motors and programs (Table XXII). Because of the low gas velocities in the grain port (maximum Mach No. = 0.12), erosive burning was not considered in the current analysis.

Ballistic performance of this motor will be recomputed when the actual propellant weights and grain dimensions are obtained and a final ballistic prediction will be made. An analysis of internal flow conditions within the propellant grain will also be made using the final motor cured grain configuration.

CONFIDENTIAL

TABLE XX

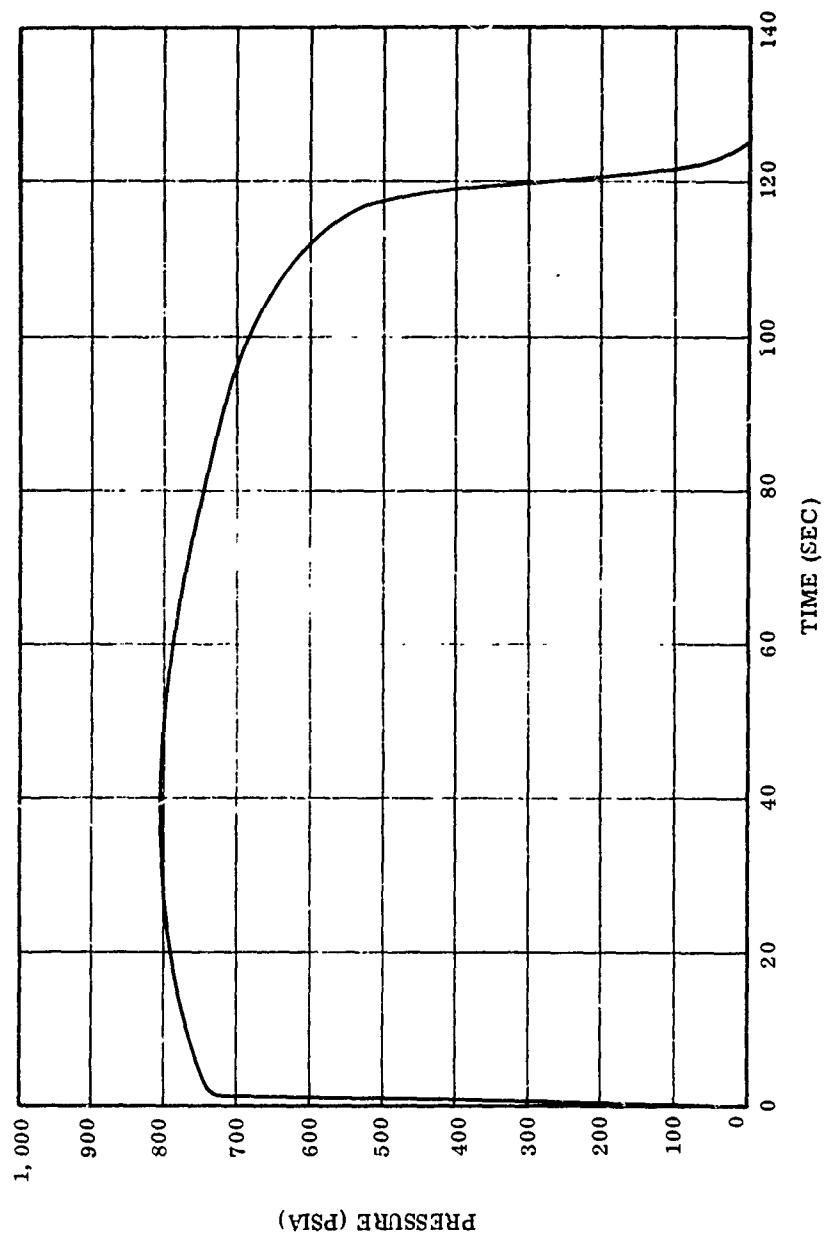
TU-312L.02 ROCKET MOTOR

BALLISTIC PERFORMANCE PARAMETERS

	70°F		100°F	
	Vacuum	Utah	Vacuum	Utah
Web Time Parameters				
Web Time (sec)*	117.8	117.8	114.23	114.23
Average Pressure (psia)	744	744	767	767
Maximum Pressure (psia)	806	806	830	830
MEOP (psia)	854	854	880	880
Average Thrust (lbf)	1,078,700	1,006,500	1,111,900	1,037,800
Maximum Thrust (lbf)	1,151,700	1,077,700	1,187,200	1,113,200
Action Time Parameters				
Action Time (sec)**	121.3	121.3	117.7	117.7
Average Pressure (psia)	732	732	755	755
Average Thrust (lbf)	1,062,700	990,400	1,095,421	1,023,320
Impulse (lbf-sec)	128,889,100	120,124,600	128,889,500	120,402,700
Specific Impulse (lbf-sec/lbm)	260.8	243.0	260.8	243.5

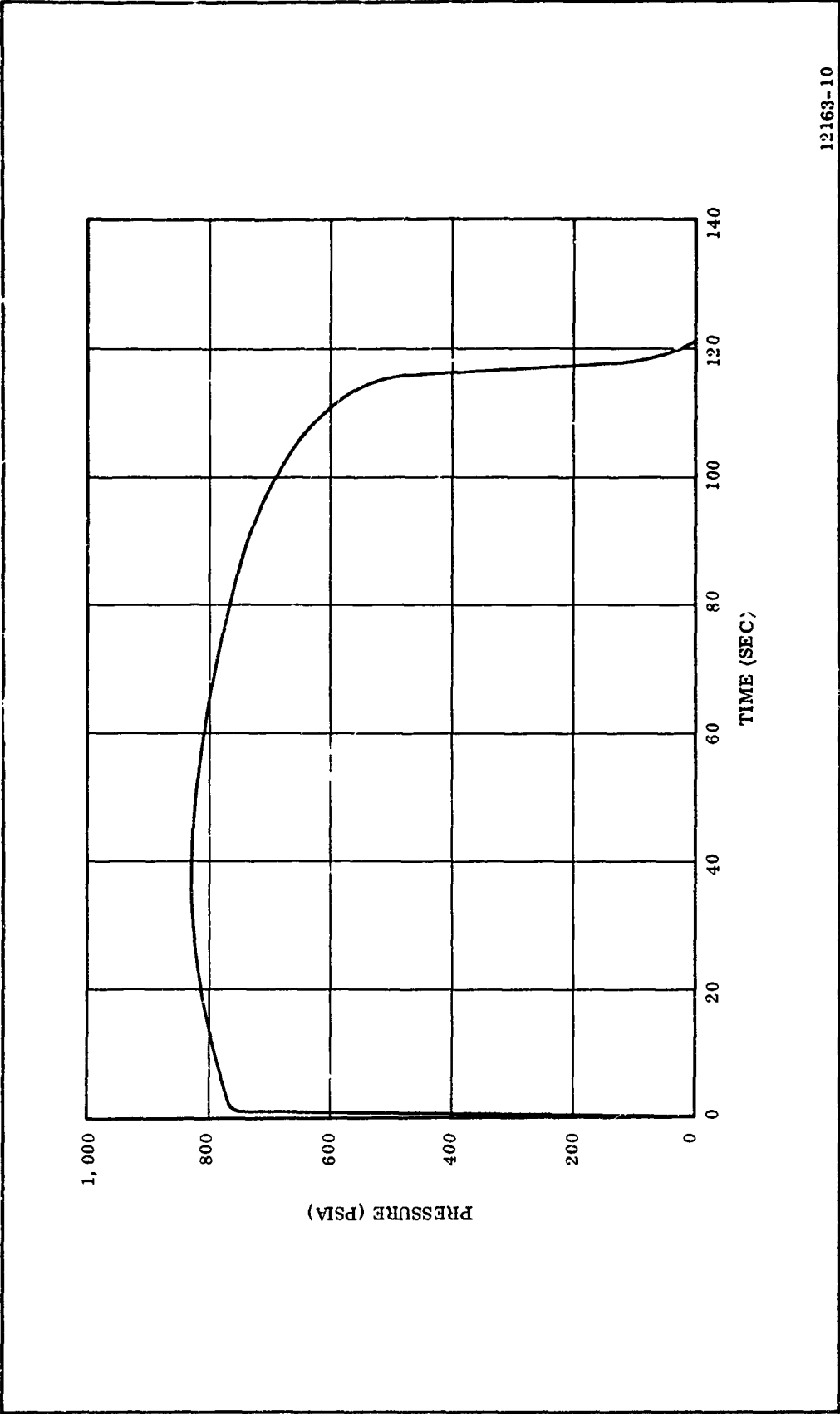
*Burning time is the interval from 75 percent of maximum pressure during rise to the point of pressure-time trace which lies on the line bisecting the angle formed by the tangents to the trace prior to and immediately after the beginning of tailoff.

**Action time is the interval from 75 percent of maximum pressure during rise to 10 percent of maximum pressure during tailoff.



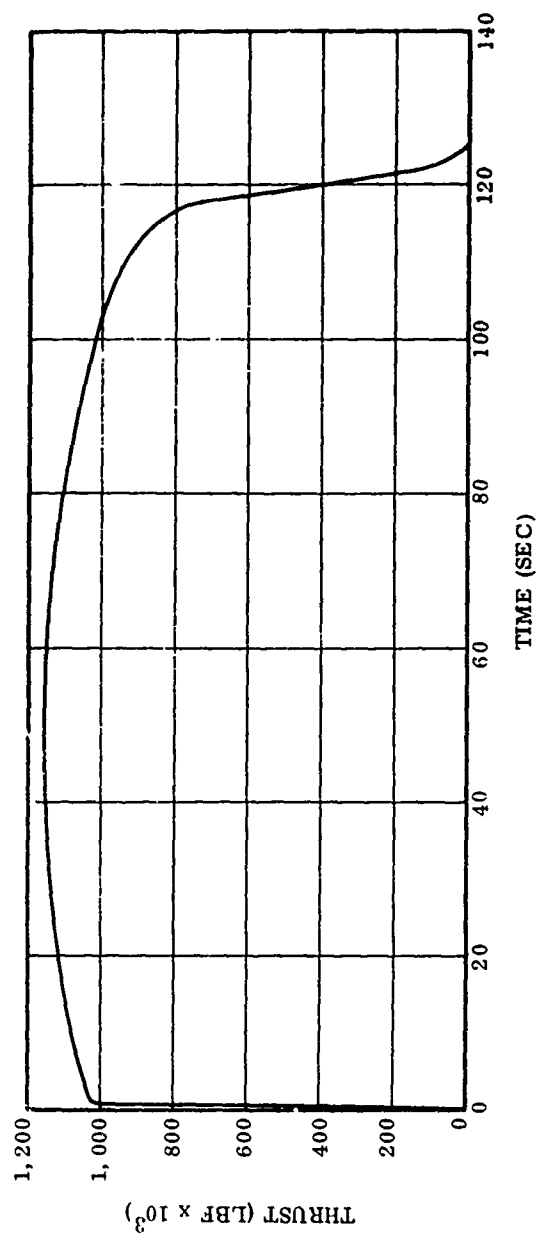
12163-11

Figure 53. TU-312L.02 Motor Chamber Pressure vs Time at 70° F



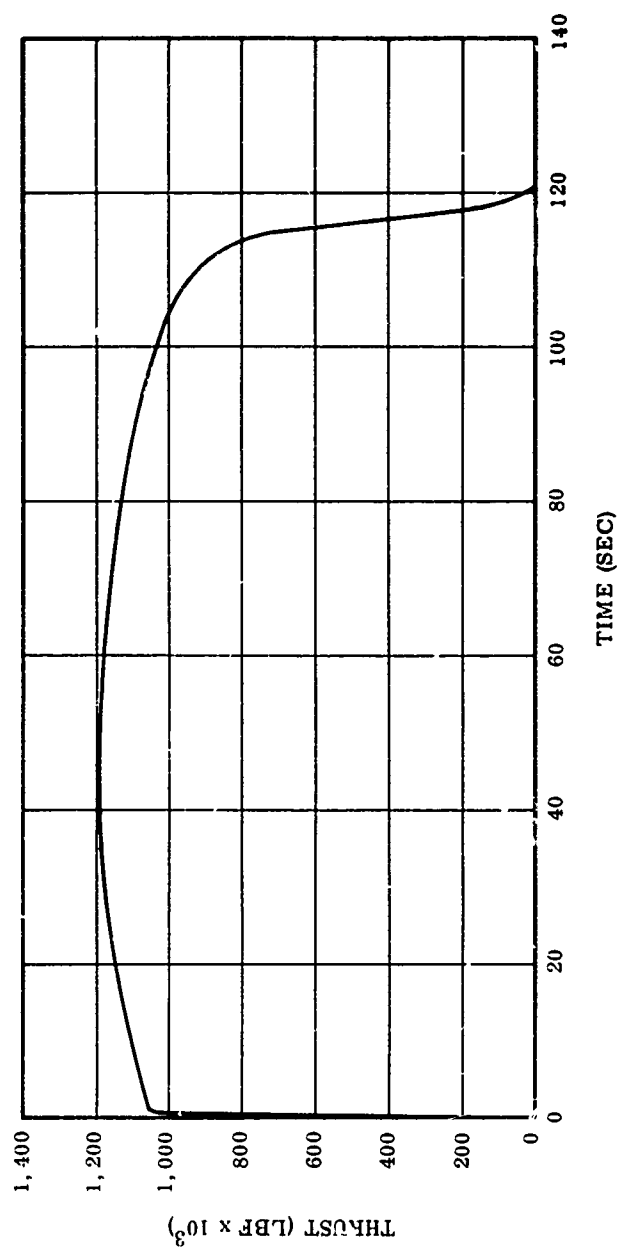
12163-10

Figure 54. TU-312L.02 Motor Chamber Pressure vs Time at 100° F



12163-9

Figure 55. TU-312L.02 Motor Thrust vs Time at 70° F (Vacuum Conditions)



12163-8

Figure 56. TU-312L.02 Motor Vacuum Thrust vs Time at 100°F

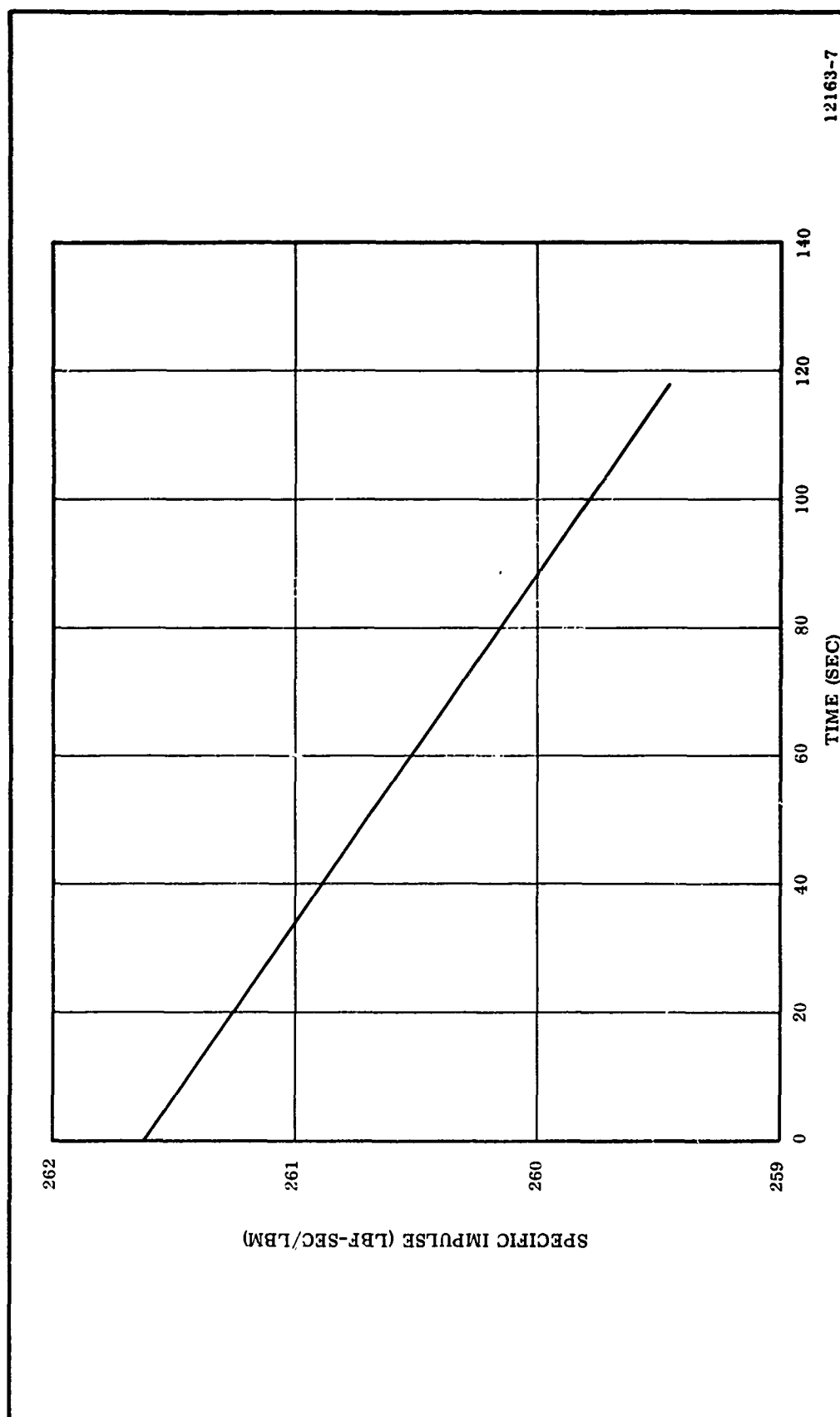


Figure 57. TU-312L.02 Motor Vacuum Specific Impulse vs Time at 70 to 100° F

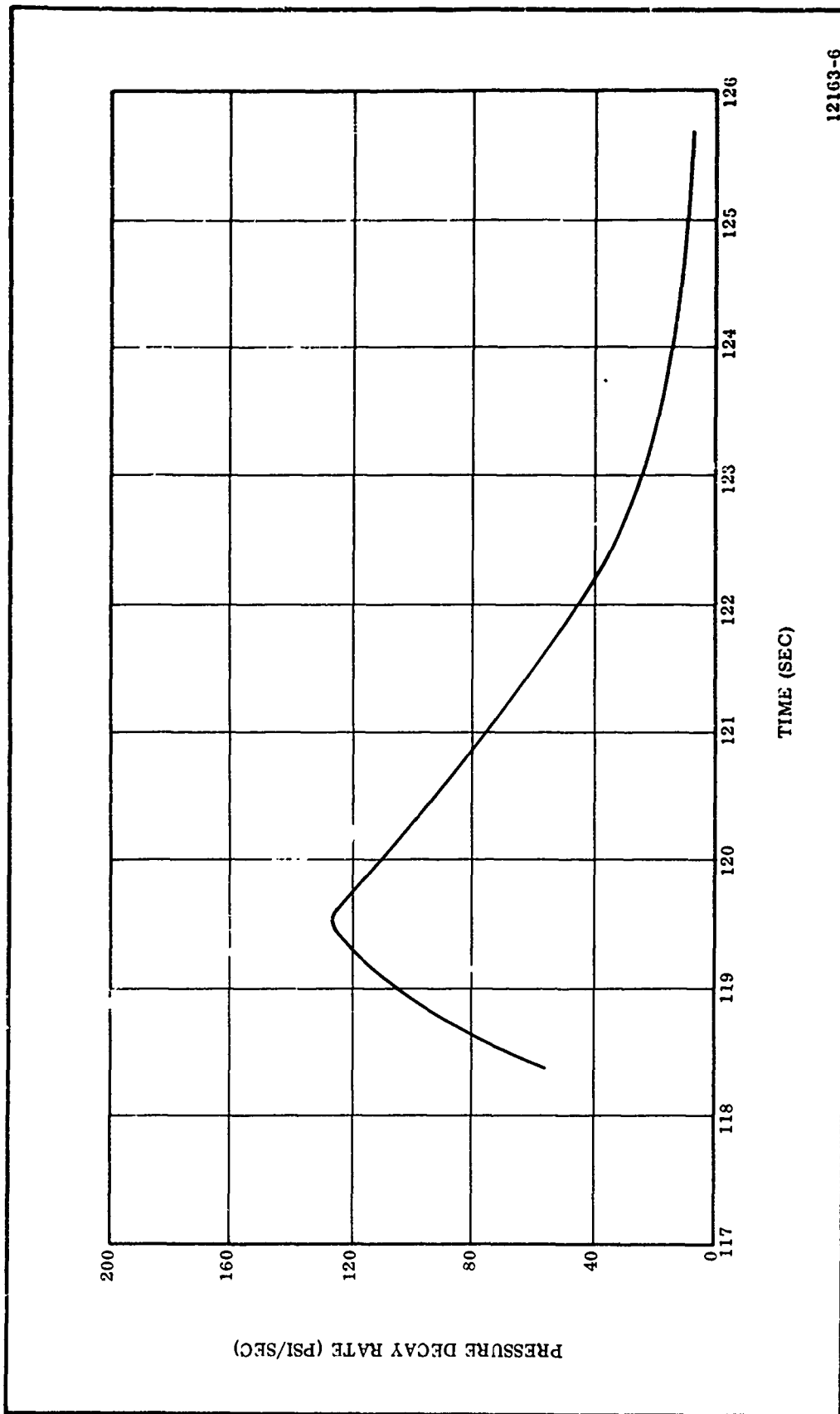
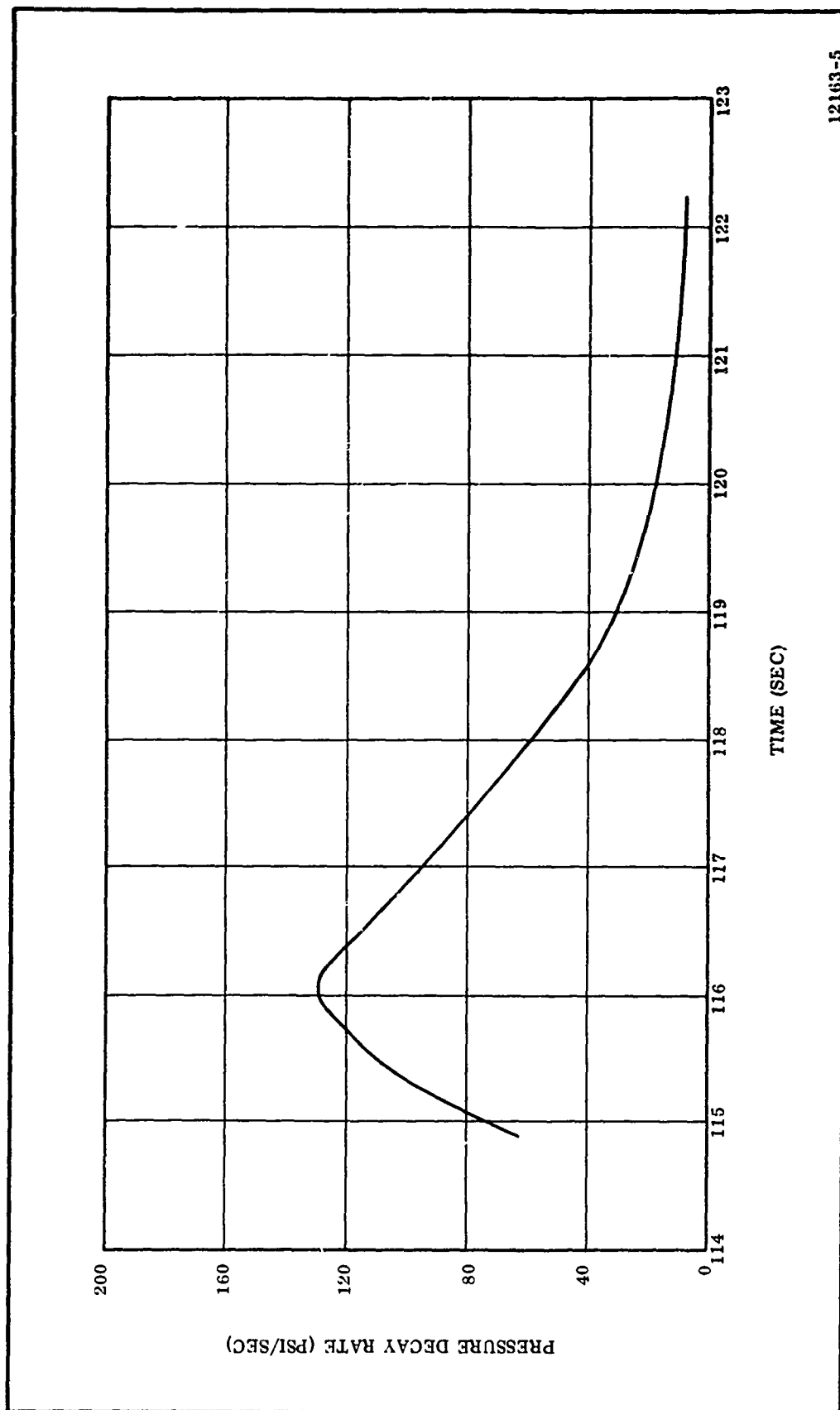
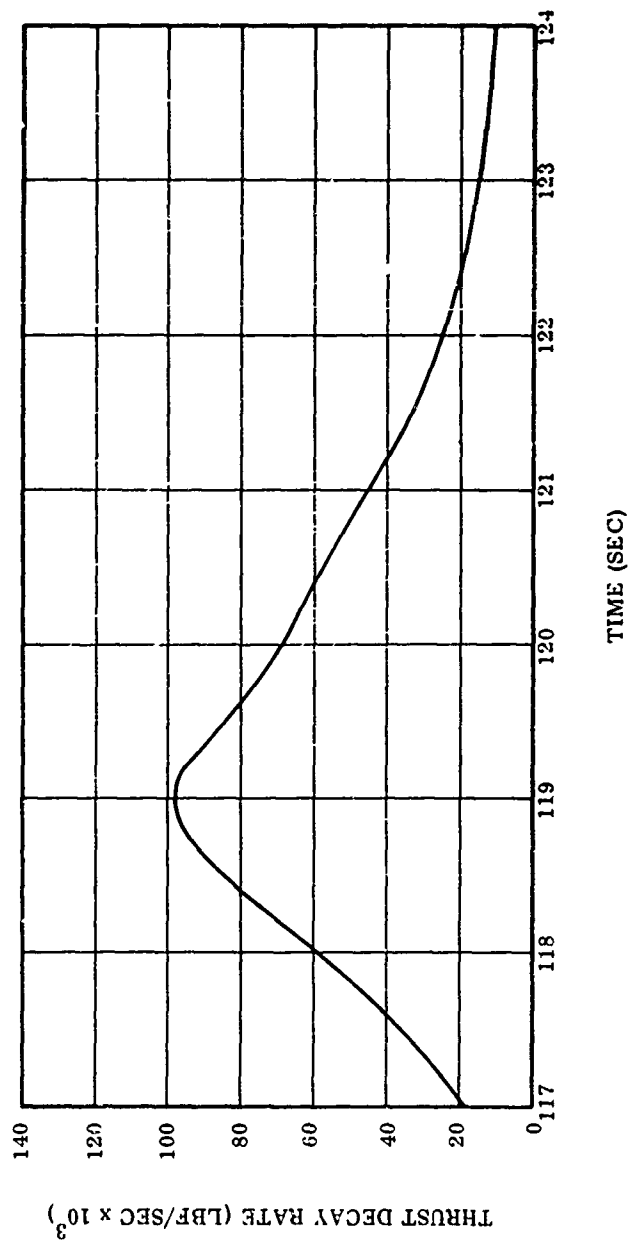


Figure 58. TU-312L.02 Motor Pressure Decay Rate vs Time at 70°F



12163-5

Figure 59. TU-312L.02 Motor Pressure Decay Rate vs Time at 100° F



12163-4

Figure 60. TU-312L.02 Motor Vacuum Thrust Decay Rate vs Time at 70° F

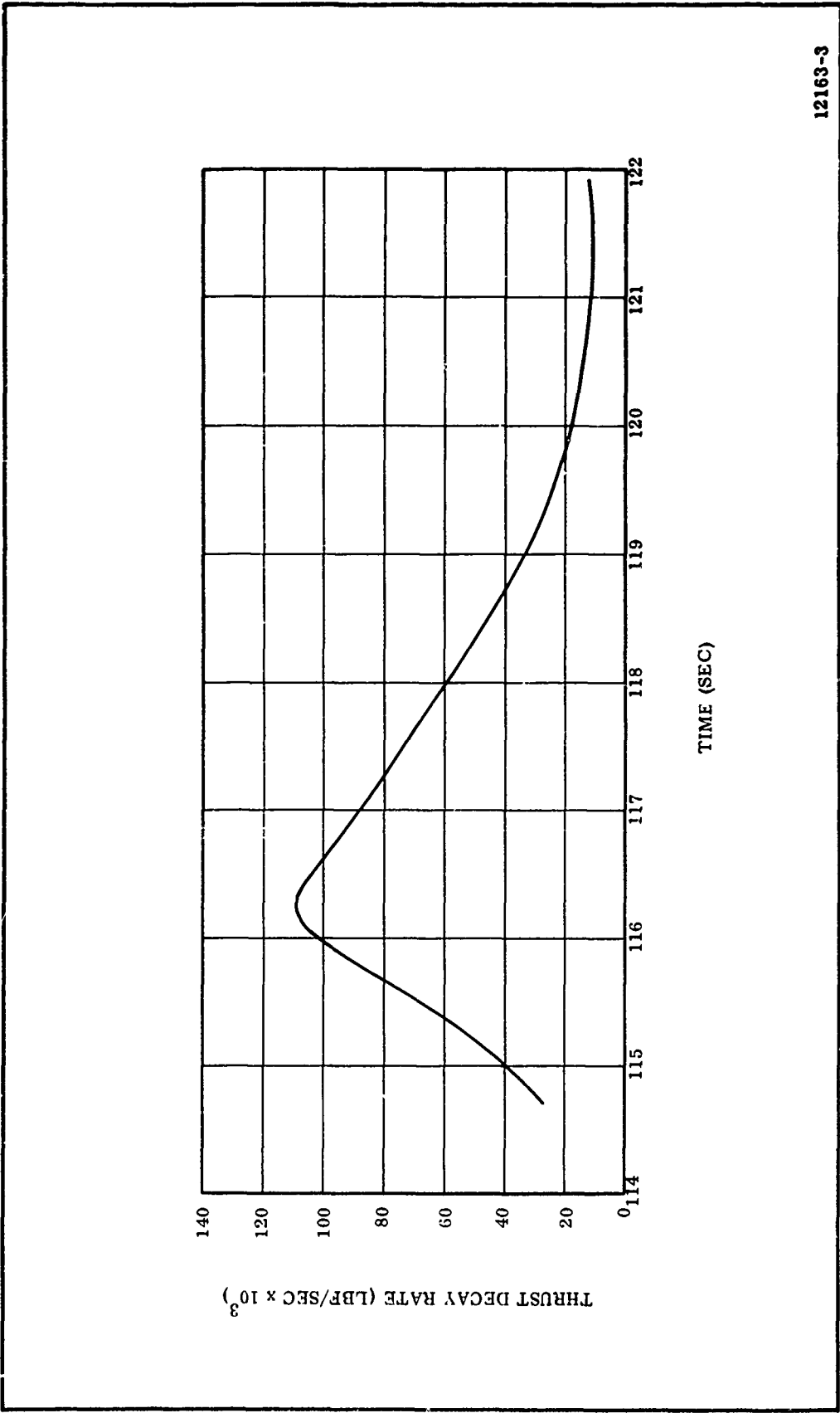


Figure 61. TU-312L.02 Motor Vacuum Thrust Decay Rate vs Time at 100°F

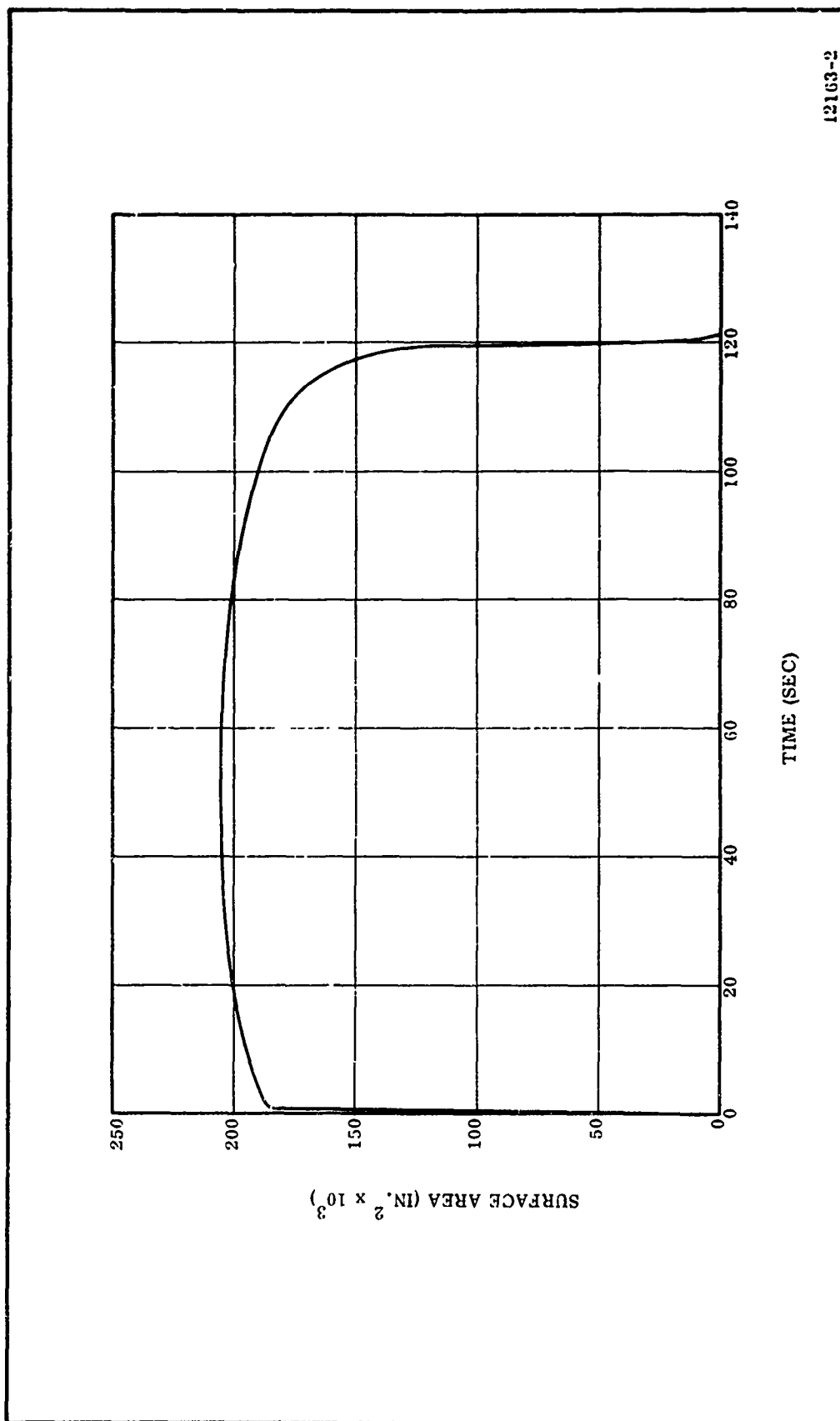
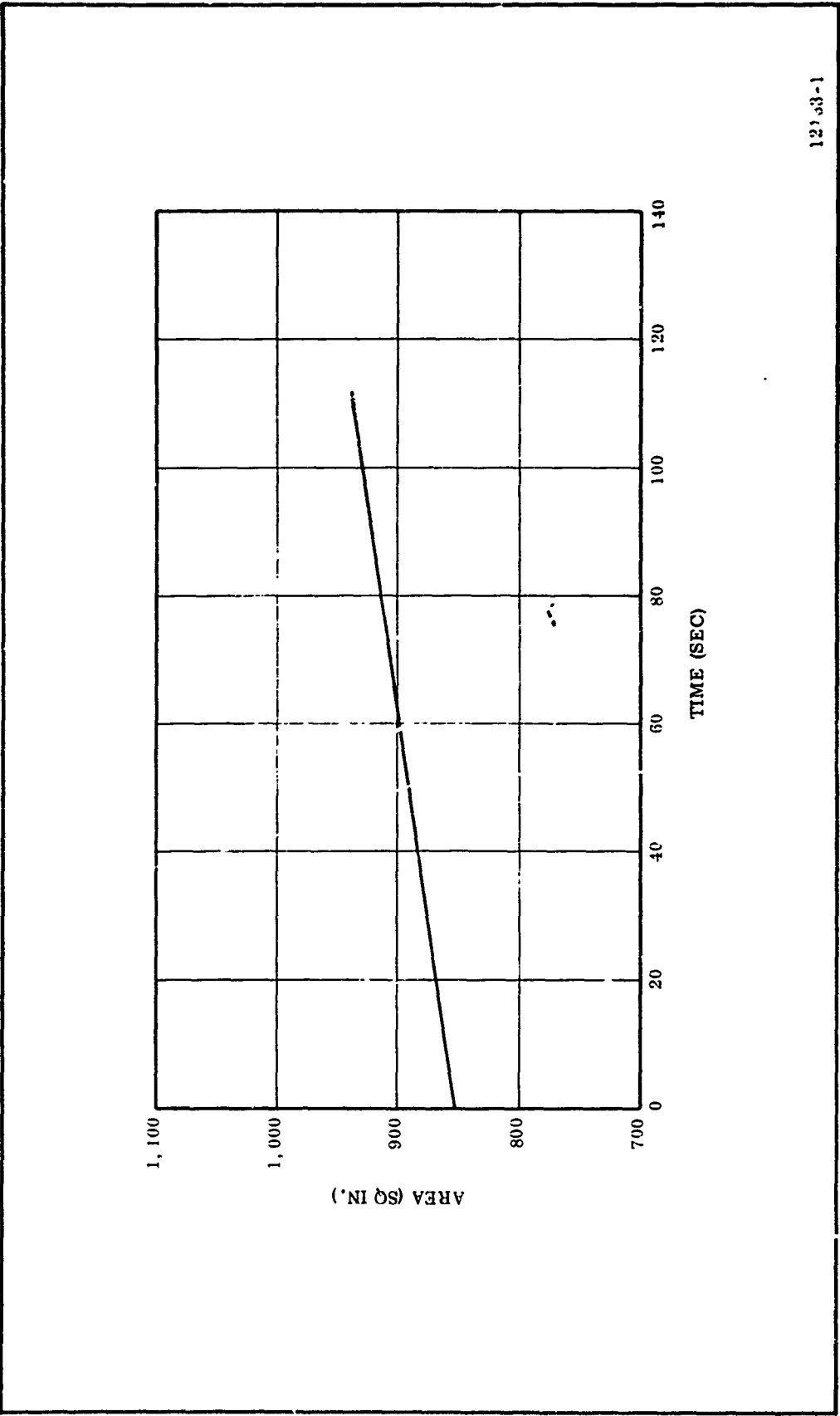


Figure 62. TU-312L.02 Motor Surface Area vs Time



12133-1

Figure 63. TU-312L 02 Motor Throat Area vs Time

CONFIDENTIAL

TABLE XXI

TP-H1011 PROPELLANT COMPOSITION

<u>Material</u>	<u>Percent Composition by Weight*</u>	<u>Function</u>
Ammonium Perchlorate Ground and Unground	70.00 \pm 0.30**	Oxidizer
Aluminum Powder	16.00 \pm 0.30	Fuel
HB Epoxy Resin Type II	14.00 \pm 0.50***	Fuel and Binder

*Total solids = 86 \pm 0.50 percent by weight.

**Ratio of ground to unground ammonium perchlorate is determined from raw material standardization to achieve the desired burn rate.

***Ratio of HB to epoxy resin is determined from raw material standardization to achieve the desired modulus of elasticity.

CONFIDENTIAL

Thiokol

TABLE XXII

BALLISTIC PROPERTIES OF TP-H1011 PROPELLANT

Theoretical specific impulse* $\frac{(\text{lbf-sec})}{(\text{lbm})}$	262.7
Predicted reference specific impulse** $\frac{(\text{lbf-sec})}{(\text{lbm})}$	248
Burning rate equation (70°)*** $\frac{(\text{in.})}{(\text{sec})}$	$r = 0.3274 \frac{(PC)^{0.21}}{P_o}$
Ratio of specific heats	1.18
Theoretical mass flow coefficient $\frac{(1)}{(\text{sec})}$	0.0062
Temperature coefficient of pressure KN (%/°F, max.)	0.12

*14.7 psia ambient pressure; 1,000 psia chamber pressure; optimum sea level expansion ratio; 0 deg nozzle half angle; (Cm) = 1.0.

**14.7 psia ambient pressure; 1,000 psia chamber pressure; optimum sea level expansion ratio; 15 deg nozzle half angle; nozzle efficiency (Cm) = 0.974.

***Burning rate pressure exponent (n) was determined from 5 in. diameter motors fired in previous Thiokol motor contracts.

CONFIDENTIAL

SECTION VII

IGNITION SYSTEM

A. IGNITION SYSTEM DESCRIPTION

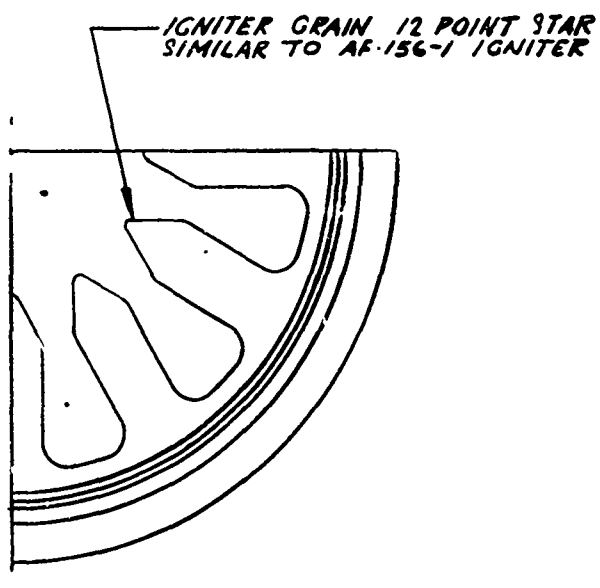
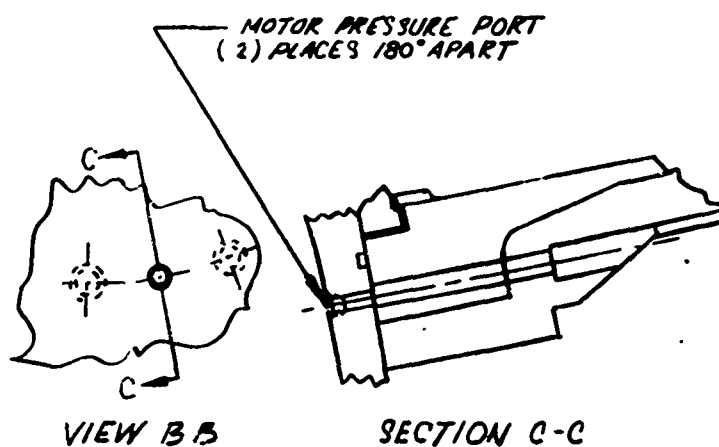
A head end PYROGEN ignition system (Figure 64) was selected to ignite the 156-8 (TU-312L.02) motor. This system is similar in design to the aft end ignition system used to ignite the AF 156-1 motor (Figure 65).

The ignition assembly selected during this first quarter consists of five main subassemblies: (1) safety and arming device, (2) pyrotechnic booster assembly, (3) initiating PYROGEN igniter, (4) booster PYROGEN igniter, and (5) the igniter cap (adapter). Each item is described below.

1. SAFETY AND ARMING DEVICE (S & A)

The S & A device selected for the TU-312L.02 ignition system is currently being used on the Stage I, II, and III MINUTEMAN motors. Thiokol developed this device for the Stage I ignition system and later it was standardized for all three stages. The S & A has been qualified to the latest Air Force requirements and over 2,500 have been produced for various development, qualification, flight test, and production programs.

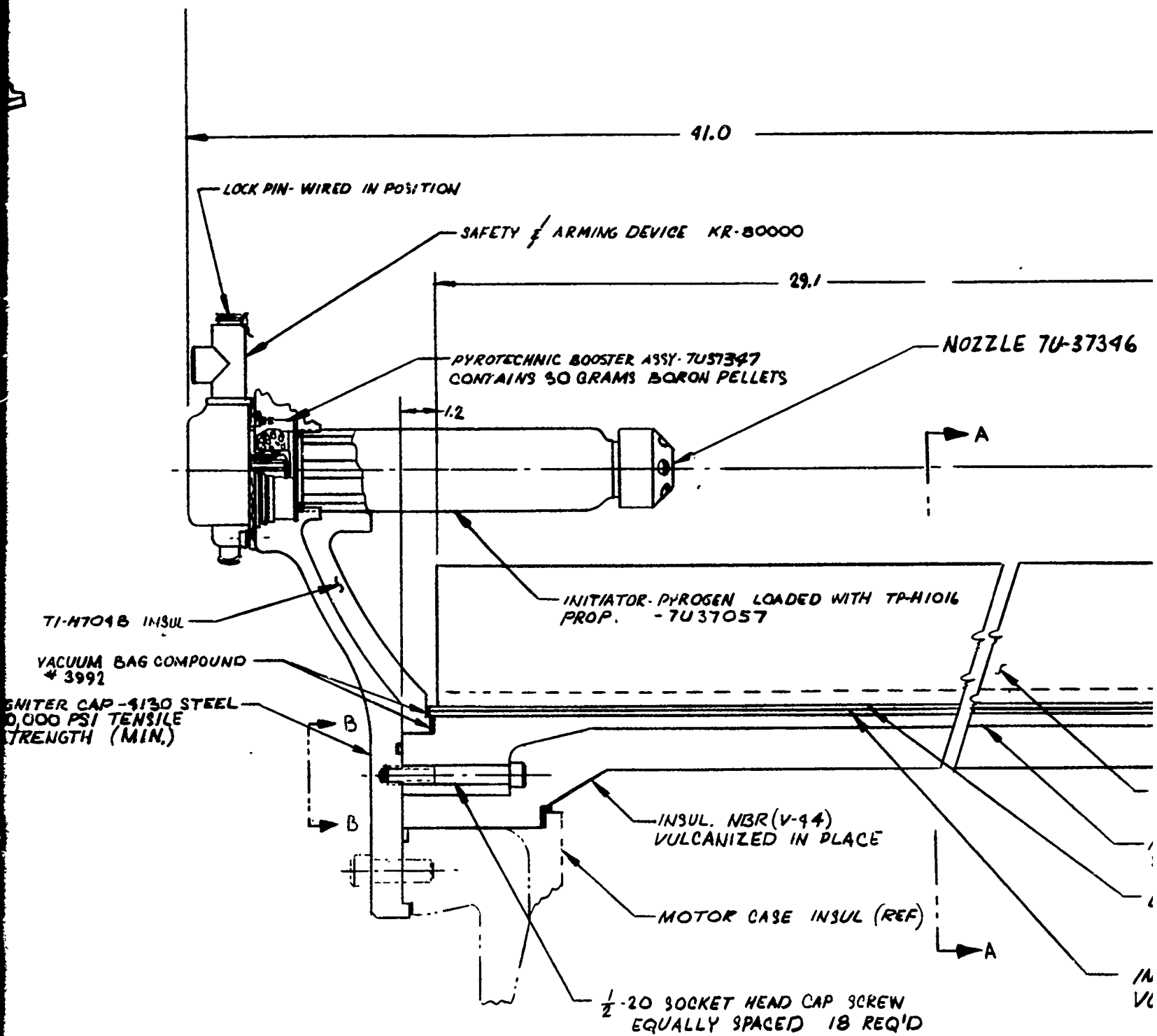
Upon initiation, two ES-003 electrical squibs start the ignition train for the motor ignition sequence. In the safe position, the squibs are electrically shorted and mechanically isolated from the ignition train. The S & A has a visual indicator, mechanical lockpin, separate connectors for the control and firing circuits, hermetic seals, and other safety features which minimize the possibility of inadvertent firing.



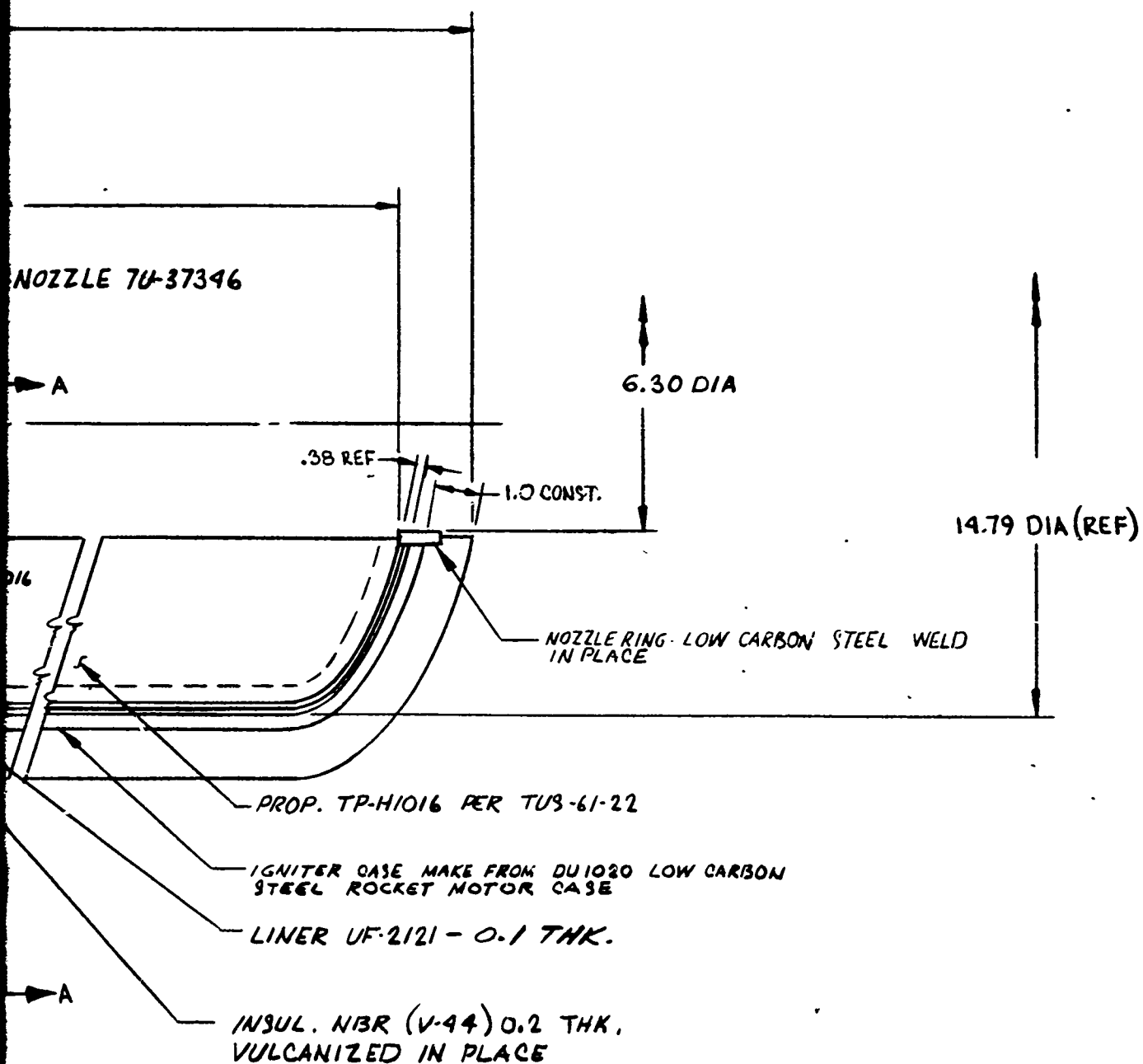
TI-H704B INSUL

VACUUM BAG COMPOUND
3992

IGNITER CAP - 4130 STEEL -
90,000 PSI TENSILE
STRENGTH (MIN.)



2



3

IGNITION SYSTEM
LAYOUT - TU-312 L. 02
TUL 11928 B

Figure 64. PYROCEN Ignition System
138



Figure 65. TU-312L.02 Motor Igniter

A lockwire secures the lockpin in place to insure assembly of the S & A device to the PYROGEN igniter in the unarmed (safe) condition. The lockwire and lockpin must be removed manually before the device can be electrically armed. This feature satisfies the RFP requirement that it shall not be possible to install the S & A device in the motor while it is in the armed condition. This lockwire-lockpin arrangement was used on the S & A of the AF 156-7 rocket motor under Contract AF 04(695)-773 (Bid Package 15), which had an identical safety requirement.

2. PYROTECHNIC BOOSTER

The pyrotechnic booster provides the ignition train between the S & A device and the initiating PYROGEN igniter. It contains 30 gm of 2A boron-potassium nitrate pellets, and the container is identical to the design used on the Stage I MINUTEMAN and AF 156-1 motors.

3. INITIATING PYROGEN

The initiating PYROGEN igniter for the TU-312L 02 motor ignites the booster PYROGEN igniter. It has the same design used to ignite the booster PYROGEN igniter for the AF 156-1 motor previously static fired at the Wasatch Division (Figure 65). Adequate ignition of the booster igniter grain configuration to be used in this system has been demonstrated using the multiple port nozzle design.

Loaded with TP-H1016 propellant (Stage I MINUTEMAN igniter propellant), the initiating PYROGEN igniter produces a mass discharge rate for booster igniter ignition of 3.5 lb/sec for approximately 0.3 second. The case length is 11.5 inches. The loaded case for this igniter was successfully tested five times before it was used in the ignitio system for the AF 156-1 motor. The case and grain designs were originally developed for the MACE ignition system.

4. BOOSTER PYROGEN

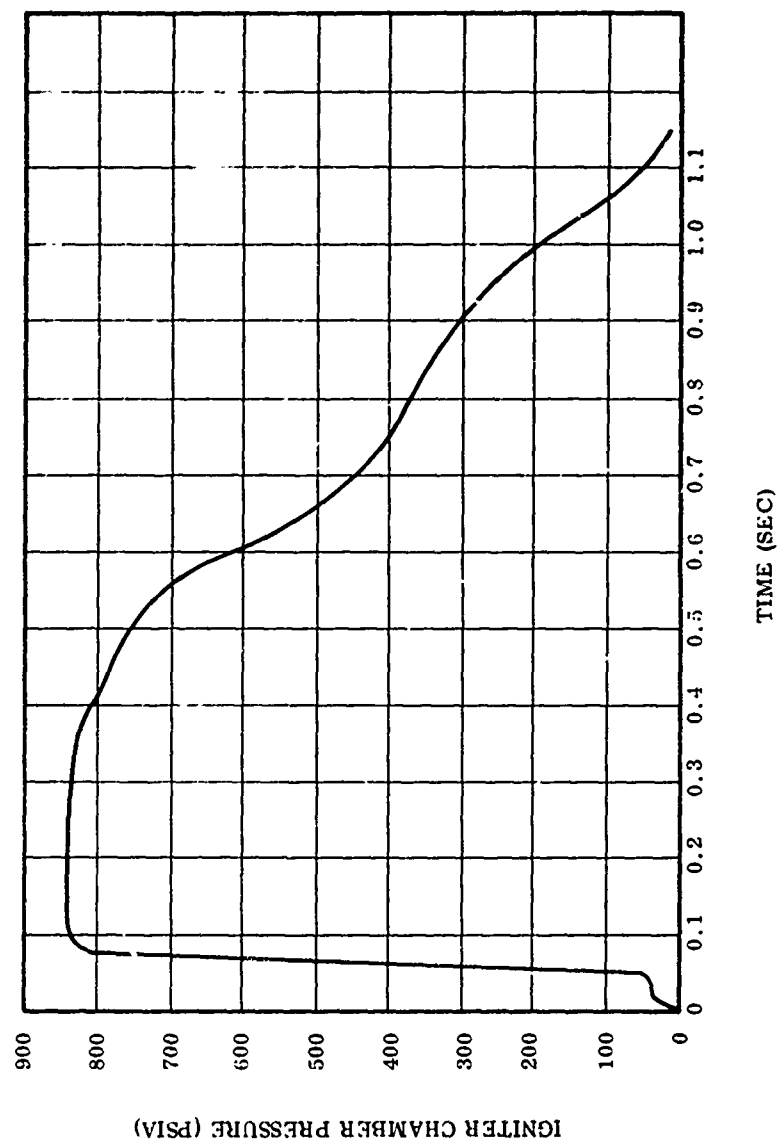
The booster PYROGEN igniter assembly consists of an existing rocket motor case, asbestos filled NBR (V-44) external and internal insulation, UF-2121 liner, and TP-H1016 propellant. The grain is cast in the same 12 point star configuration used in the booster PYROGEN which ignited the AF 156-1 motor. The igniter will operate at a pressure of 820 psia and provide a mass discharge rate of 158 lb/sec for approximately 0.6 sec after which pressure and mass flow drop off for a total burning time of approximately 1.1 sec (Figure 66).

At 820 psi, the booster PYROGEN igniter case will have a pressure safety factor greater than two. (Section D presents the case structural analysis.) The igniter case of low carbon steel is 30 in. long and 15.5 in. in diameter. It will be fabricated by modifying an existing motor case by removing skirt and handling lugs. The head end dome will be modified by opening the port and welding it in a low carbon steel ring to serve as the igniter nozzle. The selection of a steel case for the TU-312L.02 igniter was based upon economic considerations rather than weight performance.

The steel case must be insulated internally and externally to prevent melting during the motor firing. Thermodynamic calculations indicate that 0.030 in. of insulation will prevent melting from the inside; however, to protect the bond of the external case insulation to the steel case, it is necessary to install additional internal insulation. The proposed design will use 0.20 in. of NBR layup, vulcanized in place, and 0.10 in. of UF-2121 liner. This thickness controls the propellant web thickness to provide the required burning time and provide more than enough insulation on the internal surfaces to prevent bond failure of the external insulation.

5. IGNITER CAP (ADAPTER)

The igniter cap adapts the initiating PYROGEN, booster PYROGEN, booster assembly, and the safety and arming device into one integral unit. The igniter cap



12163-16

Figure 66. TU-312L.02 Igniter Predicted Performance

is made from annealed 4130 steel. The 90,000 psi material tensile strength of the annealed condition steel is adequate to withstand the pressure loading (Section D presents the igniter cap structural analysis).

B. IGNITER BALLISTIC DESIGN AND MOTOR IGNITION TRANSIENT

The empirical PYROGEN igniter coefficient is the primary tool for determining the required size of a PYROGEN igniter. This relationship states that when the ratio of igniter mass flow rate (lb/sec) divided by the motor throat area (sq in.) is in the range of 0.15 to 0.25, satisfactory ignition will result. Thus, an approximate PYROGEN igniter motor mass flow rate can be established for a motor having specified nozzle dimensions. Usually, the values selected for the PYROGEN igniter coefficient have been in the range of 0.17 to 0.20. The proposed igniter has a mass flow rate of 158 lb/sec, which results in a coefficient of 0.185.

Motor ignition is achieved through the action of a pyrotechnic charge and two PYROGEN igniters. The sequence of ignition is (1) the S & A device is electrically armed and two electrical squibs are initiated, (2) the flame and pressure created by the squibs ruptures two windows (diaphragms) and ignites the booster assembly, (3) the flame from the booster charge ignites the initiating PYROGEN igniter, and (4) the initiating PYROGEN igniter exhaust gas flow and flame ignite the booster PYROGEN igniter. The ignition transient of a motor is made up of four relatively distinct time periods identified as follows.

1. Igniter response time.
2. Time to achieve motor pressure-igniter output equilibrium prior to motor propellant ignition.
3. Lag time or time between equilibrium pressure achievement and first ignition of motor propellant.
4. Flame spreading time or time from end of lag time until all surfaces of the motor grain have been ignited.

Thiokol has predicted the ignition transients expected for the TU-312L.02 motor. The prediction includes an equilibrium calculation which begins at the end of lag time and ends upon achievement of motor equilibrium pressure. The prediction is based on the ballistic and physical characteristics of the TU-312L.02 motor grain, the ignition parameters of the ignition, estimated time of first ignition, and flame spreading rates over all surfaces in the motor. Motor pressure, thrust, mass flow rate, and surface area ignited plus igniter pressure and mass flow rate are computed as functions of time.

The predicted chamber pressure transient and thrust vs time during ignition transient for the TU-312L.02 motor is illustrated in Figures 67 and 68. This prediction is based on the ignition system performance demonstrated by the AF 156-1 motor. The igniter pressure superimposed upon the motor pressure at equilibrium will not produce a pressure in excess of the motor MEOP. The maximum predicted ignition pressure of the motor is 779 psi.

The response time associated with igniting the AF 156-1 initiating PYROGEN was 0.038 sec. The AF 156-1 booster PYROGEN took an additional 0.044 sec to achieve 75 percent of its first level operating pressure. This resulted in a time lapse of 0.080 sec between time zero and the first pressure rise in the main motor (igniter response time). From comparing the sizes of the AF 156-1 booster ignition and TU-312L.02 PYROGEN igniter, a TU-312L.02 ignition delay of 0.073 sec is predicted.

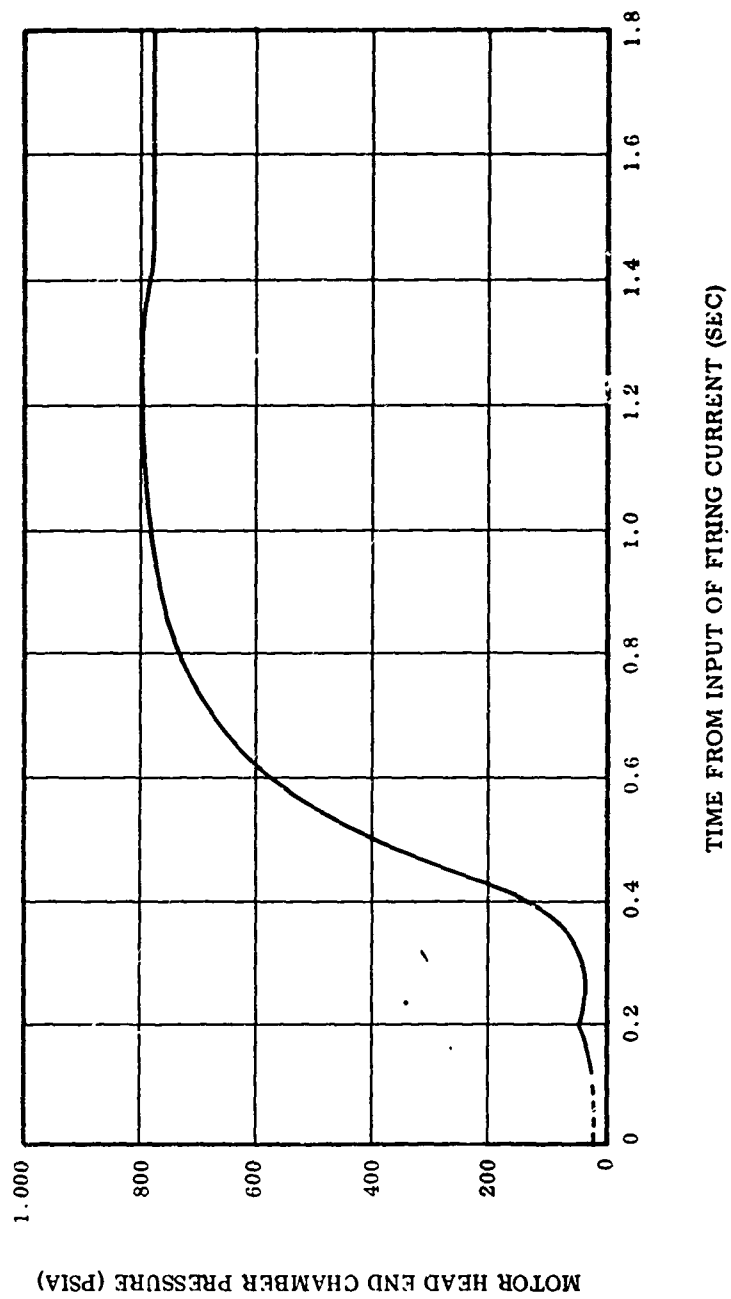
The pressure produced by the igniter in the motor is approximated by the following formula.

$$P_c = \frac{\dot{M}_i c^*}{A_t g}$$

Where:

P_c = Equilibrium pressure (psia).

\dot{M}_i = Igniter mass flow rate (lb/sec).



12163-17

Figure 67. Predicted TU-312L.02 Motor Ignition Transient

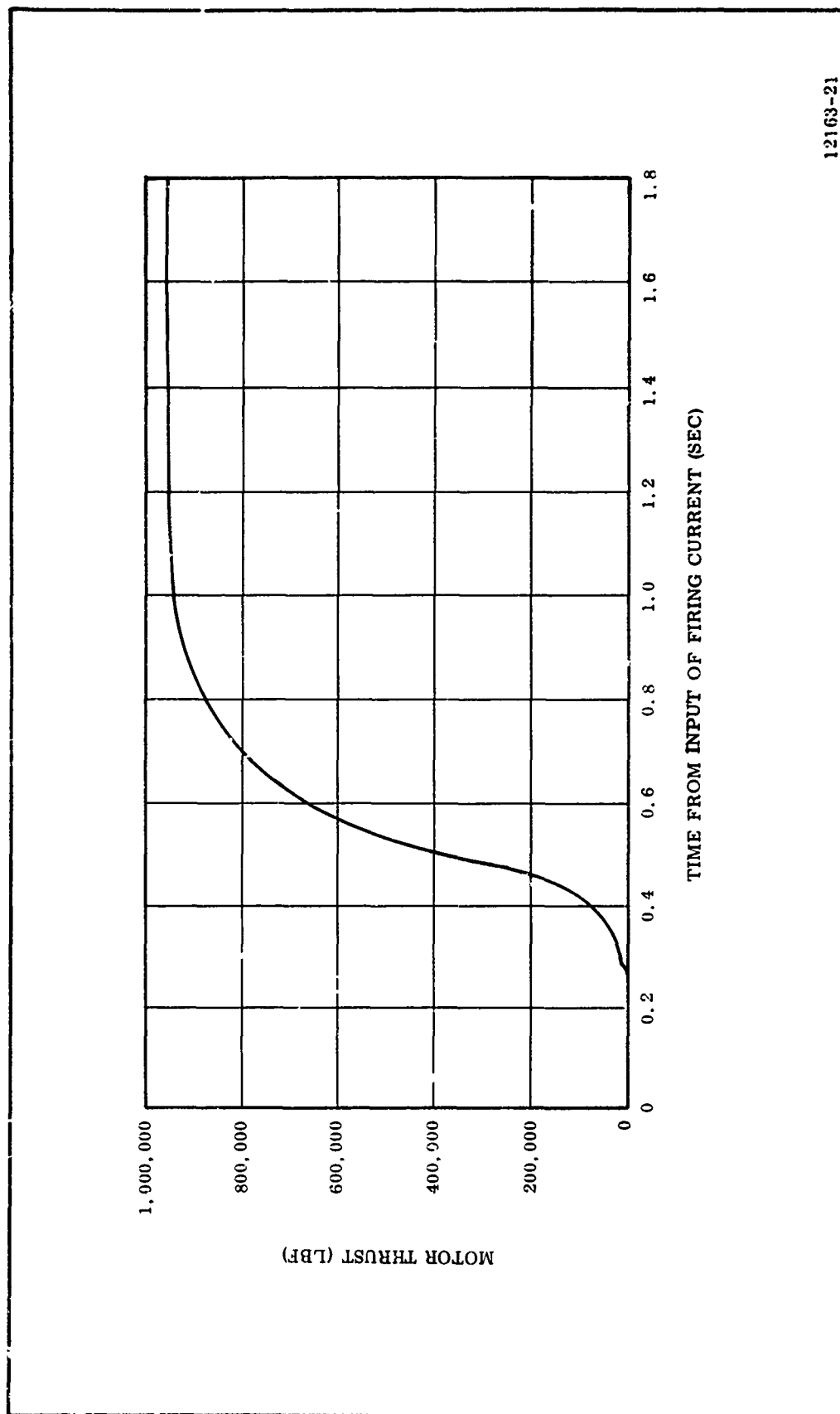


Figure 68. Predicted TU-312L.02 Motor Thrust vs Time During Ignition Transient (Utah Conditions)

- c^* = Igniter characteristic velocity (ft/sec).
- A_t = Motor throat area (sq in.).
- g = Gravitational constant (ft/sq in.).

This equation represents an ideal condition and would logically predict higher than actual pressures. In actuality, the pressures achieved are about 20 percent higher than predicted. The additional pressure is probably due to compression of the air in the motor by the igniter output before the column of air begins to flow out the motor nozzle. Including the 20 percent historical increase, the predicted motor chamber pressure produced by the igniter is 47.5 psia.

The time required to achieve equilibrium pressure is calculated by an equation derived by evaluating the relationships of igniter exhaust gas weight required to produce the equilibrium pressure and the time required by the igniter to produce the necessary weight of gas. This equation is:

$$t = \frac{L^*}{12C^* (\Omega)^2}$$

Where:

- t = Time to achieve equilibrium.
- L^* = Characteristic length (in.).
- Ω = Function of propellant gas specific heat ratio.
- C^* = Characteristic exhaust velocity (ft/sec).

This relationship has been validated by plotting time to equilibrium as a function of L^* from actual test data. The empirical and theoretical lines (Figure 69) are approximately parallel. A difference exists between the empirical and theoretical curves because the actual flame temperature in the motor chamber is less than the stagnation temperature and the igniter does not reach its full mass flow instantaneously. The high L^* of the TU-312L.02 motor (3,237 in.) is in excess of any value for which actual equilibrium times are available. It appears from Figure 69

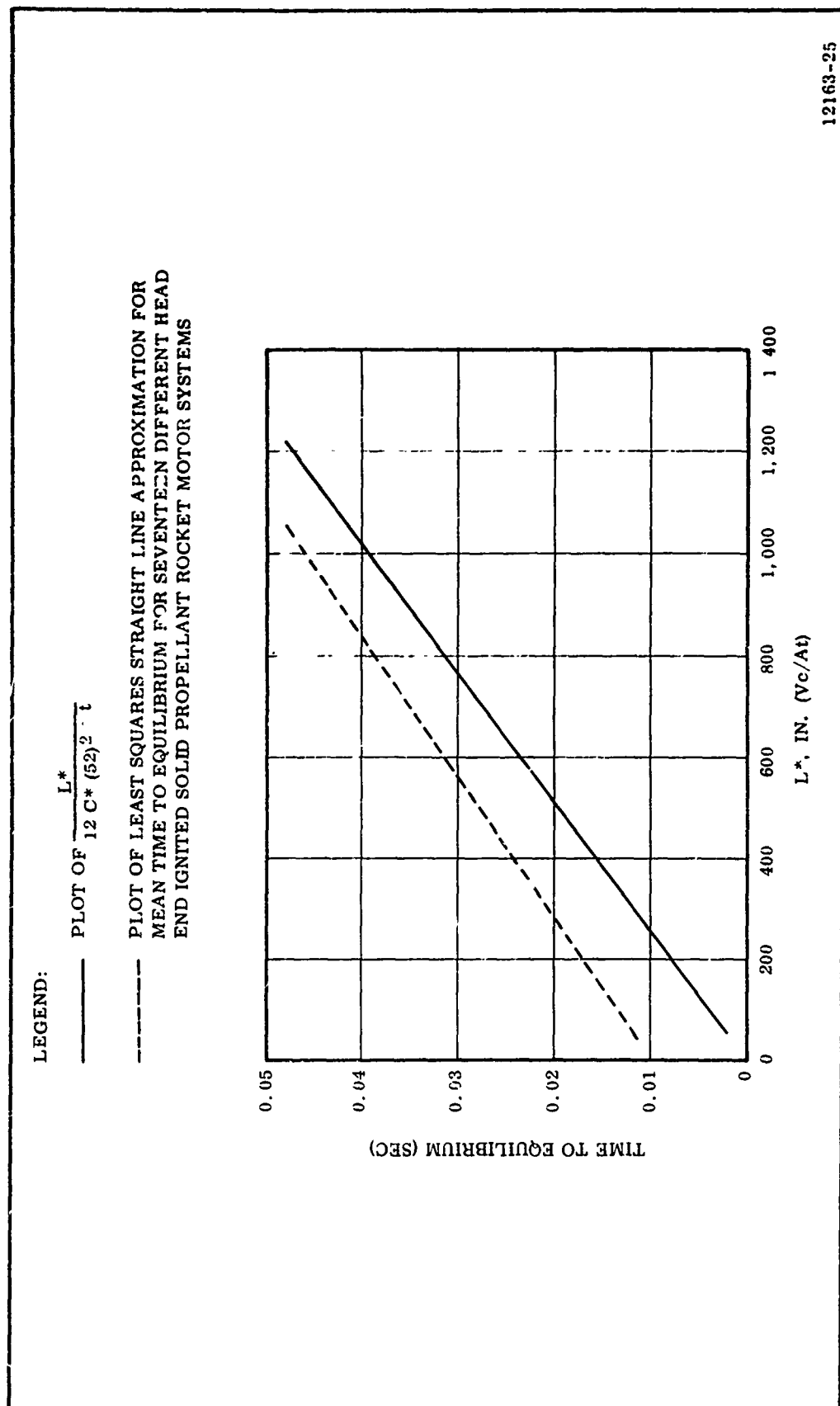


Figure 69. Time from First Motor Chamber Pressure Rise to Initial Equilibrium as Function of Motor Characteristic Length

that the theoretical and actual lines converge at high values of L^* so the above equation was used without correction to predict a time to equilibrium of 0.133 second.

Lag time is the time required for the igniter combustion products to heat the motor propellant at one spot on the surface above its autoignition temperature. For calculation purposes, this first point of ignition is located geometrically by a layout of igniter exhaust plume and the motor grain. The time to achieve the autoignition temperature is calculated by an equation which describes the heat transfer from a moving gas stream to an infinite plate. The equation generally takes the form of:

$$\tau = \frac{C_p \rho K (T_s - T_a)^2}{Q_T^2} \psi^2$$

Where:

- τ = Lag time (sec).
- C_p = Motor propellant heat capacity (Btu/lb-°F).
- ρ = Motor propellant density (lb/cu ft).
- K = Motor propellant thermal conductivity (Btu/hr-ft²-°F).
- T_s = Surface temperature of the propellant during steady state combustion (°R).
- T_a = Ambient temperature of the propellant (°R).
- Q_T = Heat flux rate (Btu/ft²-sec).
- ψ^2 = Constant, theoretically equal to $\Pi/2$; in practice, ψ^2 approaches 1.

A method of calculating Q_T was presented by United Technology Center (UTC)* in which total heat flux, Q_T , is broken down into its radiative and convective components:

$$Q_T = Q_{RAD} - Q_{CONV}$$

Where:

$$Q_{RAD} = \text{Radiative heat flux.}$$

$$Q_{CONV} = \text{Convective heat flux.}$$

Radiative heat flux is calculated by the following equation.

$$Q_{RAD} = \sigma \epsilon (T_p^4 - T_a^4)$$

Where:

$$\sigma = \text{Stephan Boltzmann radiation constant,} \\ 0.1714 \times 10^{-8} \text{ Btu/hr-ft}^2\text{-}^\circ\text{R}^4.$$

$$\epsilon = \text{Emissivity of the igniter gases.}$$

$$T_p = \text{Igniter plume temperature (}^\circ\text{F).}$$

$$T_a = \text{Propellant ambient temperature (}^\circ\text{R).}$$

UTC presented a figure from which emissivity could be taken as a function of port diameter and chamber pressure. For a diameter of 74 in. and a pressure of two atmospheres, the emissivity was found to be 0.135. Using a flame temperature of 5,220°R and an ambient temperature of 520°R, the radiative heat flux was found to be 172,000 Btu/hr-ft². UTC also presented a figure from which Q_{CONV} as a function of igniter mass flow rate and port diameter could be selected. For a port diameter of 74 in., Q_{CONV} is 65,000 Btu/hr-ft², giving a total Q_T of 237,000 Btu/hr-ft² or 66 Btu/ft²-sec.

*United Technology Center: Theoretical and Experimental Investigations of Ignition Systems of Very Large Solid Propellant Motors (U). Final Report, Contract AF 04(611)-7559; Sunnyvale, California; United Technology Center, May 1963; CONFIDENTIAL.

For the TU-312L.02 igniter, the lag time of 0.31 sec is primarily a result of the large free volume of the motor. The time lapse of the TU-312L.02 motor propellant includes heat-up time and the time of pressurization to equilibrium.

The flame spreading period covers the time from first ignition until all the surfaces are ignited. Flame spreading rates are estimated from analysis of actual motor data. Rates vary from about 7,000 in./sec down the port to about 250 in./sec down a stagnant slot. These rates vary with port diameter, flow directions, driving forces, etc., and must be selected with care for performance prediction. Based on predicted flame spreading rates of 250 in./sec down the slots, 5,000 in./sec down the main port, and 1,000 in./sec in the head end port, the ignition transient shown in Figure 68 was predicted. Table XXIII shows the TU-312L.02 igniter predicted performance.

TABLE XXIII

TU-312L.02 IGNITER PREDICTED PERFORMANCE

<u>Characteristics</u>	<u>Value</u>
Mass Flow Rate lb/sec (first level 0.56 sec)	158
Burning Time (sec)	0.6
Maximum Operating Pressure (psia)	850
Average Operating Pressure, first level (psia)	820
Average Operating Pressure, second level (psia)	350
Ignition Delay, 10 percent P_{max} for Booster PYROGEN (sec)	0.050
Ignition Interval Booster PYROGEN T_o to 90 percent P_{max} (sec)	0.076
Motor Ignition Delay Time, T_o to 75 percent P_{max} (sec)	0.58
Maximum Motor Pressure at Ignition (psia)	748
Igniter Coefficient (lb/sec) sq in.	0.185

C. IGNITER INSULATION

1. CASE INTERNAL INSULATION

The case internal insulation protects the igniter case from overheating during both igniter and motor firings and controls the web thickness of the propellant grain. The internal insulation consists of two 0.1 in. thick plies of asbestos filled NBR (V-44) laid up and vulcanized in place. One tenth inch of UF-2121 liner is applied over the NBR to provide a high strength bond to the TP-H1016 propellant. The insulation/liner/propellant bond system concept has an extensive successful history at Thiokol.

2. CASE EXTERNAL INSULATION

The igniter case external insulation will prevent the steel case from melting during the motor firing, thus precluding the ejection of fragments of the igniter case. The external insulation consists of 1.0 in. of asbestos filled NBR laid up and vulcanized in place. The insulation thickness is based on a char rate of 5.5 mil/sec with 1.5 safety factor. The thickness is more than adequate because a char rate of 3.2 mil/sec has been Thiokol's experience for motor head end applications in the past.

3. IGNITER CAP INSULATION

The insulation applied to the internal dome of the igniter cap will be 0.7 in. of TI-H704B. TI-H704B insulation was demonstrated by Thiokol as the case insulation in four Stage I MINUTEMAN size motors, the ignition system insulation on a 120 in. diameter motor, and as the case insulation in a 156 in. diameter motor. The insulation is a mastic insulation containing primarily HC binder, asbestos, and

carbon black. It is most effective in low velocity areas and was selected as a PYROGEN igniter insulation because of its relatively low cost, ease of application in any configuration, and ability to cure at ambient temperature.

4. IGNITER INSULATION INTERFACES

Vacuum putty will be used to seal and provide thermal joints when assembling the initiator PYROGEN loaded case and the booster PYROGEN loaded case to the igniter cap (Figure 64). These parts are toleranced so that a minimum of 0.1 and a maximum of 0.25 in. of this putty will be used at joint interfaces.

D. PHYSICAL CHARACTERISTICS, IGNITION SYSTEM PROPELLANT, AND IGNITER INSULATION

1. STRESS ANALYSIS

The TU-312L.02 ignition system was structurally analyzed to determine its compatibility with the forward polar boss and surrounding areas. Structural components of the system which were subjected to analysis included the forward polar boss, igniter cap, igniter case, and attachment bolts. To determine the most severe loading, two conditions were investigated.

1. Ignition-booster igniter case pressurized to MEOP
(1,000 psi), TU-312L.02 motor unpressurized.
2. TU-312L.02 main stage motor pressurized to MEOP
(848 psi), booster igniter case at equilibrium pressure.

Analytical results of these conditions are summarized in Figures 70 and 71. The margins of safety shown were calculated from stresses existing at the appropriate MEOP and ultimate material strengths. Structural materials and their mechanical properties are presented in Table XXIV. A minimum margin of safety of 0.32 occurs in the igniter cap during condition No. 2. Margins of safety throughout all igniter structural components are shown on Figures 70 and 71.

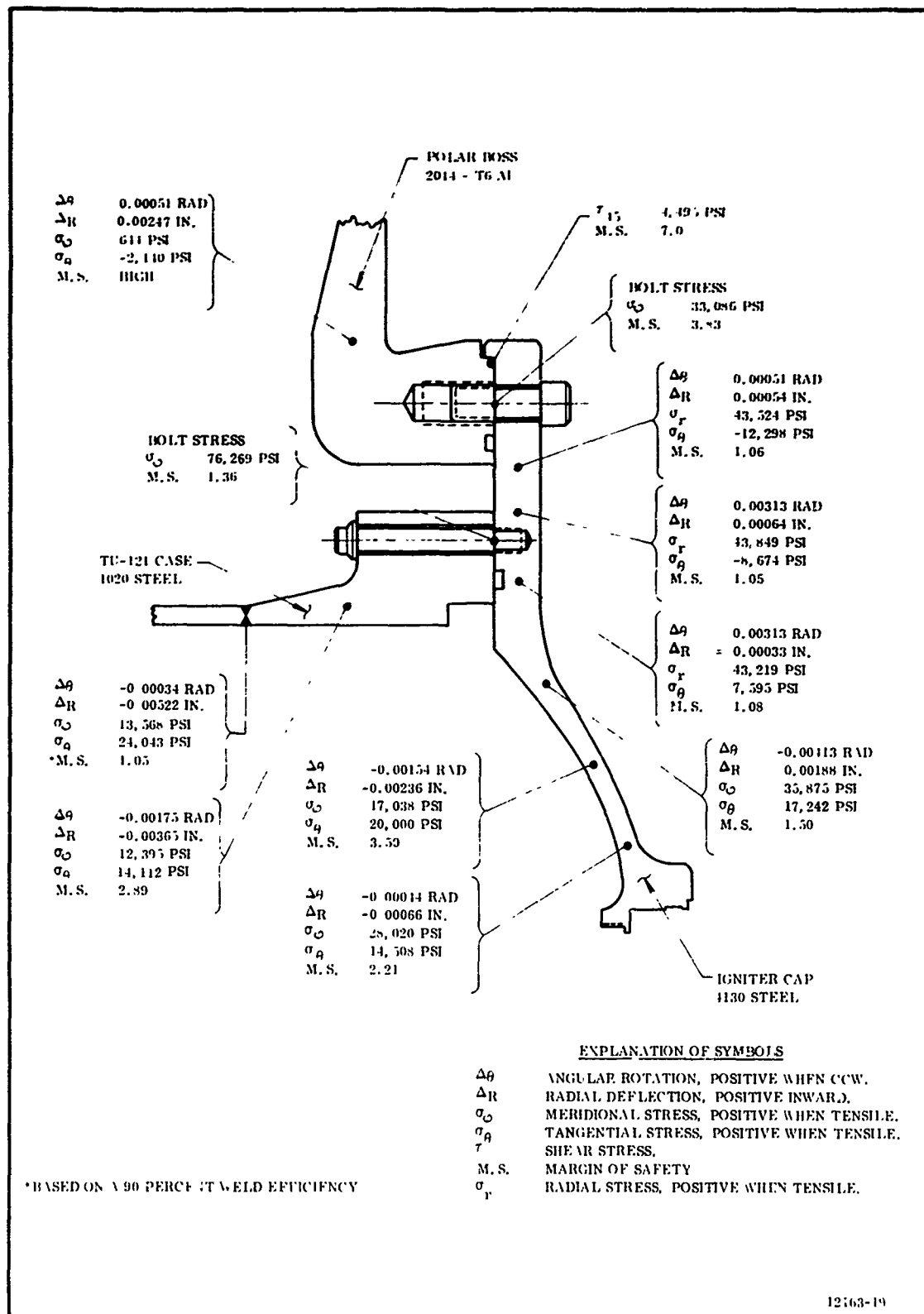


Figure 70. Summary of Analysis on TU-312L.02 Ignition System
Condition II (MEOP = 1,000 psi)

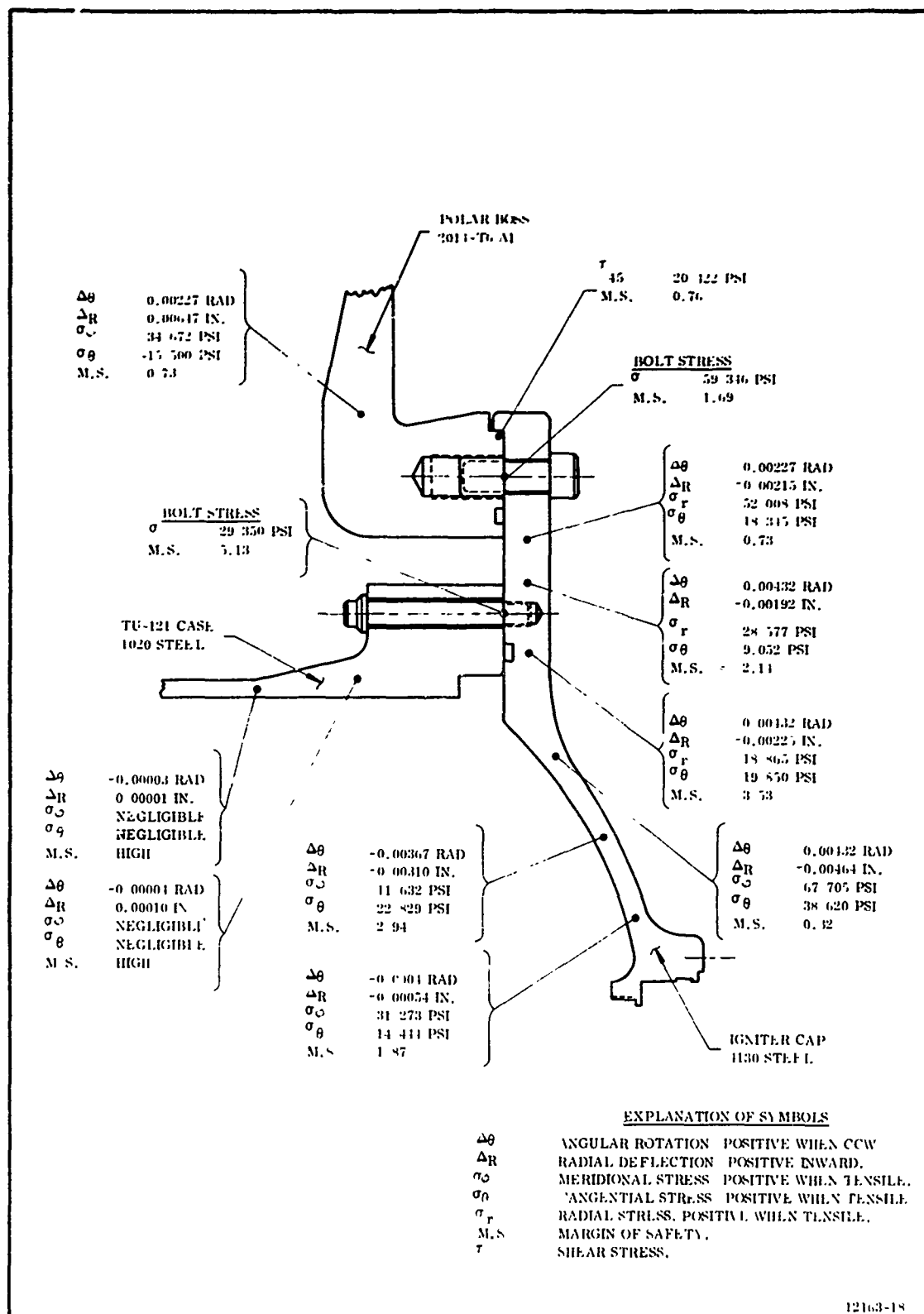


Figure 71. Summary of Analysis on TU-312L.02 Ignition System
Condition II (MEOP = 848 psi)

TABLE XXIV
IGNITION SYSTEM STRUCTURAL MATERIALS

<u>2014-T6 Aluminum</u>	<u>Component</u>
$F_{tu} = 60,000 \text{ psi}$	
$F_{ty} = 55,000 \text{ psi}$	Polar Boss
$F_{su} = 36,000 \text{ psi}$	(Ref Drawing 9U37466)
$E = 10.5 \times 10^6 \text{ psi}$	
 <u>4130 Steel</u>	
$F_{tu} = 90,000 \text{ psi}$	Igniter Cap
$F_{ty} = 70,000 \text{ psi}$	(Ref Drawing 7U37344)
$F_{su} = 54,000 \text{ psi}$	
$E = 29 \times 10^6 \text{ psi}$	
 <u>1020 Steel</u>	
$F_{tu} = 55,000 \text{ psi}$	Igniter Case
$F_{ty} = 36,000 \text{ psi}$	(Ref Drawing DU1020)
$F_{su} = 35,000 \text{ psi}$	
$E = 29 \times 10^6 \text{ psi}$	
 <u>Bolt (NAS 1351-10)</u>	
5/8 - 18 UNF	Igniter Cap to Polar
$F_{tu} = 160,000 \text{ psi}$	Boss Attachment
$E = 30 \times 10^6 \text{ psi}$	
 <u>Bolt (NAS 628-44)</u>	
1/2 - 20 UNF	Igniter Cap to Case
$F_{tu} = 180,000 \text{ psi}$	Attachment
$E = 30 \times 10^6 \text{ psi}$	
where: F_{tu} = ultimate tensile strength	F_{su} = shear strength
F_{ty} = yield tensile strength	E = modulus

2. IGNITER WEIGHTS

The weights for the PYROGEN igniter are listed below.

	<u>Weight (lb)</u>
Loaded Case Booster PYROGEN	
Case	260.750
External Insulation	87.644
Internal Insulation	13.290
UF-2121 Liner	4.070
TP-H1016 Propellant	131.912
Initiating PYROGEN	
Case	3.879
Liner	0.029
TP-H1016 Propellant	1.234
Nozzle	1.375
Booster Assembly	0.583
S & A Device	4.780
Igniter Cap	145.154
Miscellaneous	<u>8.178</u>
TOTAL	662.034

3. IGNITION SYSTEM PROPELLANT

The composition of the propellant (designated TP-H1016) for the ignition system is listed on the following page.

CONFIDENTIAL

<u>Constituent</u>	<u>Percent Composition by Weight</u>
Ammonium Perchlorate	77
Aluminum Powder	2
HB and ERL*	18
Ferric Oxide	3

*The ratio of HB to ERL is determined from raw material standardization to achieve the desired physical properties.

The physical properties of TP-H1016 propellant are listed below.

<u>Item</u>	<u>Value</u>	
	<u>Minimum</u>	<u>Maximum</u>
Density (lb/in. ³)	0.0599	0.0611
Maximum Stress (psi)	140	227
Strain at Maximum Stress (in./in.)	0.20	0.33
Modulus of Elasticity (psi)	500	1,200

TP-H1016 propellant has the following ballistic properties.

Characteristic Velocity, C* (ft/sec)	4,945
Density (lb/in. ³)	0.0605
Exponent Burning Rate, n	0.44
Burning Rate at 1,000 psi (in./sec)	0.84

TP-H1016 propellant autoignition occurs as shown below.

<u>Temperature (°F)</u>	<u>Time (min)</u>
390	60
408	40
445	20
496	10

4. INSULATION INGREDIENTS, AND PHYSICAL AND THERMAL PROPERTIES

The insulation selected for the head end cap of the ignition system is designated TI-H704B. The composition of this insulation is asbestos and carbon black filled HC polymer mastic material. The formulation of this material is listed below (Ref Specification SB-SP-356A).

<u>Ingredients</u>	<u>Weight Percent</u>
Binders	45.0
Asbestos	30.0
Carbon Black	15.0
Diammonium Phosphate	<u>10.0</u>
	100.0

The physical properties and thermal properties of TI-H704B insulation are as follows.

Cured Density at $77 \pm 3^\circ \text{F}$ (g/cc)	1.30
Cured Thermal Properties	
Specific Heat (cal/g $^\circ\text{C}$)	0.325
Thermal Conductivity (cal/cm sec $^\circ\text{C}$)	9.15×10^{-4}
Thermal Diffusivity (cm 2 /sec)	2.35×10^{-3}

5. PHYSICAL AND THERMAL PROPERTIES OF IGNITER EXTERNAL INSULATION AND LINER

For the physical and thermal properties of igniter external insulation (NBR) internal case insulation and igniter liner (UF-2121), see Section V, Insulation and Liner.

E. IGNITION BENCH TESTS

The ignition system consists of components previously demonstrated in the AF 156-1 motor test. The only modification to the AF 156-1 igniter is that the booster PYROGEN igniter is somewhat shorter. Consequently, only minimal bench testing is required to verify components and performance. This testing will include the static firing of one complete igniter assembly with a simulated S & A mechanism and without external insulation. The primary objective of this test is to evaluate igniter performance parameters such as igniter response time, igniter ignition delay, booster PYROGEN lag time, and booster PYROGEN pressures. Instrumentation will consist of pressure gages on the booster PYROGEN igniter.

The TU-312L.02 ignition system for the bench tests will be temperature conditioned for a minimum of 12 hr at 80° F. The motor will be static tested within 30 min after removal from conditioning. The ignition system will be installed in a delta test stand firing arrangement with pressure transducers installed to record igniter pressure. A documentary camera will be positioned to obtain photographic coverage of the static test. Pressure will be recorded as a function of time to provide data for analyzing igniter performance. After the igniter is tested, it will be examined for hot spots or any abnormalities. Still photos will be made before and after the static test.

The bench test ignition system configuration (7U37340-02) is identical to the ignition system that will ignite the 156-8 motor except that the firing train test fixture will replace the S & A device (for economical reasons) and the booster loaded case assembly (7U37341) does not have external insulation. The external insulation is required only for igniters subjected to heat during motor firing and assures that the ignition system will remain in one integral configuration during the motor firing.

The firing train test fixture simulates the KR80000 S & A device. Using the firing train test fixture eliminates device switch decks, motor assembly, reset assembly, and toggle assemblies. These items are not required since the device is manually armed at the test site during the final motor preparation.

SECTION VIII

PROGRAM SCHEDULE

The period of performance covered by this report is from 2 May 1966 to 31 Jul 1966. The contract provides for static testing the 156-8 motor within 240 days of the contract date. The program schedule (Figure 2) shows that the 156-8 motor will be tested on 23 Dec 1966. This schedule reflects actual performance up through 31 Jul 1966 and currently planned performance from that point through the remainder of the program. All reports and documentation requirements as listed in DD Form 1423 were submitted as shown in Figure 3. Analysis of the pertinent tasks appears below.

A. SUBSCALE JOINT SEAL DEVELOPMENT

At the end of the report period, this task was 99.08 percent complete. The design and test plan have been submitted and approved. The subscale vessel for the demonstration of the joint seal concept was fabricated and successfully hydrotested to 1,100 psig.

B. MOTOR DESIGN AND ANALYSIS

The following design drawings were submitted and approved by the Air Force during this quarter.

1. Joint seal.
2. Insulation and liner.
3. Propellant grain.
4. Ignition system.

C. MOTOR INSULATION AND LINER

All materials were placed on order and the compatibility test plan was submitted and approved. The old bladder was removed from the case segments and the new one installed. The layup of joint insulation is scheduled for early August.

Work on all other tasks was started where required by the program schedule. At the end of the report period, this program was 26.86 percent complete.

Security Classification

DOCUMENT CONTROL DATA - R&D		
(Security classification of title, body of abstract and indexing annotation must be entered when the overall report is classified)		
1. ORIGINATING ACTIVITY (Corporate author) Thiokol Chemical Corporation Wasatch Division Brigham City, Utah 84302		2a. REPORT SECURITY CLASSIFICATION Confidential
		2b. GROUP 4
3. REPORT TITLE Quarterly Technical Report No. 1 Demonstration of 156 Inch Motor with Segmented Fiberglass Case and Ablative Nozzle		
4. DESCRIPTIVE NOTES (Type of report and inclusive dates) Quarterly Technical Report (QTR) - 2 May thru 31 July 1966		
5. AUTHOR(S) (Last name, first name, initial) C. G. Kennedy		
6. REPORT DATE 30 August 1966	7a. TOTAL NO. OF PAGES 180	7b. NO. OF REFS 1 page
8a. CONTRACT OR GRANT NO. AF 04(611)-11603 b. PROJECT NO. 623A601 c. d.	9a. ORIGINATOR'S REPORT NUMBER(S) 0817-64-0995 9b. OTHER REPORT NO(S) (Any other numbers that may be assigned this report) 1066-12163 AFRPL-TR-66-222	
10. AVAILABILITY/LIMITATION NOTICES In addition to security requirements which apply to this document and must be met, it may be further distributed by the holder only with specific prior approval of: SSD (SSBS); Los Angeles Air Force Station, Air Force Unit Post Office, Los Angeles, California 90045		
11. SUPPLEMENTARY NOTES N/A	12. SPONSORING MILITARY ACTIVITY Air Force Rocket Propulsion Laboratory Edwards, California 93523	
13. ABSTRACT This program was established by the Air Force Rocket Propulsion Laboratory to demonstrate a segmented fiberglass case and an ambient pressure cured ablative nozzle in an actual motor firing. The development of manufacturing processes and handling techniques for the insulating and loading of a segmented fiberglass case is a primary objective of this program. The segmented fiberglass case was designed by Thiokol Chemical Corporation and fabricated by B. F. Goodrich Company under Air Force Materials Laboratory (AFML) Contract AF 33(657)-11303; the fixed ablative nozzle was fabricated by Thompson Ramo Wooldridge Incorporated under AFML Contract AF 33(657)-11301. The technical effort on this demonstration program was initiated on 2 May 1966. A subscale vessel was designed, fabricated, and tested during this first quarter to demonstrate joint sealing techniques for the 156 in. diameter segmented fiberglass case. The nozzle was delivered to the Wasatch Division, and effort in preparing the case segments for loading was initiated. The design of the 156 in. motor, including insulation, propellant grain, igniter, and ballistic performance, was completed.		

DD FORM 1473
1 JAN 64

Security Classification

14	KEY WORDS	LINK A		LINK B		LINK C	
		ROLE	WT	ROLE	WT	ROLE	WT
N/A							

INSTRUCTIONS

1. ORIGINATING ACTIVITY: Enter the name and address of the contractor, subcontractor, grantee, Department of Defense activity or other organization (corporate author) issuing the report.

2a. REPORT SECURITY CLASSIFICATION: Enter the overall security classification of the report. Indicate whether "Restricted Data" is included. Marking is to be in accordance with appropriate security regulations.

2b. GROUP: Automatic downgrading is specified in DoD Directive 5200.10 and Armed Forces Industrial Manual. Enter the group number. Also, when applicable, show that optional markings have been used for Group 3 and Group 4 as authorized.

3. REPORT TITLE: Enter the complete report title in all capital letters. Titles in all cases should be unclassified. If a meaningful title cannot be selected without classification, show title classification in all capitals in parenthesis immediately following the title.

4. DESCRIPTIVE NOTES: If appropriate, enter the type of report, e.g., interim, progress, summary, annual, or final. Give the inclusive dates when a specific reporting period is covered.

5. AUTHOR(S): Enter the name(s) of author(s) as shown on or in the report. Enter last name, first name, middle initial. If military, show rank and branch of service. The name of the principal author is an absolute minimum requirement.

6. REPORT DATE: Enter the date of the report as day, month, year, or month, year. If more than one date appears on the report, use date of publication.

7a. TOTAL NUMBER OF PAGES: The total page count should follow normal pagination procedures, i.e., enter the number of pages containing information.

7b. NUMBER OF REFERENCES: Enter the total number of references cited in the report.

8a. CONTRACT OR GRANT NUMBER: If appropriate, enter the applicable number of the contract or grant under which the report was written.

8b, 8c, & 8d. PROJECT NUMBER: Enter the appropriate military department identification, such as project number, subproject number, system numbers, task number, etc.

9a. ORIGINATOR'S REPORT NUMBER(S): Enter the official report number by which the document will be identified and controlled by the originating activity. This number must be unique to this report.

9b. OTHER REPORT NUMBER(S): If the report has been assigned any other report numbers (either by the originator or by the sponsor), also enter this number(s).

10. AVAILABILITY/LIMITATION NOTICES: Enter any limitations on further dissemination of the report, other than those imposed by security classification, using standard statements such as:

- "Qualified requesters may obtain copies of this report from DDC."
- "Foreign announcement and dissemination of this report by DDC is not authorized."
- "U. S. Government agencies may obtain copies of this report directly from DDC. Other qualified DDC users shall request through _____."
- "U. S. military agencies may obtain copies of this report directly from DDC. Other qualified users shall request through _____."
- "All distribution this report is controlled. Qualified DDC users shall request through _____."

If the report has been furnished to the Office of Technical Services, Department of Commerce, for sale to the public, indicate this fact and enter the price, if known.

11. SUPPLEMENTARY NOTES: Use for additional explanatory notes.

12. SPONSORING MILITARY ACTIVITY: Enter the name of the departmental project office or laboratory sponsoring (paying for) the research and development. Include address.

13. ABSTRACT: Enter an abstract giving a brief and factual summary of the document indicative of the report, even though it may also appear elsewhere in the body of the technical report. If additional space is required, a continuation sheet shall be attached.

It is highly desirable that the abstract of classified reports be unclassified. Each paragraph of the abstract shall end with an indication of the military security classification of the information in the paragraph, represented as (TS), (S), (C), or (U).

There is no limitation on the length of the abstract. However, the suggested length is from 150 to 225 words.

14. KEY WORDS: Key words are technically meaningful terms or short phrases that characterize a report and may be used as index entries for cataloging the report. Key words must be selected so that no security classification is required. Identifiers, such as equipment model designation, trade name, military project code name, geographic location, may be used as key words but will be followed by an indication of technical context. The assignment of links, rules, and weights is optional.